https://ntrs.nasa.gov/search.jsp?R=19730010512 2020-03-23T03:24:12+00:00Z

N73-19239
CR-128749

CASE FILE
COPY

Lockheed

MISSILES & SPACE COMPANY

A GROUP DIVISION OF LOCKHEED AIRCRAFT CORPORATION

SUNNYVALE, CALIFORNIA

COPY NO.

REPORT NO. GCS/3267/6211

DATED January 30 1973

REVISED

NAS 9-12075

LOCKHEED MISSILES & SPACE COMPANY

A GROUP DIVISION OF LOCKHEED AIRCRAFT CORPORATION

SUNNYVALE, CALIFORNIA

TITLE

COMPUTER SIMULATION OF SPACE STATION COMPUTER STEERED HIGH GAIN ANTENNA -

FINAL REPORT

SUBMITTED UNDER

EFFECTIVE UNDER

MODEL _____ APPROVED BY _____

PREPARED BY S. W. Beach
S. W. Beach
Guidance & Control Systems

APPROVED BY John B. Damonte
John B. Damonte, Manager
Antenna Systems

CHECKED BY D. G. Simcox
D. G. Simcox

APPROVED BY J. J. Rodden
J. J. Rodden, Manager
Guidance & Control Systems

REVISIONS

DATE	REV BY	PAGES AFFECTED	REMARKS

FORM LMSC 402-3

TABLE OF CONTENTS

TABLE OF CONTENTS (Continued)

1.0 INTRODUCTION

The purpose of this final report is to summarize the mathematical modeling and programming of the complete simulation program. Much of the material included is taken from earilier reports (Task 1 through Task 4) but is repeated here in order to provide a complete description in a single document.

Appendix A – Deck Setup and Input Variables – is also nearly identical to the separate document – Space Station Antenna Simulation Digital Computer Program Operating Requirements – and is included here both for completeness and to show the input parameter values used in the program run of Appendix C – Trade-off Study Simulation Results.

2.0 BASIC PROGRAM STRUCTURE

The simulation program described in this report is an application of a general purpose simulation package (DEADAM) maintained by Dept. 62-11, LMSCI, Sunnyvale, Calif. This foundation program provides for reading input data cards, numerically integrating up to 50 first order differential equations (not necessarily linear or continuous), and monitoring up to 48 variables on printed output and on plots.

For constructing a particular simulation program communication with the DEADAM package is accomplished through the subroutine SETUP in which the details of the differential equations and output variables are defined, usually with the aid of additional subroutines called from SETUP.

The computations done by or called for by the SETUP subroutine for the "Computer Steered High Gain Antenna Simulation" are indicated in Figure A-1 and are described in detail in the following sections of this report.

For efficient computation of pointing requirements (gimbal angles), a simplified simulation program is included which uses a different version of the SETUP subroutine (SETUP/PØINT). The computations called for by this program are a subset of those illustrated in Figure A-1 and are indicated in Figure A-2.

3.0 SIMULATED SYSTEM MODELLING

The system being simulated by the "Computer Steered High Gain Antenna Simulation" program consists of 1) a high gain antenna, 2) an antenna gimbal control system, 3) an on board computer, and 4) the environment in which 1), 2), and 3) are to operate. The interconnection of the mathematical models of these four subsystems is indicated in Figure 3.0-1.

3.1.1 Antenna Model

This section describes the mathematical model used by the simulation program for the radiating system (antenna) and has been extracted from the Task 1 Report - Math Modeling of High Gain Antenna - dated 1 March 1972.

The programming of this modeling is contained in the subroutines MØNPLS and THERMD which are called by SETUP to computer gain along the actual line of sight, monopulse system output signals, and shift in the line of sight due to solar heating deformations; and in the subroutines GAIN, AXIS, and MØDEL which are called by the antenna initialization routine ANTIN only once (per case) to determine parameters used by MØNPLS and THERMD.

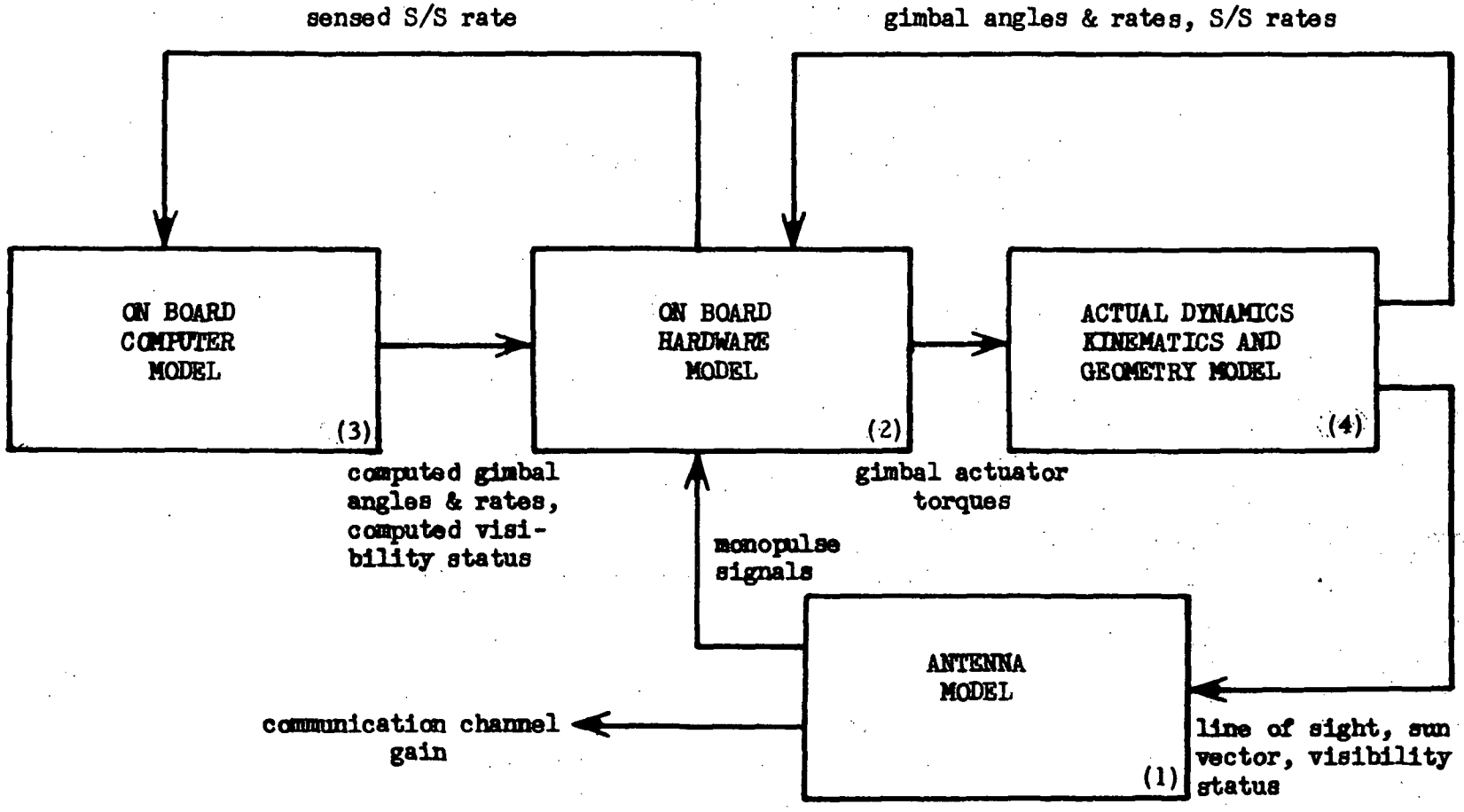

Figure 3.0-1 Interconnection of Subsystems

3.1.2 AN OVERVIEW

A simplified schematic diagram of the radiating system model is shown in Fig. A-2.1. Each of the elements in this figure will be discussed separately in later sections. In this section we shall present an overview of the radiating system model and the interrelationship of the basic elements.

The input portion of the program takes all of the input data needed for the calculation of gain except for the coordinate angles θ and ϕ and the coordinates of the sun with respect to the reflector. It has been assumed, in setting the input up this way, that the computer program will be used primarily in a "simulation" mode -- that is, to simulate the operation of an actual or proposed system. This means that all the adjustable design parameters are introduced in the input block of the program and represent one particular system. All these input parameters will remain fixed throughout a run. The most rapidly varying coordinates then will be the LOS coordinate angles and the coordinates of the sun. Thus, with one input block of data we should be able to simulate the operation of the system throughout an orbit or an operational situation, but making parametric variations of certain design parameters (such as reflector diameter) for a fixed orientation of the LOS would require re-inputting the basic data.

In addition to the basic design parameters, the input data base will contain a number of flags to select various options available within the program.

One of the flags contained in the input data base is SMP which selects either the simple gain and beamwidth calculation or the more complex computation. If SMP=1, then the peak gain and beamwidth will be calculated from simple formulas. If SMP=0, then the peak gain of the antenna along its nominal boresight axis and the beamwidth are calculated using the current distribution method. The latter option will have several feed options and reflector options associated with it.

The output of either of these calculations is the peak gain of the antenna and the half-power beamwidth with the beam direction defined as being along the nominal boresight axis of the antenna. This output is then corrected for thermal effects. The angular position of the sun relative to the reflector is fed into a correction calculation block. Based on this sun position, the direction of the peak of the antenna beam will be shifted from its nominal position, using a table of values based on ATS F and G experience. The maximum gain value will also be reduced in the same way.

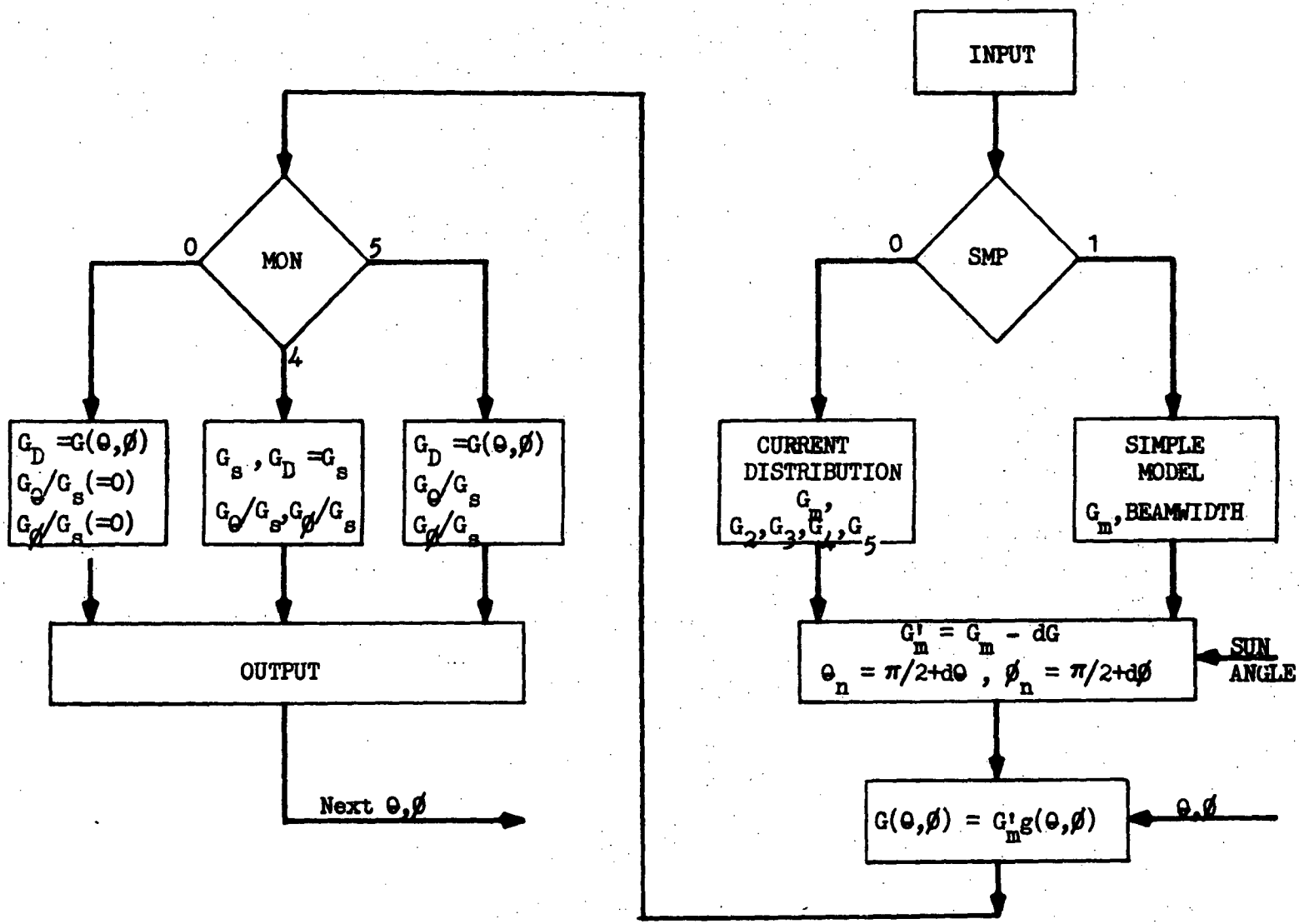

Figure A-2.1 OVERVIEW OF RADIATING SYSTEM MODEL

Following this correction, a pair of coordinate values θ and ϕ representing the LOS to the relay satellite will be entered. The computation of these coordinate angles will take into account any movement of the reflector boresight that results from steering -- that is, the angles θ and ϕ represent the true position of the LOS with respect to the nominal boresight axis of the reflector. Using these coordinates, the gain in the direction θ and ϕ will be calculated using a simple approximation formula for the peak of the main beam. This gain is that associated with a single feed located at the focal point of the reflector. For either the non-monopulse option or the five-horn monopulse option, this would be the gain of the communications channel in the LOS direction.

Another of the flags contained in the input data base is MON, which sets up the calculation of monopulse sum and difference signals where desired. For MON=O, no monopulse signals are calculated and the gain value already determined is simply read out. Then the next values of θ and ϕ and sun angle are read and the calculation is continued. For MON=4, a four-horn monopulse system is assumed. Using design parameters contained in the input data base, sum and difference signal gain values are calculated. The sum channel gain value is also the communications channel gain value. After output, the program goes on to the next LOS position. For MON=5, the calculation is the same as for the 4 horn system, except that the communication channel gain value is the same as it would be for MON=O.

One very important point should be noted here. Even if the complicated form of gain calculation is selected, this computation is performed only once to determine the peak gain of the antenna and the half-power beamwidth. Once this computation is made, it is not repeated as new values of θ and ϕ are entered. The complex computation simply determines the maximum gain of the antenna and the relative gain at any angle is found using this peak gain value and an approximation formula. The gain at the actual position of the LOS could be determined directly from the complicated form of the computation, but the error in using an approximation is comparable to (and probably less than) the computational accuracy of the complicated computation itself. The accuracy is certainly good enough for engineering purposes at any rate, and so it was not deemed prudent to use the complicated computation more than once per run as it requires a large amount of computer time compared with that required by the approximation. There are some limitations to the foregoing statements, so we shall present the rationale here in detail.

3.1.3 ACCURACY OF THE GAUSSIAN PATTERN APPROXIMATION

The current distribution method will be used (when desired) to calculate the peak gain on axis and the gain at four symmetrically located points off axis (in the vicinity of the half-power level). From these data an elliptical paraboloid will be fitted to the peak of the main beam. For the case of a symmetrical main beam aligned with the nominal boresight axis, the current distribution method will determine G_m and β, where 2β is the half-power beamwidth of the antenna pattern. Then the main beam within the half-power contour will be approximated by the formula

$$G(\alpha) = G_m \exp -p(\alpha/\beta)^2 \tag{3.1}$$

where $G(\alpha)$ is the gain in a direction which makes an angle α with respect to the boresight axis. In the above p is a constant.

The pattern shape given by Eq. (3.1) is a Gaussian curve and this approximation is sometimes called the Gaussian approximation. When converted to decibels, the equation becomes that of a parabola.

$$10 \log_{10} G(\alpha) = 10 \log_{10} G_m - 3.010 (\alpha/\beta)^2 \tag{3.2}$$

For this reason, the approximation is often called the parabolic approximation. For the more general case where the pattern beamwidths in two orthogonal planes are not equal, Eq. (3.2) must be generalized to the form of an elliptical paraboloid.

A study was made of the accuracy of Eq. (3.2) compared to some typical theoretical pattern shapes. Specifically, the gain pattern functions chosen were

$$g(\alpha) = \left(2^n \, n! \, \frac{J_n'(u)}{u^n}\right)^2 G_m \tag{3.3}$$

where $u = (\pi D / \lambda) \sin\alpha$, D is the aperture diameter and λ is the wavelength. These are the pattern shapes that result from circular apertures of uniform phase having an amplitude distribution of the form

$$A(r) = (1 - r^2)^{n-1} \tag{3.4}$$

where r (≤ 1) is the normalized radius of the aperture.

When $G(\alpha)/Gm$ as given by Eq. (3.1) is matched to Eq. (3.3) at the peak ($\alpha = 0$) and at the half power point ($\alpha = \beta$), the error curve shown in Figure A-3.1 is the result. This is a plot of the equation

$$\Delta G = -3.010 \ (\alpha / \beta)^2 - 10 \log_{10} \left(\frac{g(\alpha)}{G_m} \right) \qquad (3.5)$$

for $n = 1$ and $n = 4$. Although in Fig. 3.2 D/λ was 200, there was no significant difference for $20 \leq D/\lambda \leq 500$. From the figure it can be seen that the Gaussian approximation gives a gain not more than 0.05 dB too low within the half-power contour, although it deteriorates rapidly when $\alpha > \beta$.

As we shall mention later, the computational accuracy of the current distribution method is about 0.07 dB. While the Gaussian approximation would not properly represent specially shaped beams, such as those having flat tops, it should be an accurate representation of normal pencil beam patterns applicable to communications problems. The accuracy of this representation is better than 0.05 dB within the half-power contour and improves as we approach the peak of the beam.

Beyond the half-power contour the Gaussian approximation begins to produce erroneous results. But for the computer-steered system, a misalignment of more than half a half-power beamwidth would cause serious doubts concerning the efficacy of the computer-steering method since the misalignment loss would exceed 3 dB.

The Gaussian approximation will also be used in the monopulse case, not only for the data or communication channel, but also to form the monopulse error signals. Although initial misalignment during acquisition may be greater than β, giving some error in gain, the monopulse will track toward the beam peak to reduce the error to within acceptable limits when the acquisition phase ends and the self-tracking phase begins.

The approximation will be used to save computer time since the current distribution integration process is quite costly compared to the simpler approximation. The approximation is considered sufficiently accurate for practical engineering purposes. Beamwidth and the angle between the LOS and the beam axis will be read out to flag situations where the approximation begins to deteriorate.

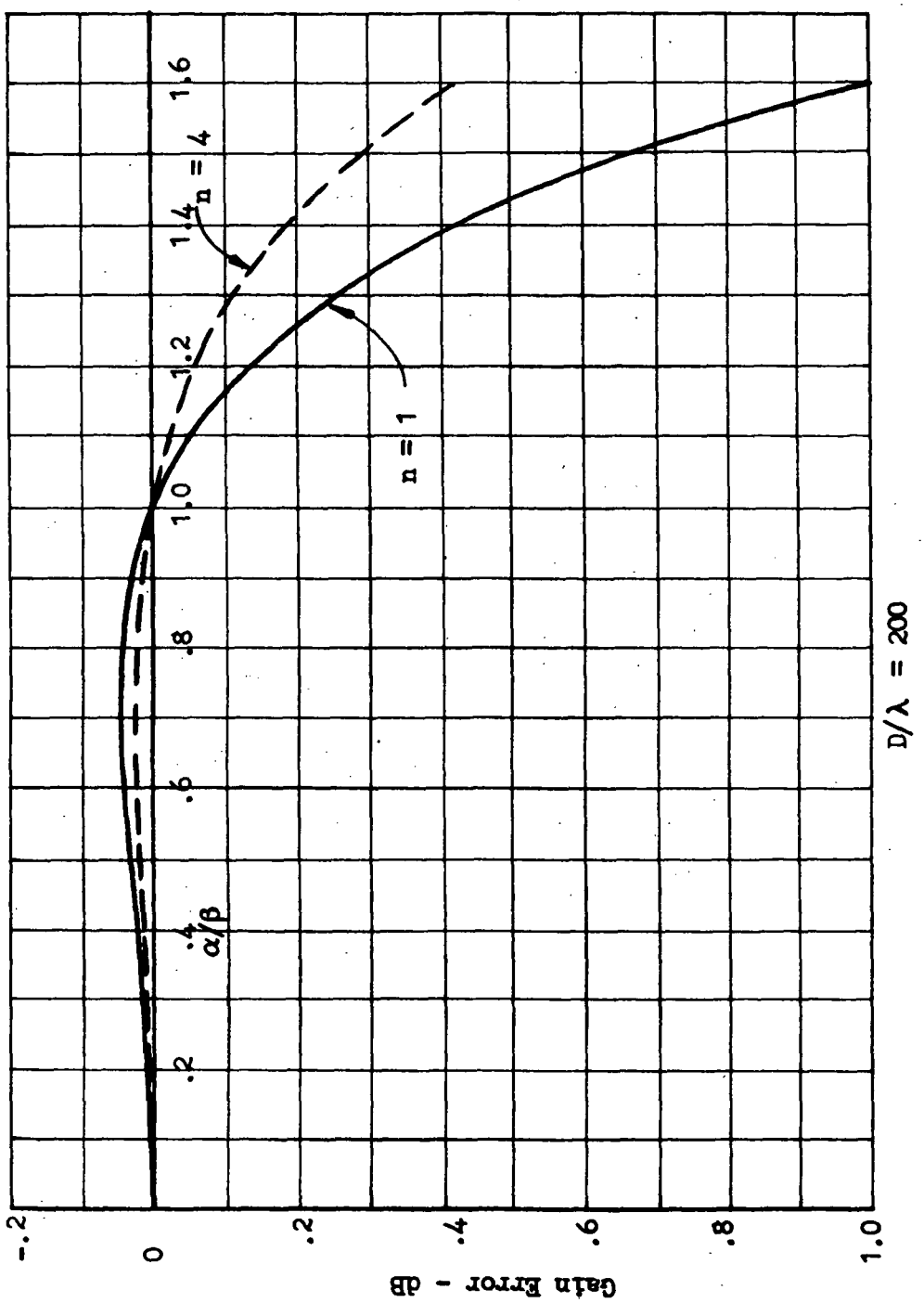

Figure A-3.1 GAIN ERROR OF GAUSSIAN APPROXIMATION

3.1.4 INPUT

The radiating system model receives data for calculation from four different sources: the built-in data files, external data files, the input subroutine, and other elements of the simulation program.

The built-in data files are as follows:

1. Standard Feed Gain Function. This is an experimental feed gain function data file which can be used in the program to calculate the reflector gain. This data file will represent a typical experimental feed designed to provide a tapered aperture illumination with approximately a -10 dB edge taper.

2. Thermal Gain Degradation Data File. This is a data file representing the peak gain degradation of a typical unfurlable reflector antenna as a function of sun position. It is used, as explained in Section A-7, to provide correction for thermal distortion effects.

3. Thermal Beamshift Data File. This is a data file representing the beamshift of a typical unfurlable reflector antenna as a function of sun position. It is used to provide for correction for thermal distortion effects.

Any of the built-in data files may be updated as required to reflect a current design case.

The one external data file is an experimental feed gain function data file which the user must provide.

The only data that the model receives from other elements of the simulation program are the coordinates of the LOS and the coordinates of the sun in reflector reference coordinates. These data are the independent variables for each single run. When the model is run by itself without the balance of the simulation master program, these data must be supplied on cards.

All of the remaining parameters necessary for the calculations performed by the radiating system model are supplied by the user on cards through the input subroutine. Some of the input parameters act as flags for selecting various options which may be exercised. The important input parameters are:

BMW....This is the beamwidth factor. This is the product of the half-power beamwidth and the aperture size in wavelengths. See Eq. 5.3.

CSN....This parameter flags the feed option to be used, as follows:

CSN $<$ 0: Selects either the built-in or the external experimental feed data file. See Sections A-6.3.4 and A-6.3.5.

$0 \leq$ CSN $\leq$ 999: Uses analytical function for feed gain function. Value of CSN is used in the analytical gain function. See Sections A-6.3.2 and A-6.3.3.

CSN $>$ 999: Uses function that provides uniform aperture illumination. See Section A-6.3.1.

DBK....This is the diameter of an area that blocks the reflector aperture. See Section A-6.5. DBK is in inches.

DIA....This is the reflector diameter in inches.

EFF....This is the aperture efficiency in percent.

FTV....This is the feed to vertex distance in inches. If FTV=0, the feed is placed at the nominal focal point of the reflector.

GFE....This is normally the peak gain of the feed. GFE and CSN determine the exact feed option, as follows:

CSN <0; GFE <0: The built-in reference experimental feed pattern is used. See Section A-6.3.5.

CSN <0; GFE ≥ 0: The external experimental feed pattern is selected. See Section A-6.3.4.

$0 \leq$ CSN $\leq$ 999; GFE ≤ 0: Uses analytical function for feed gain function with peak gain value for feed computed internally. See Section A-6.3.2.

$0 \leq CSN < 999$; GFE > 0: Uses analytical function for feed gain function with GFE as the peak gain value for the feed. See Section A-6.3.3.

GHZ....This is the frequency in GigaHertz.

HUB....This is the radius of the hub of the reflector in inches. By hub is meant any portion of the reflector at the vertex which is either a hole in the surface or a surface area not meant to be part of the reflector (as, for example, a flat plate covering a hole).

MON....This is the monopulse flag, as follows:

MON=0: does not calculate monopulse error signals.

MON=4: Assumes a four-horn monopulse system.

MON=5: Assumes a five-horn monopulse system.

See Section 3.1.

PAN....Flags the choice surface.

PAN ≤ 0: Selects perfect paraboloid. See Section A-6.4.1.

PAN > 0: Selects perfect Flex-Rib surface and sets the number of panels equal to PAN. See Section A-6.4.2.

POL....Selects polarization of the feed.

POL = 1: dipole mode of linear polarization.

POL = 2: slot mode of linear polarization.

POL = 3: right hand circular polarization.

POL = 4: left hand circular polarization.

PPW....This stands for points per wavelength and determines the rate at which the aperture is sampled to calculate the integral for gain. A built-in trap will require at least 600 points to be used to evaluate the integral. See Section 3.1.

SMP....This flags the simple or the complex model.

SMP=0: The gain is determined by the current distribution method. See Section 3.1.

SMP=1: The gain is determined by the simple model. See Section 3.1.

TDT(6,3)....This is a data array which defines the method of extrapolating the gain degradation and beamshift data for thermal distortion to other reflector diameters and frequencies. See Section 3.1.

XAP....This is the cross over angle in the ϕ plane for either monopulse case.

XAT....This is the cross over angle in the θ plane for either monopulse case.

XVP....This is the cross over level in the ϕ plane for either monopulse case.

XVT....This is the cross over level in the θ plane for either monopulse case.

(NOTE: At least one and no more than two of the parameters XAP, XAT, XVP, XVT will have a non-zero value whenever monopulse is called for. The monopulse may be specified by offset angles XAP and/or XAT or by cross over levels XVP and/or XVT (but not both). If only one non-zero value is given, the case is assumed to be symmetrical. Thus if XAP$\neq$0 and XAT=0 then the program sets XAT=XAP. See Section A-9.)

3.1.5 PEAK GAIN AND BEAMWIDTH CALCULATION - SIMPLE CASE

If SMP=1, the simple model is selected. This causes the peak gain to be calculated using the formula

$$G = \eta \left(\frac{\pi D}{\lambda} \right)^2 \tag{5.1}$$

where η = the overall antenna aperture efficiency, D = the aperture diameter and λ = the wavelength. The wavelength in inches is calculated from the equation

$$\lambda = 11.802854/f \tag{5.2}$$

where f = the frequency in GigaHertz. The quantities η, D, and f are represented by EFF, DIA, and GHZ, respectively, in the input subroutine. If EFF=0, the EFF is set equal to 0.55 (considered to be a typical value).

The half-power beamwidth β_o is determined by

$$\beta_o = \beta_r \frac{\lambda}{D} \text{ degrees} \tag{5.3}$$

where β_r is the beamwidth factor represented by BMW in the input subroutine. If BMW=0, BMW is set equal to 70 (a typical value) in the simple case computation.

Note that in the simple case the beam is assumed to be rotationally symmetric.

There is no justification for the use of the simple case formulas given above on the basis of accuracy. These formulas have been accepted for years in the antenna design field as representing typical designs. Normally, they would be used because specific design information is lacking about the antenna to be used. On the other hand, the simple model will normally be quite satisfactory when parametric tradeoffs not related to the radiating system itself are being studied.

By making the proper use of input data the simple model can be used to represent an actual antenna having known characteristics. Thus, if we have measured the gain and beamwidth of a specific antenna, we may use Eq. 5.1 and Eq. 5.3 to calculate η and β_r (EFF and BMW) which may then be set as input quantities.

3.1.6 PEAK GAIN AND BEAMWIDTH CALCULATION - CURRENT DISTRIBUTION METHOD.

3.1.6.1 GENERAL EQUATIONS

The gain of the antenna will be calculated by the "current distribution" method. The reflector is assumed to be illuminated by a point source feed (one producing spherical phase fronts at the reflector). The feed produces a surface current distribution on the reflector, and to find the total radiation at any point in the far-zone of the reflector, we sum (integrate) the vector contributions of elements of surface current.

The current distribution method is a standard procedure in the antenna science. We shall omit the basic derivation which starts with the boundary conditions at the reflector surface, and instead will use the radiation integral given by Silver* as our starting point. In the following the notation $\bar{E}$ will be used to indicate that E is a vector.

The total field at a point (R, θ, ϕ) in the far-zone of the reflector is

$$\bar{E} = \frac{e^{-j\kappa R}}{R} \left[\frac{P_{rad}}{2\pi} \sqrt{\frac{\mu}{\epsilon}} \right]^{\frac{1}{2}} \left[\sqrt{G(\theta,\phi)}\ \bar{e}(\theta, \phi) - j \frac{\bar{I}_T}{\lambda} \right] \quad (6.1)$$

where $\kappa = 2\pi / \lambda$

λ = wavelength

P_{rad} = the total radiated power

μ and ϵ are the constitutive parameters of the medium

$G_f(\theta,\phi)$ = the (scalar) gain function of the feed.

$\bar{e}(\theta,\phi)$ is a unit vector everywhere defining the polarization of the feed pattern.

- - - -

*S. Silver (ed.), Microwave Antenna Theory and Design, McGraw-Hill Book Co., New York, 1949, p150.

The vector $\bar{I}_T$ is the component of the complex vector $\bar{I}$ which is perpendicular to the direction of propagation. That is,

$$\bar{I}_T = \bar{i}_\theta \left(\bar{i}_\theta \cdot \bar{I} \right) + \bar{i}_\phi \left(\bar{i}_\phi \cdot \bar{I} \right) \tag{6.2}$$

The vector $\bar{I}$ is given by

$$\bar{I} = \int_s \frac{G_f(\psi,\xi)}{\rho} \left[\bar{n} \times \left(\bar{i}_\rho \times \bar{e} \right) \right] \epsilon^{-jk(1 - \bar{i}_\rho \cdot \bar{i}_R)\rho} dS \tag{6.3}$$

The coordinate systems are shown in Fig. A-6.1. The feed is located at the origin. Points on the reflector are located by spherical coordinates (ρ, ψ, ξ) or by rectangular coordinates (x, y, z). The variables of integration can be chosen from either of these two systems. The far-field observation point is located by the spherical coordinates (R, θ, ϕ). The corresponding rectangular coordinates (X, Y, Z) are also shown to aid in visualizing the transformations that follow.

In Eq. 6.3 $\bar{i}_\rho$ is a unit vector in a direction toward a point on the reflector while $\bar{i}_R$ is a unit vector in a direction toward the far field observation point. The quantities G_f and $\bar{e}$ have already been defined. The vector $\bar{n}$ is a unit vector normal to the reflector surface.

In Eq. 6.1 the product $\sqrt{G_f}\,\bar{e}$ accounts for the back radiation of the feed in a direction toward the observation point. Normally in high gain antenna systems with well-designed, directive feeds, this contribution is negligible in comparison to the summed contributions of the reflector currents. Therefore, we shall neglect back radiation here.

Neglecting back radiation, we find that the gain function of the reflector system is

$$G(\theta, \phi) = \eta_r \frac{\bar{I}_T \cdot \bar{I}_T^*}{\chi^2} \tag{6.4}$$

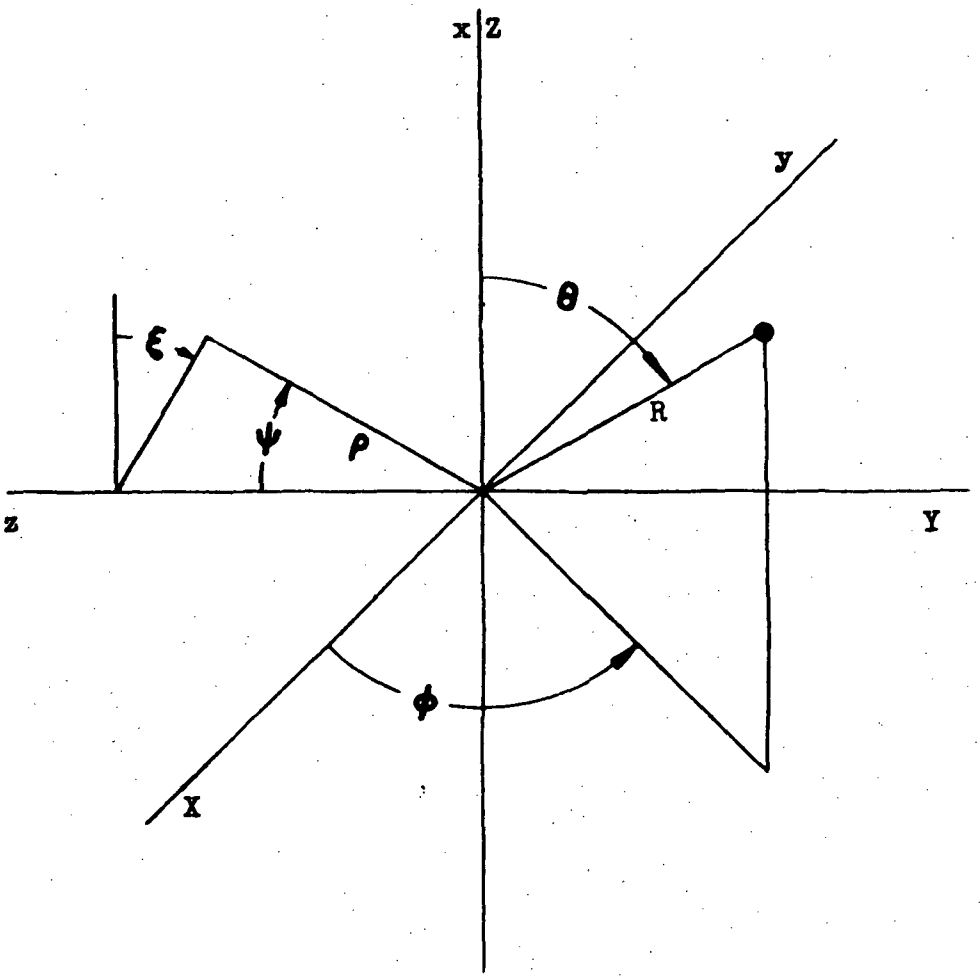

Figure A-6.1 COORDINATE SYSTEM

where η_r is the radiation efficiency of the antenna. That is

$$\eta_r = \frac{P_{rad}}{P_{in}} \tag{6.5}$$

where P_{in} is the total input power. The radiation efficiency accounts for only the dissipative losses in the antenna.

The problem then reduces to the evaluation of the complex vector integral $\bar{I}$.

3.1.6.2 CALCULATION OF THE VECTOR I

The vector $\bar{I}$ is evaluated by numerical methods on the computer. The general expression for $\bar{I}$ is given by Eq. 6.3. The integration is performed over S, the surface of the reflector. Either spherical or rectangular coordinates may be used as variables of integration; we shall use the latter here.

The quantity $\sqrt{G_f}$ in Eq. 6.3 is numerically proportional to the electric field strength of the feed as a function of direction. In this form there is an implication that only the main lobe of the feed radiation falls upon the reflector. The first factor in the integrand, $\sqrt{G_f}/\rho$, is the feed pattern adjusted for the relative space attenuation to various points on the reflector.

The bracketed expression in the integrand is the only vector part of the integral. This term accounts for the conditions of reflection at the reflector surface. The exponential term is the phase factor. For a perfect paraboloid the phase factor is reducible to $\exp(-2jkF)$, a constant.

The reflector influences the value of $\bar{I}$ through ρ, the distance from the feed phase center to a point on the surface, and through $\bar{n}$, the vector normal. We shall discuss feed and reflector surface options in following sections and confine our attention here to the remaining parts of the integrand.

The key element to be considered is the vector $\bar{V}$ defined by

$$\bar{V} = \bar{n} \times (\bar{i}_\rho \times \bar{e}) \tag{6.6}$$

If we resolve $\bar{V}$ into components parallel to the rectangular coordinate axes, the unit vectors $\bar{i}_x$, $\bar{i}_y$, and $\bar{i}_z$ are invariant in direction and magnitude as we move across the reflector. Thus we may remove the aforementioned vectors from under the integral sign and (when we take real and imaginary parts) reduce the complex vector integral $\bar{I}$ to a set of six real integrals. Of course, we may resolve $\bar{V}$ into rectangular coordinate components regardless of whether we choose spherical or rectangular coordinates as the variables of integration.

The vector $\bar{e}$ describes the polarization of the feed pattern as a function of direction. Since the reflector is in the far zone of the feed, the longitudinal component of $\bar{e}$ is zero. Even if this were not so, the longitudinal component of $\bar{e}$ would make no contribution to the integral since

$$\bar{i}_\rho \times \bar{i}_\rho \ (\bar{i}_\rho \cdot \bar{e}) \equiv 0 \tag{6.7}$$

Thus, without any loss of generality we may take the polarization vector to be

$$\bar{e} = \bar{i}_\theta \ B_\theta + \bar{i}_\phi \ B_\phi \tag{6.8}$$

with the constraint

$$|B_\theta|^2 + |B_\phi|^2 = 1 \tag{6.9}$$

We could have defined $\bar{e}$ in terms of its rectangular coordinate components. But then even the simplest polarization would require using all three rectangular components. We might be tempted to let $\bar{e} = \bar{1}_x$ (or $\bar{1}_y$) be a linear polarization, but this would mean that as the wave progresses toward the reflector, the electric field vector would remain parallel to the x (or y) axis and this is not typical of practical feeds. If we define $\bar{e}$ in terms of the spherical coordinate components of the (ρ , ψ , ξ) system, the longitudinal component may be discarded, but this definition has the effect of specifying radial and circumferential components of polarization on the reflector surface .

Defining $\bar{e}$ in terms of the far-field spherical coordinates (R , θ, Φ) accomplishes two things. First, the relationship between the feed polarization and the polarization of the resultant far-zone field of the reflector is obvious. Secondly, the θ and ϕ components of feed radiation are easy to visualize and are typical of practical antennas.

When $B_\theta = 1$, $B_\phi = 0$, we have a linear polarization similar to that of a dipole antenna. We shall refer to this as the "dipole" mode of polarization. On the other hand when $B_\phi = 1$, $B_\theta = 0$, the linear polarization is similar to that of a slot antenna. Since B_θ and B_ϕ can be complex and can each be functions of θ and ϕ, it is possible to construct any arbitrary polarization vector. For example, circular polarizations may be formed by setting $B_\theta = 1/\sqrt{2}$ and $B_\phi = \pm j/\sqrt{2}$

Although we originally set up $\bar{e}$ in terms of spherical coordinate components, we will eventually need to resolve $\bar{e}$ into rectangular coordinate components to perform the indicated vector operations. Also we need to find the θ and ϕ components of the far field radiation to compute $\bar{\bar{I}}_T$. Thus we shall need unit vectors $\bar{1}_R$, $\bar{1}_\theta$, and $\bar{1}_\phi$ expressed in both reflector and far field coordinates. Letting

$$A = \sqrt{y^2 + z^2} \tag{6.10}$$

we have

$$\bar{i}_R = \bar{i}_\rho = \bar{i}_x \frac{x}{\rho} + \bar{i}_y \frac{y}{\rho} + \bar{i}_z \frac{z}{\rho} \tag{6.11}$$

$$\bar{i}_\theta = -\bar{i}_x \frac{A}{\rho} + \bar{i}_y \frac{xy}{\rho A} + \bar{i}_z \frac{xz}{\rho A} \tag{6.12}$$

$$\bar{i}_\theta = -\bar{i}_y \frac{z}{A} + \bar{i}_z \frac{y}{A} \tag{6.13}$$

and

$$\bar{i}_R = \bar{i}_x \cos\theta - \bar{i}_y \sin\theta \cos\phi - \bar{i}_z \sin\theta \sin\phi \tag{6.14}$$

$$\bar{i}_\theta = -\bar{i}_x \sin\theta - \bar{i}_y \cos\theta \cos\phi - \bar{i}_z \cos\theta \sin\phi \tag{6.15}$$

$$\bar{i}_\phi = +\bar{i}_y \sin\phi - \bar{i}_z \cos\phi \tag{6.16}$$

Writing the vector $\bar{n}$ in the form

$$\bar{n} = \bar{i}_x n_x + \bar{i}_y n_y + \bar{i}_z n_z \tag{6.17}$$

we have

$$\bar{V} = \bar{i}_x \left[\frac{n_y}{A} \left(B_\theta y - B_\phi \frac{xz}{\rho} \right) + \frac{n_z}{A} \left(z B_\theta + xy \frac{B_\phi}{\rho} \right) \right]$$

$$+ \bar{i}_y \left[\frac{n_z}{} \left(\frac{A B_\phi}{\rho} \right) - \frac{n_x}{A} \left(y B_\theta - xz \frac{B_\phi}{\rho} \right) \right] \tag{6.18}$$

$$+ \bar{i}_z \left[\frac{-n_x}{A} \left(z B_\theta + \frac{xy B_\phi}{\rho} \right) - n_y \frac{(A B_\phi)}{\rho} \right]$$

The surface element ds is

$$dS = \frac{dx\, dy}{-n_z} \tag{6.19}$$

Since the product ∇ds contains components of $\bar{n}$ in both the numerator and denominator, it is immaterial whether the normal is directed toward or away from the origin.

For the phase factor we must evaluate the expression Γ where

$$\Gamma = \rho \left(1 - \bar{i}_\rho \cdot \bar{i}_R\right) \tag{6.20}$$

This turns out to be

$$\Gamma = \rho - x \cos\theta + y \sin\theta \cos\phi + Z \sin\theta \sin\phi \tag{6.21}$$

Thus

$$I = -\iint \frac{\sqrt{G_f}\ \bar{V}\ e^{-jk\Gamma}}{\rho\ n_z}\ dxdy \qquad (6.22)$$

where $\bar{V}$ is given by Eq. 6.18 and Γ by Eq. 6.21.

We shall now consider feed and reflector options available in the model.

3.1.6.3 FEED OPTIONS

The feed pattern is represented in Eq. 6.3 by the product $\sqrt{G_f(\psi,\xi)}\,\bar{e}(\psi,\xi)$ The factor $\sqrt{G_f}$ represents the amplitude pattern (on a field strength basis) and the vector $\bar{e}$ defines the polarization. The phase factor for the feed is unity. The feed radiation at the reflector surface is represented by $\sqrt{G_f}\ \bar{e}\ e^{-jk\rho}/\rho$ which corresponds to a far-field representation of the feed radiation. The analysis assumes that the reflector surface is everywhere in the far zone of the feed.

Various input parameters permit us to select from five different feed options. These range from a simple theoretical feed gain function to an exact description of the feed pattern which has been determined by measurement. The use of any of these options will be dictated by the amount of information that is available about the feed and by the purpose of making the particular computer run.

3.1.6.3.1 Uniform Illumination

Uniform aperture illumination represents an important special case. This gives the upper bound of gain for in-phase aperture illumination and is the basis for defining 100 per cent aperture efficiency. There are two ways to calculate the maximum gain for uniform illumination. One is by the simple formula

$$G_m = \left(\frac{\pi D}{\lambda}\right)^2 \qquad (6.23)$$

which is simply Eq. 5.1 with $\eta \pm 1$. This does not allow us to determine the losses due to aperture blockage or due to surface distortions. It assumes a perfect paraboloidal reflector of diameter D and an unblocked aperture.

The second method is to let

$$G_f(\psi, \xi) = C, \rho(\psi, \xi) \tag{6.24}$$

in Eq. 6.22, where C is a constant. When this equation is used, the current integration method may be used with any of the available reflector options. Also various aperture blockages may be used. Uniform illumination gives more weighting to the edge of the reflector and less to the reflector vertex than a tapered illumination does. Since blockage is assumed to occur at the center of the aperture, using uniform illumination will tend to de-emphasize the effects of blockage. Since reflector options tend to have maximum deviation from a perfect paraboloid at the reflector edge, using uniform illumination will tend to emphasize the effects of surface distortions.

Frankly, including the uniform illumination option in the current-distribution computation will be of limited value in the final program, but it is easy to include and may be of some value for diagnostic purposes. The use of uniform illumination with a perfect paraboloid and no blockage is an important reference case that can be used to check the computational accuracy of the computer program, for example. The result obtained can be compared with the value of G_m obtained from Eq. 6.23 and the accuracy thereby determined.

Thus the uniform illumination case will be included in the complex model. However, the gain function will not be that determined by Eq. 6.24 which would make the illumination uniform for the particular reflector model chosen. Instead the gain function will be that which provides uniform illumination for a perfect paraboloid with the feed at the focal point. For this case

$$G_f(\psi, \xi) = \cot^2 \frac{\psi_m}{2} \sec^4 \left(\frac{\psi}{2} \right) \tag{6.25}$$

or

$$G_f(\psi, \xi) = \frac{16 F^2}{D^2} \sec^4 \left(\frac{\psi}{2} \right) \tag{6.26}$$

The illumination function is then

$$\frac{\sqrt{G_f}}{\rho} = \frac{4F}{D\rho} \sec^2 \left(\frac{\psi}{2} \right) \tag{6.27}$$

which for a perfect paraboloid reduces to

$$\frac{\sqrt{G_f}}{\rho} = \frac{4}{D} \tag{6.28}$$

This option is called by setting CSN > 999 in the input subroutine.

3.1.6.3.2 Theoretical Feed Gain Functions

An analytical function may be used to represent the feed gain function. A typical function is given by

$$G_f(\psi, \xi) = 2(m+1)\cos^m\psi \qquad (6.29)$$

for $0 \leq \psi \leq 90^\circ$ and

$$G_f(\psi, \xi) = 0 \qquad (6.30)$$

for $90 < \psi \leq 180^\circ$.

Silver* uses this function in his treatment of reflector antenna properties. We have used this function extensively in deriving design curves for reflector systems. We have found that it gives good relative gain values when treating reflector antenna design problems parametrically. This would indicate that the pattern shapes are reasonable representations of typical feed patterns. Patterns for this gain function are shown in Fig. A-6.2.

The peak gain value obtained when using these functions is not correct. These functions produce gains which are higher than those obtained in practice. This is because a practical feed whose pattern shape matches the $\cos^m\psi$ curve will have a lower gain than $2(m+1)$ for two reasons. First the theoretical feed has no radiation in the rear hemisphere ($\psi > 90^\circ$) while a practical feed will have some backradiation, however small. Second, the theoretical feed has no forward hemisphere side lobe structure. The practical feed, however, may have sidelobes or distortions of the main lobe skirt which will lower efficiency even though the distortions or sidelobes do not fall upon the reflector.

When the value of m is chosen to optimize the feed pattern for a particular reflector (a particular F/D ratio), the peak gain corresponds to an aperture efficiency of 83% or thereabouts for values of m up to 8. Typical practical values range from 55% to 65%. To be conservative the model will be set to adjust the gain of

*Op. Cit., p425

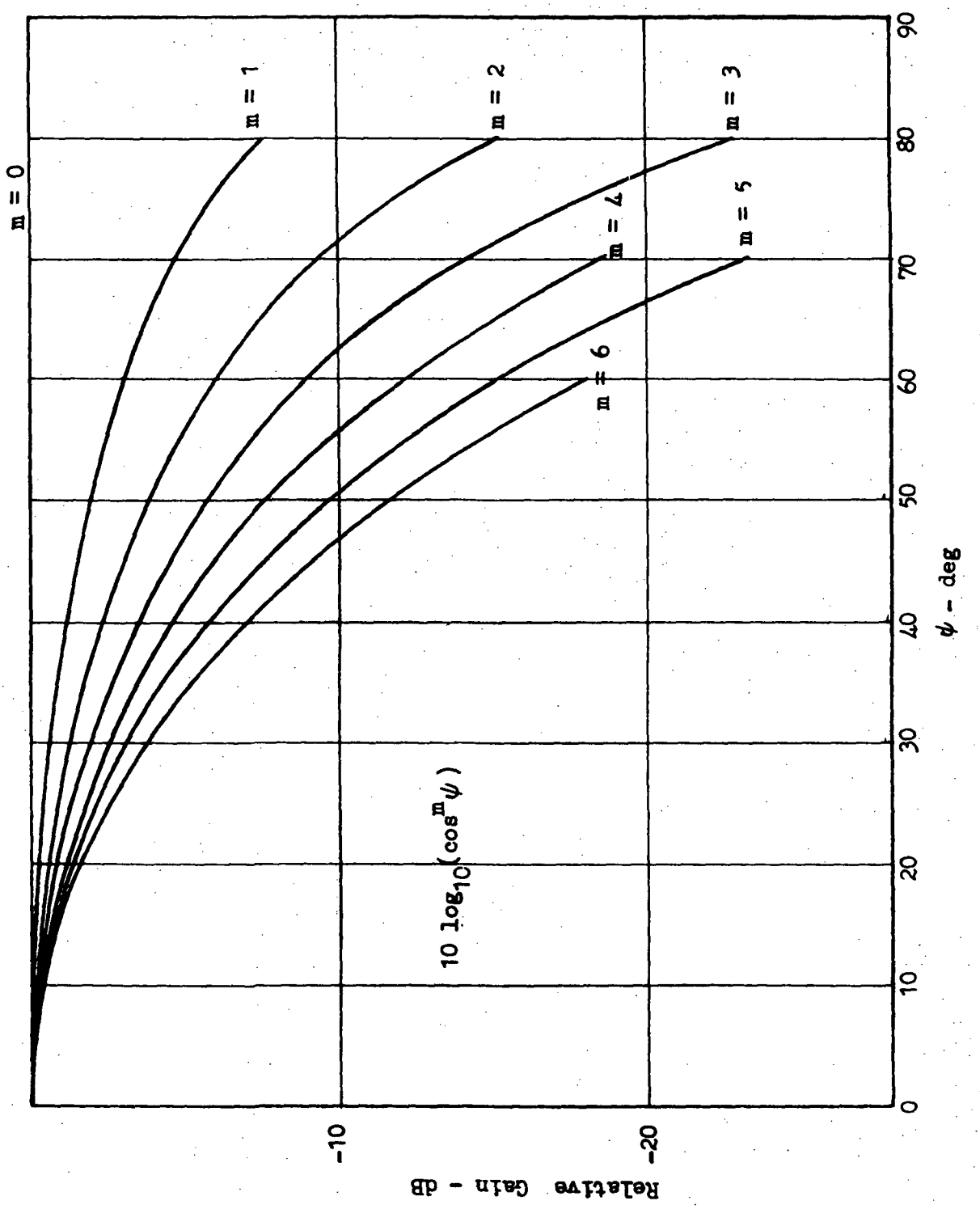

Figure A-6.2 PATTERNS OF THEORETICAL FEED GAIN FUNCTION

the feed function to the low end of the range. Since 55/83 is approximately 2/3, Eq. 6.29 can be modified to be

$$G_f(\psi, \xi) = \frac{4}{3}(m+1)\cos^m \psi \tag{6.31}$$

This option will be called by setting CSN in the range $0 \leqslant \text{CSN} \leqslant 999$ in the input subroutine, in which case m will be set equal to CSN. The quantity GFE must also be set $\leqslant 0$.

3.1.6.3.3 Modified Theoretical Gain Function

Another way of using the theoretical gain function and at the same time obtaining realistic gain values is to use the actual feed gain as determined by measurement. In this case

$$G_f(\psi, \xi) = G_F \cos^m \psi \tag{6.32}$$

for $0 \leq \psi \leq 90^o$ and

$$G_f(\psi, \xi) = 0 \tag{6.33}$$

for $90^o < \psi \leqslant 180^o$. The quantity G_F is the measured feed gain.

This option may be called by setting $0 \leqslant \text{CSN} \leqslant 999$ and setting $\text{GFE} > 0$. In the input subroutine GFE is the measured feed gain corresponding to G_F above.

3.1.6.3.4 Experimental Feed Patterns

We can improve the correlation between the predicted gain values which are computed by the program and experimental gain values that would be measured on the range by replacing the analytical function describing the feed gain function with the measured gain function of the feed. It is now relatively easy to determine the spherical coverage pattern of a feed in a form suitable for inclusion in the computer program.

A first order approximation might be to fit a suitable surface to the two principal plane patterns of the feed. Although this is generally better than an analytical function, it is not quite as good as using the complete pattern contour of the feed sampled at close intervals.

The experimental feed pattern data must be supplied to the computer in a format compatible with the program. The data file format to be described here is directly obtainable by measuring the feed pattern with Scientific Atlanta Radiation Distribution Equipment. If the feed pattern is measured another way, it will have to be converted to the standard format before it can be used with the computer program and no provisions for this conversion are included in the model.

The coordinate system used in measuring the feed patterns is shown in Fig. A-6.3. The feed axis is aligned with the $\psi = 0$ axis. The resulting coordinates (ψ ξ) are the same coordinates defined in Fig. A-6.1. We have developed equations for other orientations of the feed axis, but so far we have never found occasion to use them. The difficulty in using the orientation shown in Fig. A-6.3 is that the polarization rotates during the measurement of the pattern. Therefore, when the feed is nominally linearly polarized, the patterns are measured with a circularly-polarized transmitting antenna and a constant 3 dB polarization loss is assumed. When the feed is nominally circularly-polarized, the appropriate circular polarization is used for the transmitting antenna. Then when the data file is used in the computer program, either dipole or slot polarization is used for the linear case or the appropriate circular polarization is used for the circularly-polarized case.

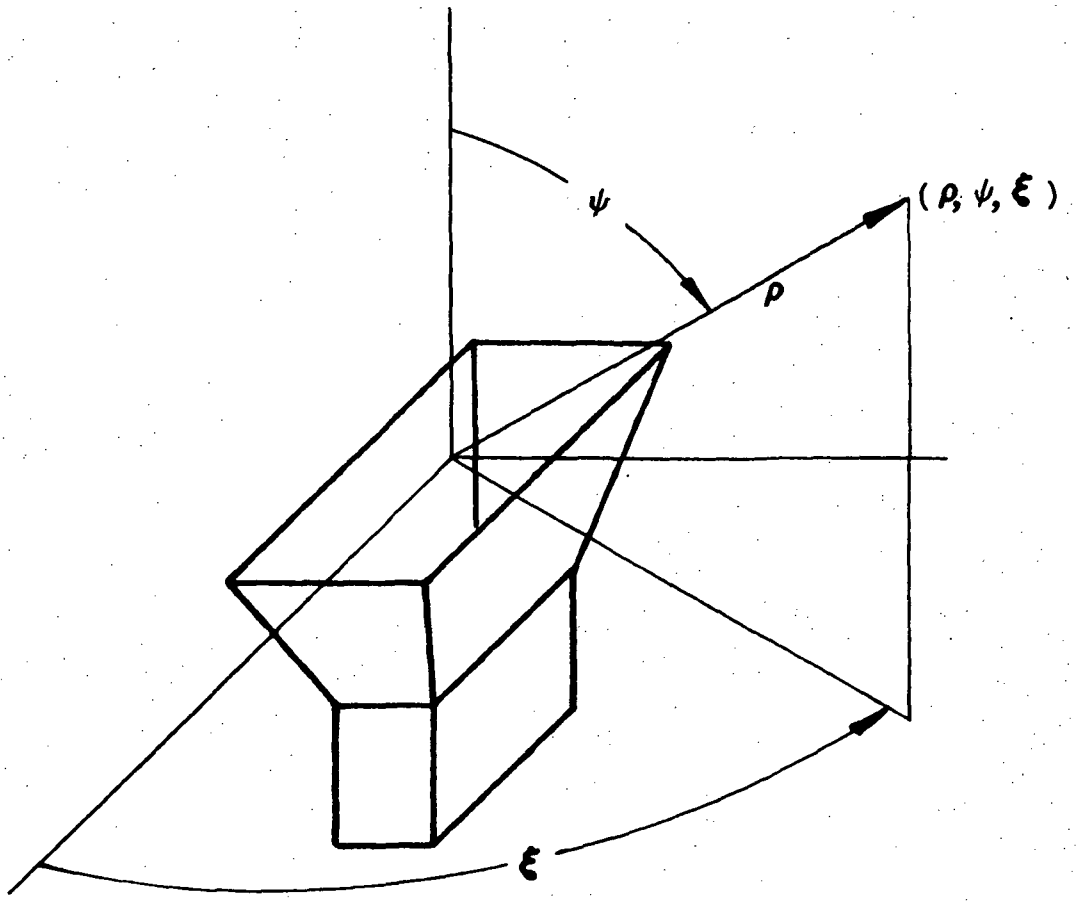

Figure A-6.3 FEED PATTERN COORDINATES

This procedure is admittedly an approximation with regard to the variation of polarization throughout the feed pattern. Equations have been developed for making a series of feed pattern measurements with different polarizations so that the vector $\underline{e}$ may be determined point by point throughout the pattern. This requires an added cost of measurement and an increased amount of computer time for each run and thus far such a complication has not been found necessary.

With the set-up shown in Fig. A-6.3 the Scientific Atlanta equipment samples the feed pattern every 2 degrees in ψ and in ξ . Starting at $\psi = 0$ and concluding at $\psi = 90^{\circ}$, the model tower is positioned in 2 degree increments. At each ψ position a complete conical pattern is obtained by rotating in ξ and sampling every 2 degrees. The data file therefore consists of 91 ψ scans each consisting of a start-of scan marker and 180 data points corresponding to the sampling in ξ . At the end of the 91st scan, a start-of-scan marker followed by an end-of-file marker occurs. The complete data file, therefore, consists of 16473 data points including markers.

The data file as measured represents only the relative gain pattern of the feed. Each value in the data file must be corrected so that it represents the actual gain of the feed in that particular direction. To do this, it is necessary to make a separate experimental measurement of the peak gain of the feed.

Having the complete feed pattern on a data file allows us to integrate the feed pattern to determine the feed directivity. This may then be compared with the measured gain value of the feed to determine the feed radiation efficiency. Also, it is possible to integrate the portion of the feed radiation intercepted by the reflector which may then be compared with the total radiation to determine the spillover efficiency.

The data points representing feed radiation are quantized to the nearest quarter dB and are limited to within the range of approximately 0 to 40 dB. The quantization gives an error of at worst ± 0.125 dB for any particular value of the feed pattern, but on the average the error is much less.

Also, the feed pattern is sampled at 2 degree intervals in both angular coordinates and this does not agree with the sampling pattern used in the

integration process. Therefore, feed pattern values at the integration sampling points must be found by interpolation. Since the feed is generally a smooth, slowly varying function over the angle subtended by the reflector, the interpolation error is not significant.

The accuracy of feed representation will be discussed further in a later section.

The experimental feed pattern option may be called in the program by setting CSN < 0 and by setting GFE ≥ 0 in the input subroutine.

3.1.6.3.5 Reference Experimental Feed Pattern

This option is the same as the experimental feed pattern option, except that an experimental feed pattern data file which is considered to be typical of practical horn feeds will be built into the program.

This option may be called by setting CSN < 0 and GFE < 0 in the input subroutine.

3.1.6.4 REFLECTOR OPTIONS

The reflector is represented in Eq. 6.3 by the scalar function and by the vector $\overline{n}$. The function $\rho = f(\psi, \xi)$ describes the variation of the distance from the origin (feed) to a particular point on the reflector surface as a function of the variables of integration. If the surface is defined in the form

$z = g(x,y)$ then

$$\rho = \sqrt{x^2 + y^2 + (g(x, y))^2} \qquad (6.34)$$

The vector $\overline{n}$ represents the variation of a unit vector normal to the reflector surface as a function of position on the reflector. The vector $\overline{n}$ can

be obtained by taking the gradient of any scalar equation equal to a constant which represents the reflector surface. Thus if

$$H = \rho - f(\psi, \xi) = 0 \tag{6.35}$$

or if

$$H = z - g(x, y) = 0 \tag{6.36}$$

(depending on how the surface is defined)

then

$$\bar{n} = \frac{\nabla H}{|\nabla H|} \tag{6.37}$$

Included in the radiating system model are two analytical representations of special reflector surfaces. One is the paraboloid and the other is the flex-rib reflector. (The latter is applicable not only to the flex-rib unfurlable reflector but also to various "umbrella" type reflectors).

For any particular kind of antenna it is possible to develop a distortion theory embodied in an equation $\rho = f(\psi, \xi)$ or $z = g(x,y)$ to represent the actual distorted surface in the presence of orbital thermal and/or dynamic effects. Then ρ (or z) and the vector $\bar{n}$ derived therefrom may be used directly in Eq. 6.3 to calculate gain as it is degraded by the orbital environment. This has been done for the flex-rib type of construction on the ATS F and G reflector project, for example.

The difficulty is that the form of the ρ or z equation depends explicitly on the distortion theory formulated for each particular type of reflector. The only type of general treatment possible is to expand the reflector surface in a general power series or similar expansion, but this becomes cumbersome when one attempts to relate it to a specific design for which a distortion theory has

been or can be developed.

Since the treatment of thermal effects has been limited in this study, we shall include only the perfect paraboloid and the perfect flex-rib surfaces. The effects of a thermally-distorted surface will be handled as we shall describe in a later section. The reader can be assured that if a particular reflector design is chosen and ρ or z equations can be derived representing the surface in the presence of the orbital environment, the basic model can be modified to include the effects of these distortions. It would also be necessary to modify the input subroutine to handle new input data.

3.1.6.4.1 The Perfect Paraboloid

The equation for a perfect paraboloid of focal length F with vertex located at (x, y, z) coordinates of (0, 0, z_D) is

$$z = z_D - \frac{x^2 + y^2}{4F} \tag{6.38}$$

Thus ρ is given by

$$\rho = \sqrt{x^2 + y^2 + \left(z_D - \frac{x^2 + y^2}{4F}\right)^2} \tag{6.39}$$

Since z_D is a constant

$$\nabla H = \nabla z_D = \nabla \left(z + \frac{x^2 + y^2}{4F}\right) \tag{6.40}$$

and

$$\nabla H = \bar{i}_x \frac{x}{2F} + \bar{i}_y \frac{y}{2F} + \bar{i}_z \tag{6.41}$$

and $\bar{n}$ can be found from Eq. 6.37 with

$$\left|\nabla H\right| = \frac{1}{2F}\sqrt{x^2 + y^2 + 4F^2} \tag{6.42}$$

This option can be called by setting PAN < 0 in the input routine.

3.1.6.4.2 The Perfect Flex-Rib Reflector

The Flex-Rib reflector may be called a sectoral approximation to a desired paraboloidal surface. The frontal view of this type of reflector is shown in Fig. A-6.4. In each wedge-shaped sector the surface is approximated by a parabolic cylinder.

The equation for a parabolic cylinder represented by the sector designated by $s = 0$ in Fig. A-6.4 is simply the equation of the x-z plane intercept, since the elements of this particular parabolic cylinder are parallel to the y axis. Thus for $s = 0$

$$z = z_D - \frac{x^2}{4F_C} \tag{6.43}$$

where F_C is the focal distance of the parabolic cylinder.

If we rotate this panel through an angle $\xi = \xi_s$, we have the equation

$$z = z_D - \frac{(x\cos\xi_s + y\sin\xi_s)^2}{4F_C} \tag{6.44}$$

In particular if we have N panels then Eq. 6.44 becomes

$$z = z_D - \frac{(x\cos\frac{2\pi s}{N} + y\sin\frac{2\pi s}{N})^2}{4F_C} \tag{6.45}$$

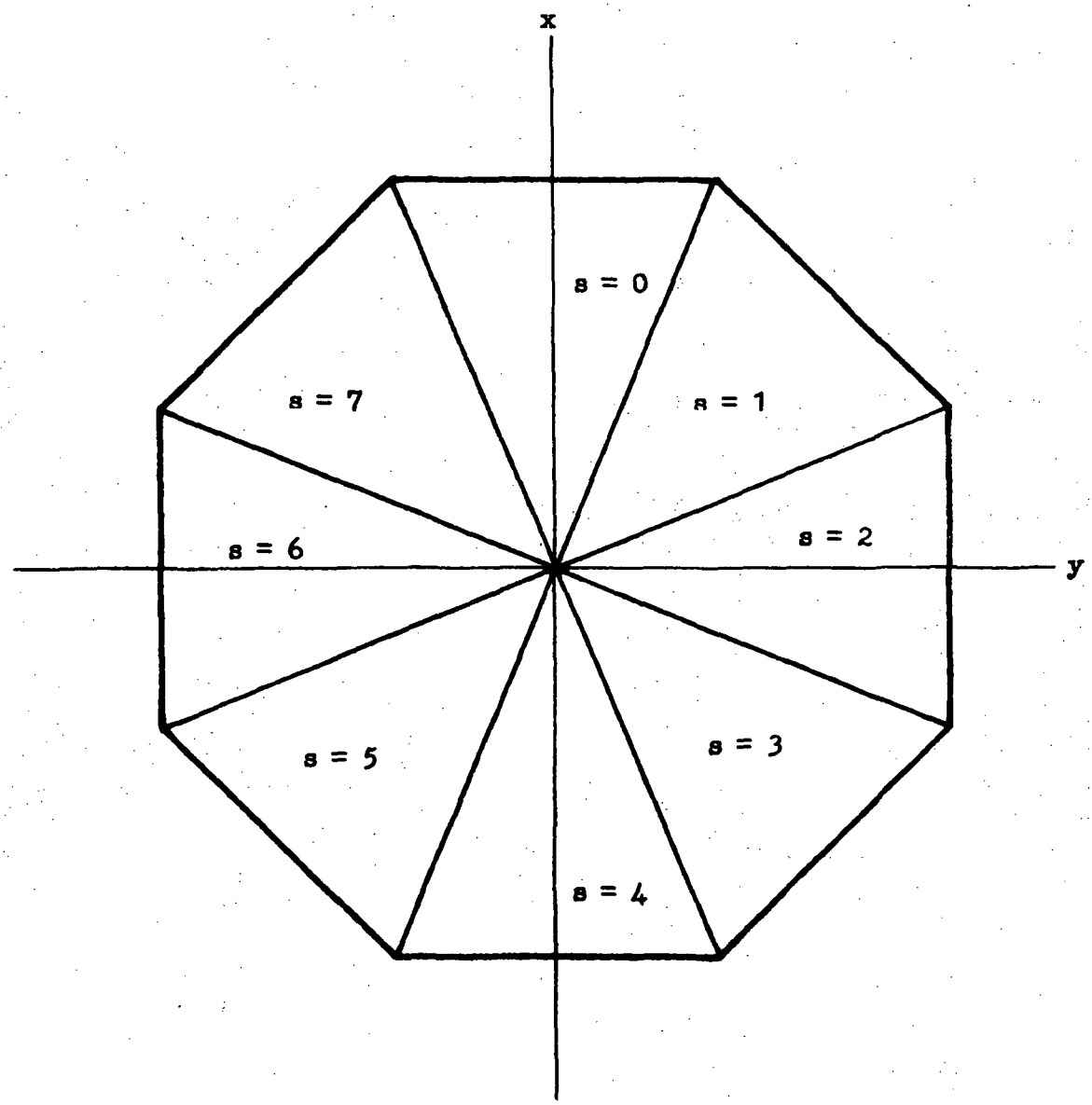

Figure A-6.4 FRONTAL VIEW FLEX RIB REFLECTOR

and the s -th panel extends over the range

$$(2s-1)\ \frac{\pi}{N} \leq \xi \leq (2s+1)\ \frac{\pi}{N}$$

We may define a parameter W as

$$W = x \cos \frac{2\pi s}{N} + y \sin \frac{2\pi s}{N} \tag{6.46}$$

This has special significance since it is the distance of a particular point on the reflector from the center of the aperture as measured, not radially, but along the centerline of its own particular panel. In terms of this parameter

$$\rho = \sqrt{x^2 + y^2 + (z_D - \frac{W^2}{4F_C})^2} \tag{6.47}$$

As in the previous section we may take z_D as the constant defining the surface. Thus

$$\nabla H = \nabla(z + \frac{W^2}{4F_C}) \tag{6.48}$$

and

$$\nabla H = \bar{i}_x \frac{W}{2F_C} \cos \frac{2\pi s}{N} + \bar{i}_y \frac{W}{2F_C} \sin \frac{2\pi s}{N} + \bar{i}_z \tag{6.49}$$

Then $\bar{n}$ can be found from Eq. 6.37 with

$$|\nabla H| = \frac{1}{2F_C} \sqrt{W^2 + 4F_C^2} \tag{6.50}$$

The quantity F_C is the focal distance of the parabolic cylinder. We must determine the relationship of F_C to F, the focal length of the "equivalent" paraboloid. To do this consider the intersection of a radial plane (ξ = a constant) with the reflector surface. Separating out the dependence on ξ in Eq. 6.45, we have

$$z = z_D - \frac{r^2}{4F_C} \cos^2 \left(\xi - \frac{2\pi s}{N}\right) \tag{6.51}$$

where $r = \rho \sin \psi$ is the offset of a point from the z-axis. Comparing Eq. 6.51 with Eq. 6.43, we conclude that the intersection of a radial plane containing the z axis and the reflector surface is a parabolic arc of focal length

$$F_i(\xi) = \frac{F_C}{\cos^2 \left(\xi - \frac{2\pi s}{N}\right)} \tag{6.52}$$

The focal length F_R of the reflector rib (which is the boundary between two adjacent panels) is obtained by setting $\xi = (2s \pm 1)\,\pi/N$. Thus

$$F_R = F_O / \cos^2\left(\frac{\pi}{N}\right) \tag{6.53}$$

We may conclude that the paraboloid which is a best fit to this surface must intersect the surface twice in each panel and will therefore have a focal length F such that $F_R > F > F_C$. As the number of panels increases without bound, the Flex-Rib surface more closely approaches a paraboloid. Since $F_R \to F_C$ as $N \to \infty$, then in the limit $F_R = F = F_C$.

A mean value of the function $F_i(\xi)$ can be found by integrating F_i over the aperture. There is, of course, no radial variation of F_i. This mean value is

$$F = F_C \left(1 + \frac{1}{3} \tan^2 \frac{\pi}{N}\right) \tag{6.54}$$

or

$$F = F_R \left(1 - \frac{2}{3} \sin^2 \frac{\pi}{N} \right) \tag{6.55}$$

We have chosen to let F, the focal length of the "equivalent" paraboloid, be this mean value of the function F_1 .

When z_D is set equal to F as defined above, the peak gain varies as a function of D/λ as shown in Fig. A-6.5. When the reflector is a good approximation to a perfect paraboloid, setting z_D to any value other than F does not improve the gain by a significant amount (something of the order of 10^{-3} dB). However, when the gain curve departs significantly from the perfect paraboloid gain curve, some of the lost gain can be recovered by moving the feed. This, however, is not a normal design region for this type of reflector since, even with refocussing, the gain degradation is severe. Thus, we can set $z_D = F$ and conclude that F is the focal length of the equivalent paraboloid for all normal reflector designs.

The perfect Flex-Rib reflector case can be called by setting $N > 0$. The variable N is represented by PAN in the input routine. For this case ρ is found from Eq. 6.47 and the vector π is found from Eq. 6.49 (normalized by Eq. 6.50). The focal lengths are related by Eq. 6.53 through Eq. 6.55.

3.1.6.5 ASSUMPTIONS AND ACCURACY

In this section we shall discuss the basic assumptions associated with using the current distribution method to calculate gain. We shall also mention some of the checks that have been made to determine the accuracy involved.

There are three basic theoretical assumptions involved in the original formulation of the general equations. First of all, the method is applicable to determining the far field radiation of the reflector antenna only. Secondly, the reflector is assumed to be in the far field of the feed. Third, direct radiation of the feed to the point of observation in the far zone is neglected.

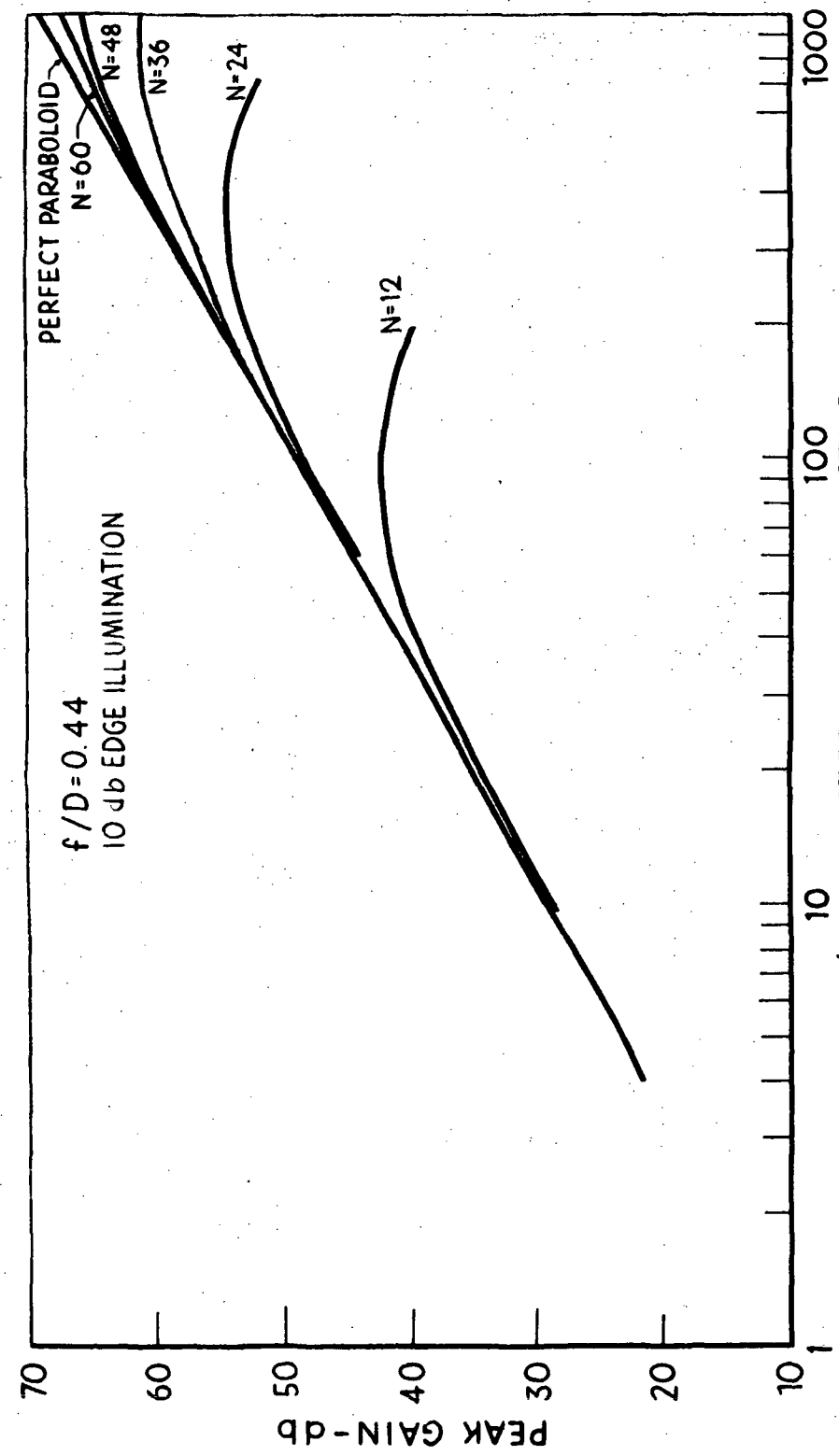

Figure A-6.5 PEAK GAIN OF FLEX RIB REFLECTOR

The usual criterion for determining the far-zone of a directive antenna is that the distance R from the antenna exceeds $2D^2/\lambda$. This will nearly always be true for orbital antennas. For example, at 100 nm altitude or at 100 nm distance between two space vehicles, it would require an antenna larger than 173 feet in diameter to fail to satisfy this criterion at X-band (10 GHz), clearly beyond the state of the art for the immediate future. The only conditions under which we might fail to satisfy the far-zone criterion are during the testing of orbital antennas on the ground on some ranges; during very close approaches of two space vehicles, as in rendezvouspr in some extremely large aperture systems intended for the transmission of power by microwave radiation. None of these situations are intended to be covered by the simulation of the antenna in this study.

When the distance from the antenna is exactly $2D^2/\lambda$, the gain loss is typically of the order of 0.05 dB. Since normally the distance will be much in excess of this minimum distance, the gain error will be reduced to an insignificant value.

The assumption that the reflector is everywhere in the far zone of the feed is not as easy to justify but normally it would be true. To illustrate, a typical horn type feed for a paraboloidal reflector would have an effective aperture of the order of 1 wavelength so as to illuminate the aperture properly. With F/D ratios of the order of 0.5, this would mean that reflectors smaller than about 2 wavelengths would fail to meet the criterion. A 2λ reflector fed by a 1λ feed would suffer severe blocking and provide only a few dB gain. In fact, it probably would be better to turn the feed around and eliminate the reflector, perhaps adding aperture to the feed horn. Thus, for normal feeds we will probably not run into a situation where the reflector is not in the far zone of the feed.

The assumption that the reflector is in the far zone of the feed is made so we can apply geometrical optics when determining the amplitude of the feed radiation at the point where it strikes the reflector. Because of this assumption, there is no phase factor relating to the feed radiation in the basic formulation. The feed is assumed to be a point source with spherical phase fronts. There may be some cases where the feed radiation does not have equal phase across the angle subtended by the reflector and when this happens, the feed cannot be considered to have a single point phase center -- thus the criterion would not be satisfied.

Normally the criterion that the reflector be in the far zone of the feed will be satisfied to a degree sufficient for all practical purposes. The user should be on the lookout for any unusual feed designs which might have a significant phase error throughout the angle subtended by the reflector. Should this occur, he may correct the results for the appropriate amount of gain degradation attributable to such phase error or he may elect to use the simple model.

The third assumption is that the back radiation of the feed can be neglected. If this is not so, the correction can be made as indicated in Eq. 6.1. Normally, well designed feeds will have a front-to-back ratio of at least 15 or 20 dB and very often considerably more. For typical feeds, the back radiation would normally be some 10 or more dB below isotropic and this would be insignificant in comparison with the peak gain of the reflector which normally would be 20 to 60 dB above isotropic. The back radiation usually would be further reduced in the normal design by obstructions behind the feed, such as feed support brackets, electronic boxes, or perhaps the space vehicle itself.

Of more importance are the practical approximations which have been made in constructing the model from the basic formulation. For some of these approximations we have not been able to obtain an estimate of the error directly attributable thereto, but we know what the overall accuracy seems to be.

We have made a basic assumption with regard to polarization. If the feed is linearly polarized, we have assumed that it is either a dipole or slot mode, as previously discussed. If the feed is circularly polarized, we assumed that the polarization is a quadrature combination of dipole and slot modes. No provision has been made for elliptically polarized feeds, since we normally try to achieve either linear or circular polarization.

The choice of the polarization modes is only important when we are using the experimental feed patterns. We have made calculations using the theoretical feed gain functions, including uniform illumination, and have found no significant difference in the results for each of the four basic polarizations.

When we are using experimental feed patterns, our assumptions regarding the polarization modes become of more importance. The difficulty is not whether the choice of dipole and slot modes is a correct one. We measure the gain function

of a linear antenna with a circularly polarized transmitting polarization and then during the integration process, we assume that the polarization is in one of the two standard linear modes. If instead the linear polarization has some other form, such as always parallel to the x-axis, we would still expect to get the same result, based on our experience with theoretical feed patterns referred to in the preceding paragraph. Similarly, if the feed polarization is circular throughout the pattern, it is immaterial what two linear polarizations are used to define circular polarization.

If the feed has elliptical polarization, we shall be disregarding a component of its radiation either when we measure the feed pattern or when we use it in the program, or both. The error that occurs is dependent on relative amplitudes of the nominal polarization component and the omitted component. Since the reflector would have integrated the discarded component just as it does the retained component and would have then added the two in complex vector fashion, we can estimate bounds on the error from the relative amplitudes of the two components.

Similarly, the four standard polarizations do not provide for the fact that some feed patterns have polarization characteristics which vary throughout the angle subtended by the reflector. This is most noticeable in frequency-independent type feeds over some portions of their operating bands. This variation tends to occur near the edge of the reflector, usually where the illumination taper tends to de-emphasize its effect. Furthermore, in a well-designed feed this variation is usually held within reasonable bounds.

Frankly, it is difficult to determine what part of the error is attributable to the departure of the actual feed polarization from the assumed state. An investigation of this effect on accuracy would be a separate study all in itself. We know that if it were a serious problem we could measure both amplitude and polarization (and even phase) of the feed pattern and put these corrections into the program. The result would be at least a four-fold increase in the test time required to measure feed characteristics, a significant increase in program storage requirements on the computer, and a significant increase in compute time for every case. The overall accuracy of the computation without this refinement is satisfactory for engineering purposes (as we shall see) so adding this complication does not seem justified.

The theoretical gain function option was primarily intended to be used as a means of evaluating parametric trade-offs. The relative accuracy for evaluating reflector designs is quite good and has been confirmed by experiment. In this test the gains of a high-precision 4 foot paraboloid and a 12 panel, 4 foot Flex-Rib reflector were compared at 4, 8, and 12 GHz. A direct substitution method was employed so that the same aperture illumination, focal distance, and frequency were used for both cases. The primary feed patterns were measured and fitted to the analytical feed functions. Then the relative gain values predicted by theory and experiment were compared. Agreement was within about 0.05 to 0.1 dB, even though the feed patterns were not exact fits to the analytical functions. This test confirmed the relative accuracy of the current integration method of gain calculation.

As mentioned before, use of the analytic function without modifying the peak gain value gives peak gain values that are unrealistic. The modification given in Eq. 6.31 should be more representative of typical antennas and should be within $\pm$ 1 dB for typical cases, though it may be in error by more than that amount for any particular case. When the analytic function is modified by using the actual peak gain of the feed, the error is estimated to be within $\pm$ 1 for the particular case considered. In these estimates, we have not included any allowance for transmission lines losses and have referenced the antenna gain to the feed terminals. The estimates in this paragraph relate to absolute accuracy -- that is, the accuracy of predicting the true gain of the antenna.

The basic radiation integral is approximated by numerical integration methods in the model. The sampling interval must be fine enough to sample accurately the illumination taper across the aperture, the reflector contour, and the electromagnetic wavelength. Electromagnetic theory would tell us that there should be one sampling point per half-wavelength across the reflector, but if this is used as a criterion, the reflector surface may not be adequately sampled when the reflector is small in terms of wavelengths. Thus a wavelength criterion is used, but a certain minimum number of points must be taken for the double summation to represent the integral.

For large reflectors, fewer points can be taken if the surface is smooth. The paraboloid, for example, requires fewer points than a many-panelled Flex-Rib because the paraboloid is a smooth surface of revolution. In many cases when doing parametric studies we have found good relative accuracy with sampling rates as low as one point for every five wavelengths, but, of course, the absolute accuracy deteriorates somewhat.

The criterion we normally use is that one point should be taken per wavelength, except that in no case should fewer than about 600 points be taken. The accuracy for one point per wavelength sampling is almost as good as that obtained for one point per half-wavelength sampling, but the integration time is only one quarter as long. For exploratory parametric studies, fewer sampling points can be taken to reduce compute time while searching for the optimum values. The proper minimum sampling rate for a given problem can be determined by increasing the sampling rate and noting where the gain value begins to stabilize. There will be some oscillation of the gain value about the true gain value as the sampling rate is increased further due to basic inaccuracies in the calculation (computer arithmetic accuracy).

To check the computational accuracy, we have used the uniform illumination feed option and the perfect paraboloid reflector option and compared the resultant gain value with that obtained by using Eq. 6.23. For one point per wavelength sampling the agreement is about 0.07 dB. This is considered to be the computational accuracy of the program. (The machine used for this test is the SDS 940 time-sharing computer . The case considered was the ATS F and G reflector at 8.25 GHz).

When using the experimental feed option, two additional errors occur. First the feed gain values are quantized to the nearest quarter-dB. Second, since the sampling of the feed pattern in the data file is not coincident with the sampling of the aperture in the integration process, feed pattern data must be interpolated at the integration sampling points. Studies of the best method of interpolation showed that linear interpolation was adequate since the feed pattern generally is quite smooth for typical designs. Moreover, taking higher order differences eventually and/or occasionally results in poorer accuracy due to the quantization of the feed pattern data. The reason for this can be seen by comparing the following

difference tables for unquantized and quantized data.

Actual Values						Quantized					
4.5						4.5					
4.6	.1					4.5	.0				
4.7	.1	.0				4.75	.25	.25			
4.8	.1	.0	.0			4.75	.0	-.25	-.50		
4.9	.1	.0	.0	.0		5.0	.25	.25	.50	1.00	
5.0	.1	.0	.0	.0	.0	5.0	.0	-.25	-.50	-1.00	-2.

Due to the rounding off, higher order differences eventually will increase causing poorer accuracy of interpolation. If we used only first and second order differences we would occasionally get poorer accuracy (near where the values change).

To check the overall computational accuracy of the program, we constructed an artificial "experimental feed" data file simulating the feed gain function that provides uniform illumination of the aperture (Eq. 6.25). The feed data file was quantized to the nearest quarter-dB, as an experimental data file would be. In the integration process linear interpolation was used. At 8.25 GHz the gain program calculated a gain of 57.873 dB for a 30-foot reflector using this data file with sampling at one point per wavelength. The gain equation for uniform illumination (Eq. 6.23) gave a gain of 57.958 dB. The difference, 0.085 dB, represents the overall computational accuracy, including machine accuracy, the representation of the double integral by the double summation, linear interpolation of the feed data, and the effects of quantizing the feed data. In this check a 500 panel Flex-Rib reflector was used to simulate a paraboloid, so the minor effect of that approximation is also included. Thus the computational accuracy using the experimental feed option is almost the same as that obtained using the theoretical feed options.

Aperture blockage by the feed assembly or other structures is accounted for by not integrating the surface currents over the projection of the blockage on the surface of the reflector. That is, the limits of integration are adjusted so as to omit portions of the reflector radiation not contributing to the on-axis gain. This approach is accurate on axis and near the refelector axis. For observation

points at wide angles to the reflector axis, it is necessary to account for the fact that the blockage would not obscure the vertex area of the reflector but some other displaced part. However, since the model is normally used to predict gain values near the axis of high gain systems, the refinement applicable to wide angles has not been included.

Blockage is considered to be a circular blockage centered about the reflector axis. If the blockage is not circular, the best procedure is to equate the area represented by the blockage to a circular blockage area for use in the program. The blockage may not be centrally located, but normally it would be near the center of the aperture. If the blockage is off center, then the model tends to give conservative results.

The apparent gain of the reflector antenna will be modified by the impedance mismatch of the feed when mounted in the reflector. This mismatch may be thought of as having two components, one the inherent mismatch of the feed in free space and the other the reaction of the reflector on the feed. The theoretical gain of the reflector/feed can be corrected if the mismatch of the feed in the reflector is known. Often this is not available. Therefore, the model calculates the magnitude and phase of the interaction of the feed and the reflector. This can be used as a bound or tolerance on the gain values obtained from the model. Normally, in a well designed system this will not be a problem, since the feed should be reasonably well matched in free space and since the normal aperture distributions for maximum gain do not provide a high degree of reflector feed interaction.

We shall cite an example to illustrate the reaction effect and indicate, at the same time, something of the overall absolute accuracy of the model. LMSC experienced a perturbation in a gain versus frequency curve of about 1.5 dB for two measurements 50 MHz apart at L-Band. Careful tests indicated this perturbation was not due to measurement error. The model was used to predict the gain at the two frequencies in question from experimentally determined feed patterns. The computed values were within 0.1 dB of the curve obtained by extrapolating smooth portions of the gain curve with no correction for mismatch. This represented an agreement of about 0.7 dB between theoretical and experimental values. When the reflection coefficient was calculated, it was found to be of the order of -11 dB with

a large phase change over the 50 MHz frequency interval. This reaction in combination with a measured free space mismatch of the feed of about 2:1 was sufficient to account for the observed gain perturbation. These were range instrumentation antennas with -22 dB edge illumination for low sidelobes. The low edge illumination resulted in relatively high concentration of energy near the center of the reflector causing more interaction with the feed than would normally be encountered in a typical general purpose antenna. The typical case where the illumination tapers to -10 or -11 dB to maximize gain results in a reflection coefficient attributable to the reflector of the order of -18 to -20 dB.

One effect which is not taken into account is the interaction of the feed support struts with the feed. This is the effect the structure has in modifying the amplitude or phase of the feed pattern (as distinguished from the blockage of the aperture caused by the feed and other support structures). Normally, the antenna designer will design the structure for minimum effect on the feed patterns, but structural considerations nearly always limit the designers ability to achieve his desires. This is probably the major factor limiting the accuracy of the model. With well-designed and simple support structures we may neglect this consideration. But the user should be on guard when complicated support structures are used (as when large masses are supported with the feed). Where this effect is not negligible, the feed pattern can be measured in the presence of the support structure to obtain a better feed model.

We have previously cited tests of the relative accuracy of the model (the tests with the 4-foot reflectors) and of the absolute accuracy of the model (tests on the range instrumentation antennas). We have also checked the absolute accuracy of the model using a feed designed for the ATS F and G verification tests and a four-foot reflector. The agreement between the gain value predicted by the model and that obtained by measurement was about 0.16 dB. The conditions of test were such that we could expect very good experimental accuracy, so this test seems to confirm the accuracy of the model.

3.1.7 CORRECTION FOR THERMAL EFFECTS

The scope of the effort in considering influence factors was limited in this study to be compatible with available funding. As a consequence, the effects of thermal distortions on the gain of the antenna along a particular LOS will be handled as a correction based on extrapolation of LMSC's experience with the ATS F and G reflector and with other systems.

The effect of a distorted reflector can be accurately handled by including in the current distribution integration model an option for a distorted reflector. The overall program sequence can be modified to calculate the actual gain of the reflector along the line of sight, rather than calculating peak gain and using the Gaussian approximation as described in Section A-3. All that is necessary to accomplish this is an analytical function which describes the distorted surface and which can be differentiated to determine the normal surface vector.

The problem of including the precise calculation of distorted surface effects is the complete lack of generality in any formulation that can be made. The description of the perfect paraboloid may apply to many types of reflector construction, such as honeycomb sandwiches or spun dishes. Similarly, the description of the perfect Flex-Rib surface also applies to the umbrella type of deployable reflector. But to include distortion effects requires developing a distortion theory for each possible method of realizing each type of surface. For example, the distortion equation of a Flex-Rib reflector would be different from that of an umbrella reflector which might have rigid ribs that fold up against the reflector axis. Similarly, there is a large amount of work involved in establishing the design parameters that optimize each type of reflector for the chosen orbit. Thus in a limited scope effort, only a correction-type treatment of thermal effects is possible.

The ATS F and G reflector designed for 8.25 GHz operation (30 foot diameter aperture) will be the primary initial basis for making a thermal correction. Beamshift and gain degradation data for this case will be extrapolated to other sizes and frequencies as required.

The peak gain and the on-axis gain of the ATS reflector at 8.25 GHz is shown as a function of orbit hour in Fig. A4-7.1. The beamshift is shown in Fig. A-7.2. Both these curves are for the configuration utilizing Chromel-R mesh. The orbit hour is directly relatable to sun angle in the xz plane of the reflector. (In far-zone coordinates this would be the ZY plane or the $\phi = \pm \pi$ plane. See Fig. A-6.1). In the simple or the complicated gain calculation, the peak gain is

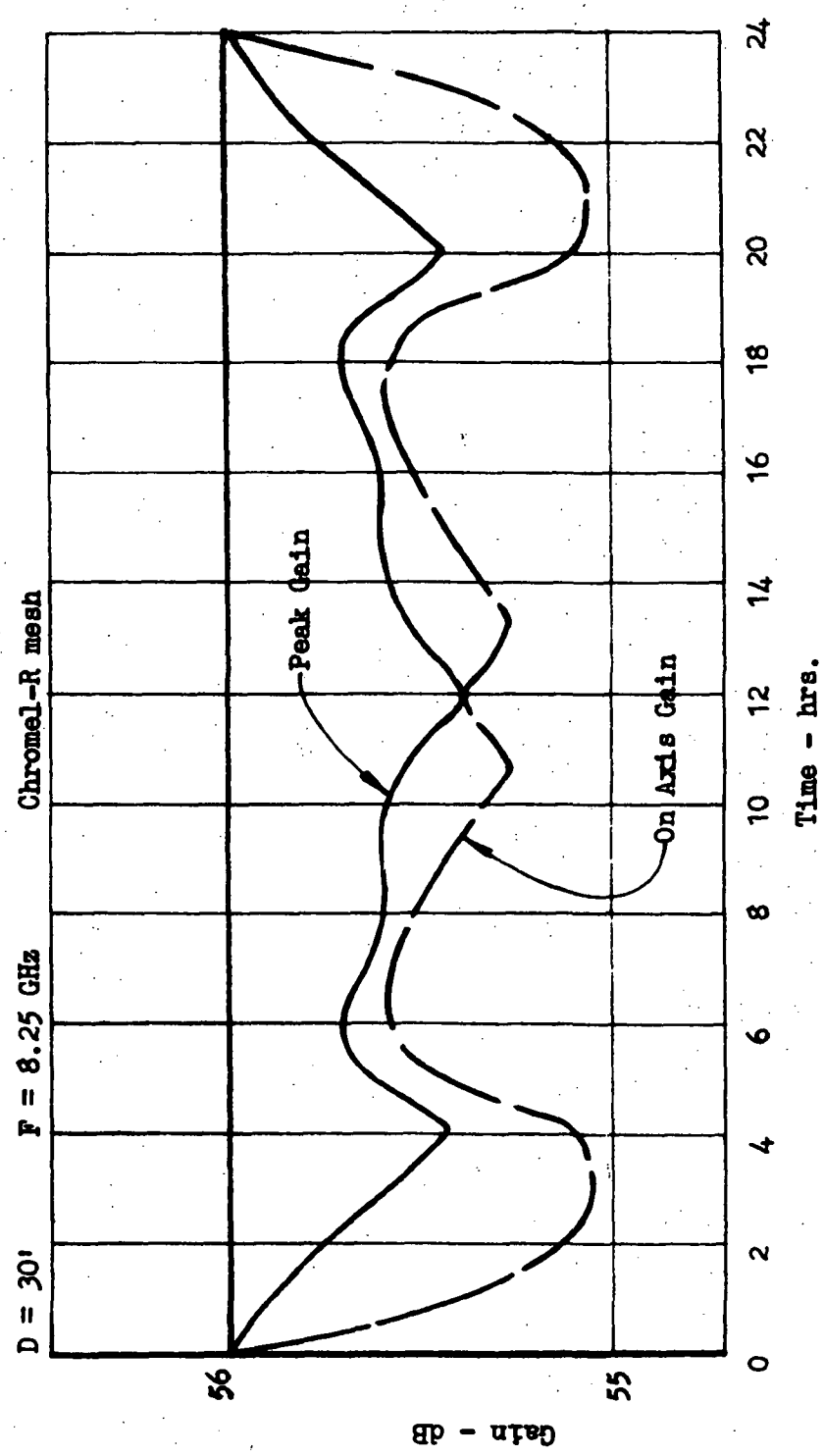

Figure A-7.1 GAIN DEGRADATION - ATS F&G REFLECTOR

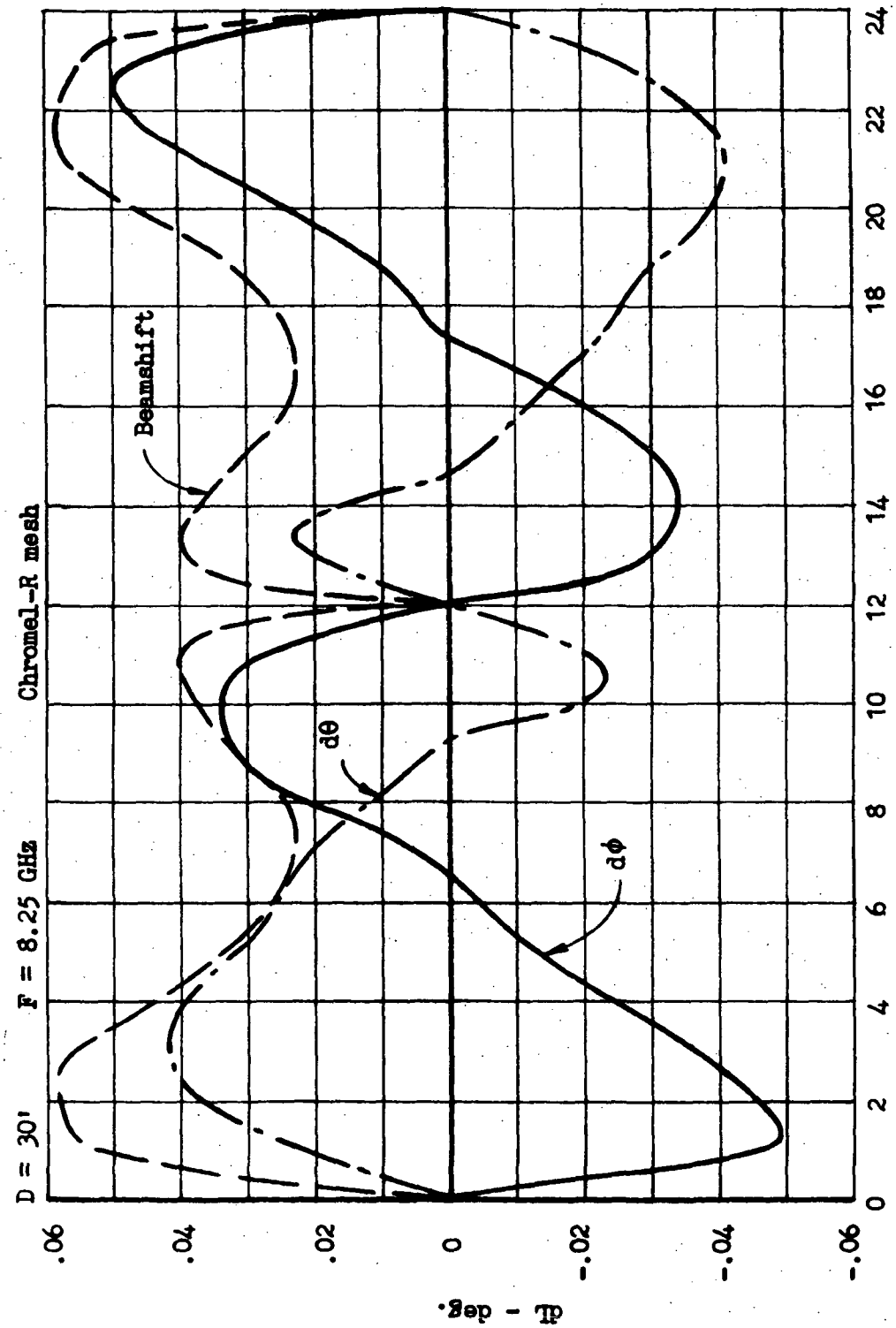

Figure A-7.2 BEAMSHIFT - ATS F&G REFLECTOR

calculated and the beam position is defined as $\theta = 90^{o}$, $\phi = 90^{o}$. The thermal correction will correct the peak gain value and provide for a new reference position for the beam. A coordinate transformation (a rotation about the reflector axis) will be used to handle the case where the sun is not in the aforementioned plane.

We shall denote the gain degradation for the reference case by ΔG_o for diameter D_o and frequency f_o. Then for any diameter D and frequency f, we will use the form

$$10 \log_{10} G_m = 10 \log_{10} G_m - \Delta G \quad \text{dB} \tag{7.1}$$

where G_{mo} is the peak gain for the undistorted case and where

$$\Delta G = \Delta G_0 \left[a_o + a_1 \frac{D}{D_o} + a_2 \frac{D^2}{D_o^2} \right] \left[b_o + b_1 \frac{f}{f_o} + b_2 \frac{f^2}{f_o^2} \right] \tag{7.2}$$

In Eq. 7.2 the parameters a_n and b_n are input constants which fit the design case best. The form of Eq. 7.2 allows some flexibility of adjustment by making changes in the input constants. Generally, some of the input constants may be zero. The form used above does require some justification.

Since most of the systematic distortion errors are monotonic, increasing functions of radius, we would expect the surface error to increase as the diameter is increased. As the surface error increases, so does the gain degradation. Thus we can expect the magnitude of the gain degradation to increase as D/D_o increases. Eq. 7.2 gives us the possibility of making a second-degree polynomial fit to the scaling effect. Similarly, frequency changes act in the same way because wavelength, which is inversely proportional to frequency, is the unit of measure in reflector antenna systems. (That is, all distances may be measured in wavelengths instead of inches).

To use the correction option, we must simply make some judgement about how the distortions of the case in hand would be extrapolated from the reference case and then assign appropriate constants. If the gain degradation data for the case at hand becomes available in some way, the reference file may be updated and then with an appropriate choice of constants no correction will be made.

The gain degradation will depend on other factors besides D and f. Amplitude distribution, focal length-to-diamter ratio, and various other parameters may all have a bearing on the actual gain degradation. But our intent here is to supply the best correction that can be made for thermal distortions consistent with the scope of the study. The manner in which this correction is made allows the program to be updated whenever distortion effects are analyzed in more detail.

Exactly the same philosophy is applied to the beamshift problem. When the sun is in the xz plane (Fig. A-6.1), the angular corrections to the position of the peak of the beam become

$$\phi_n = \frac{\pi}{2} + d\phi \tag{7.3}$$

and

$$\theta_n = \frac{\pi}{2} = d\theta \tag{7.4}$$

where

$$d\phi = d\phi_o \left[C_o + C_1 \frac{D}{D_o} + C_2 \left(\frac{D}{D_o} \right)^2 \right] \left[d_o + d_1 \frac{f}{f_o} + d_2 \left(\frac{f}{f_o} \right)^2 \right] \tag{7.5}$$

and

$$d\theta = d\theta_o \left[e_o + e_1 \frac{D}{D_o} + e_2 \left(\frac{D}{D_o} \right)^2 \right] \left[g_o + g_1 \frac{f}{f_o} + g_2 \left(\frac{f}{f_o} \right)^2 \right] \tag{7.6}$$

Using the same functional form for beamshift does not necessarily imply that the beamshift will be a function of diameter scaling ratio or of frequency scaling ratio. For example, a distortion mode corresponding to a simple tilt of the reflector, if scaled to a larger diameter, would still be a tilt of the same angle and thus would

be independent of D/D_o. Also, we would not expect the displacement of the beam to be dependent on frequency when this displacement is measured in degrees or radians. That is because we tend to think of the displacement as the result of an "effective" rotation of the reflector. The importance of this rotation arises when we measure the rotation in beamwidths and not degrees. Thus while we have included provision for dependence on diameter and frequency, there may be many cases in which the beamshift would be independent of either variable or both.

The reference file for beamshift data can be updated just as we mentioned above for the gain degradation reference file.

For purposes of providing the input signal to the monopulse model (subroutine MØNPLS) a distorted antenna reference frame (D-frame) is defined as the frame obtained from the undistorted antenna reference frame (A-frame) by applying the (small) rotation $d\varphi$ and $d\theta$ about the appropriate axes (see definitions of $d\varphi$ & $d\theta$ above). In this reference frame the peak gain of the antenna lies along the $-Z_D$ axis and the unit line of sight vector in this reference frame (LHATD) is the input to MØNPLS.

The D-frame is obtained from the A-frame by an effective single rotation $d\psi \triangleq \sqrt{(d\varphi)^2 + (d\theta)^2}$ about the $\bar{\epsilon}_\psi$ axis (see Figure A.0.1) where $\bar{\epsilon}_\psi \triangleq \frac{d\varphi}{d\psi}\,\bar{\epsilon}_\varphi + \frac{d\theta}{d\psi}\,\bar{\epsilon}_\theta$. The Euler parameters for the transformation from the A-frame to the D-frame are defined such that

$$\begin{bmatrix} q_1 \\ q_2 \\ q_3 \end{bmatrix} = \left[\bar{e}_\psi\right]_A \sin\frac{d\psi}{2}\,, \quad q_4 = \cos\frac{d\psi}{2}$$

or since $d\psi$ is small and $\bar{e}_\psi$ is a linear combination of $\bar{\epsilon}_\varphi$ and $\bar{\epsilon}_\theta$,

$$\begin{bmatrix} q_1 \\ q_2 \\ q_3 \end{bmatrix} = \frac{d\varphi}{2}\begin{bmatrix} \cos\Omega \\ \sin\Omega \\ 0 \end{bmatrix} + \frac{d\theta}{2}\begin{bmatrix} -\sin\Omega \\ \cos\Omega \\ 0 \end{bmatrix} \Rightarrow$$

$$q_1 = \tfrac{1}{2}\,(d\varphi\cos\Omega - d\theta\sin\Omega)$$

$$q_2 = \tfrac{1}{2}\,(d\varphi\sin\Omega + d\theta\cos\Omega)$$

$$q_3 = 0$$

$$q_4 = 1$$

where Ω is the angle between the X_A axis and the axis of the $d\varphi$ rotation (see Figure A.0.1). The transformation matrix ($T_{D/A}$) is obtained from these Euler parameters using the subroutine EPTØDC.

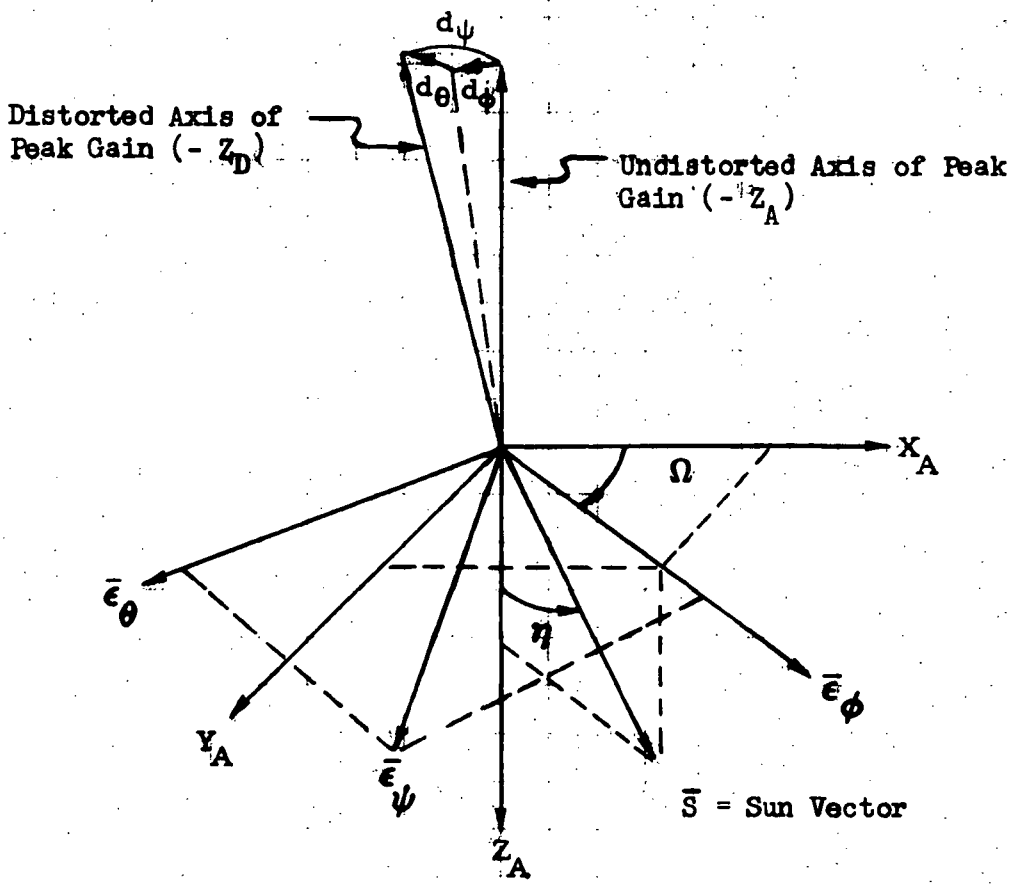
d_ψ
d_θ
d_ϕ
Distorted Axis of Peak Gain ($-Z_D$)
Undistorted Axis of Peak Gain ($-Z_A$)
X_A
Ω
$\bar{\epsilon}_\theta$
η
$\bar{\epsilon}_\phi$
Y_A
$\bar{\epsilon}_\psi$
$\bar{S}$ = Sun Vector
Z_A

Figure A.0.1

3.1.8 GAIN CALCULATION ALONG THE LOS

The first step after the input subroutine is to calculate the antenna gain at five points. The pattern of these five points is shown in Fig. A-8.1. When the current distribution method is used to calculate the gain, the gain is calculated on axis and at four angles off axis as shown in the figure. When the simple method is used, we have the same result since we know the peak gain on axis and the half-power beamwidth. Thus we have the following table of values in either case:

Gain	θ	ϕ
G_1	θ_n	ϕ_n
G_2	θ_n	$\phi_n - \delta$
G_3	θ_n	$\phi_n + \delta$
G_4	$\theta_n - \delta$	ϕ_n
G_5	$\theta_n + \delta$	ϕ_n

In the above table, θ_n, ϕ_n are the coordinates of the reference axis (in this case the beam peak). When the method has been used to calculate gain, G_2, G_3, G_4, and G_5 have the value G_1-3. dB and δ is the half-power beamwidth divided by 2. The gain values and angular coordinates may have been corrected for thermal effects.

These five gain values and their corresponding coordinates are used to fit an elliptic paraboloid to the peak of the beam. This paraboloid is then used to determine the gain along the LOS for varying coordinates of the LOS, thus saving much computer run time. The accuracy of this approximation has been discussed in Section 3.

In the vicinity of $\theta = \pi/2$, $\phi = \pi/2$, Eq. 3.2 may be generalized to the form:

$$10 \log_{10} G_m - 10 \log_{10} G(\theta, \phi) = T(\theta - \theta_o)^2 + P(\phi - \phi_o)^2 \qquad (8.1)$$

where G_m is the peak gain value and where θ_o, ϕ_o are the coordinates of the beam peak. It will happen that $G_m = G_1$, $\theta_o = \theta_n$, and $\phi_o = \phi_n$ because the reference axis θ_n, ϕ_n happens to be the beam peak in these calculations.

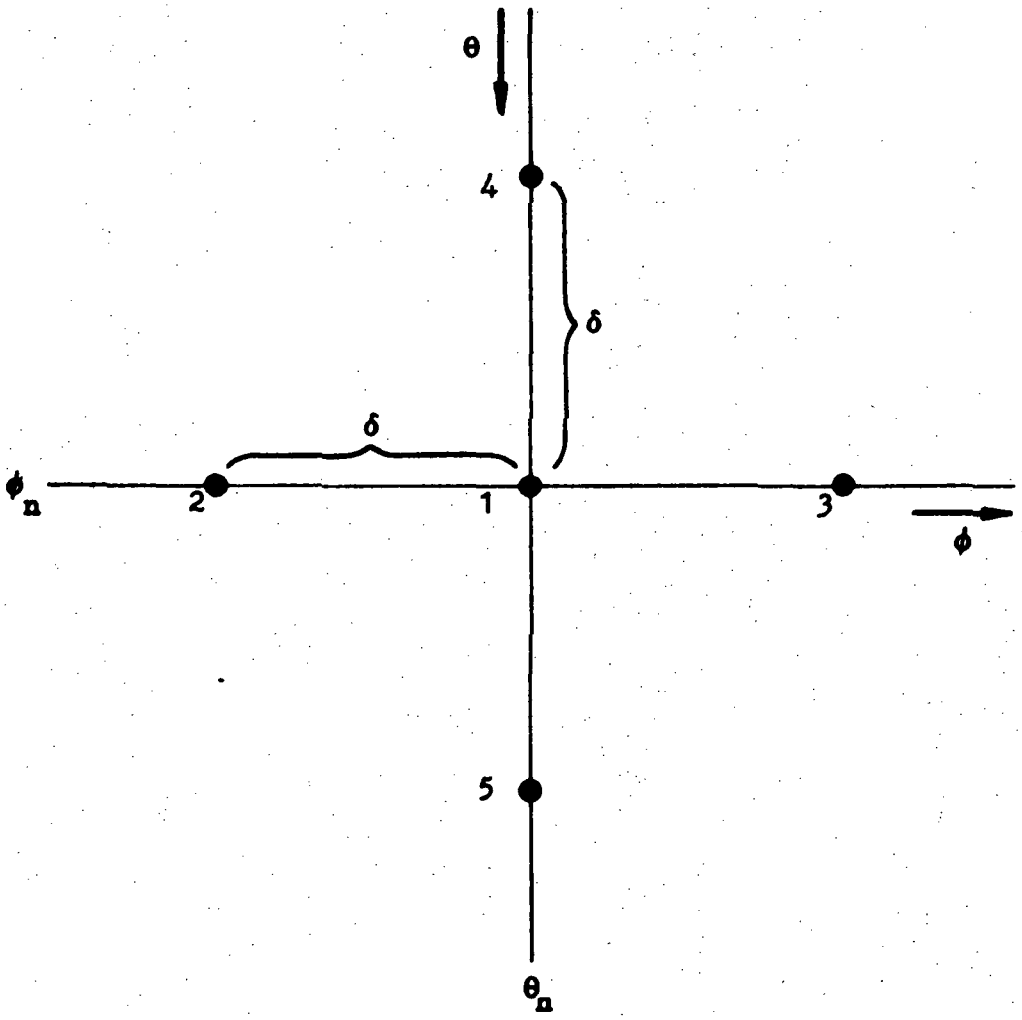

Figure A-8.1 LOCATION OF GAIN CALCULATION POINTS

In general, however, it is not necessary that this be so, and when the current distribution is applied to distorted reflectors, the peak gain and the beam position can be found by using Eq. 8.1 and five gain values as indicated in the above table.

For convenience we shall use the notation G'_x to indicate $10 \log_{10} G_x$ in the following.

In general, we find that

$$P = \frac{1}{2\delta^2} \left(2G'_1 - G'_2 - G'_3\right) \tag{8.2}$$

$$T = \frac{1}{2\delta^2} \left(2G'_1 - G'_4 - G'_5\right) \tag{8.3}$$

and that

$$\varphi_o = \varphi_n + \frac{G'_3 - G'_2}{4P\delta} \tag{8.4}$$

$$\theta_o = \theta_n + \frac{G'_5 - G'_4}{4T\delta} \tag{8.5}$$

When the beam peak lies along the reference axis then $G'_2 = G'_3$ and $G'_4 = G'_5$ so that

$$10 \log_{10} G(\theta, \varphi) = G'_1 - (G'_1 - G'_2)\left(\frac{\varphi - \varphi_o}{\delta}\right)^2 - (G'_1 - G'_4)\left(\frac{\theta - \theta_o}{\delta}\right)^2 \tag{8.6}$$

$$= G'_1 - P(\varphi - \varphi_o)^2 - T(\theta - \theta_o)^2$$

which for the calculations made in the simple model would be

$$10 \log_{10} G(\theta, \phi) = 10 \log_{10} G_1 - \frac{3.010}{(\beta)^2} \left[(\phi - \phi_o)^2 + (\theta - \theta_o)^2\right] \qquad (8.7)$$

where 2β is the half-power beamwidth. Equation 8.6 is used to represent the antenna pattern in all subsequent calculations. The parameter β is chosen in the current distribution calculation to be half the estimated half-power beamwidth to obtain good correlation over this region.

3.1.9 MONOPULSE MODEL

The monopulse system used on the high gain antenna could be either a four-horn or a five-horn configuration. In the five-horn configuration a single horn located at the focus of the reflector provides the communications channel signal; we shall denote this horn and its associated beam by the letter T. The error signals are formed from four offset feeds a, b, c, and d clustered about the focus. In the four-horn configuration the on-axis horn is omitted and the remaining horns are not displaced quite as far from the reflector axis. In this case the communications signal is the sum signal of the monopulse.

The choice between the two configurations is a tradeoff between communications channel gain and tracking capability. The sum signal of a four-horn monopulse, being the sum of four offset beams, has a lower peak gain that that provided by a single on-axis horn. Thus the five-horn configuration provides higher communications channel peak gain. On the other hand, because of the presence of the fifth horn, the remaining four horns must be displaced further from the axis of the reflector than they would be in the four-horn configuration. As a result, the four-horn approach can have higher beam crossover levels -- more nearly at the optimum level -- and provides better tracking.

The monopulse model will calculate four gain values for each position of the LOS. One of these, G_D, is the gain available along the line of sight in the communications or service channel. Another, G_S, is the gain available in the monopulse sum channel. The remaining gain values, G_θ and G_ϕ, are the monopulse error channel gains for the constant θ and constant ϕ "planes" respectively. The model allows the user to select a four-horn, or five-horn monopulse or no monopulse at all. The flag for this is MON in the input routine.

When MON=O, the model will not compute monopulse sum or difference signals. Then G_D is set equal to $G(\theta, \phi)$ as discussed in the previous section. The remaining gain values G_S, G_θ, and G_ϕ are set to zero.

When MON=5, G_D is also set equal to $G(\theta, \phi)$. The model then calculates G_S, G_θ, and G_ϕ as we shall discuss in the following paragraphs. When MON=4, the model computes G_S, G_θ, and G_ϕ and then sets $G_D = G_S$.

Each of the five beams can be represented by an equation of the form of Eq. 8.6, except that θ_o, ϕ_o must be adjusted to include the shift of

each beam off the axis represented by θ_n, ϕ_n. The coordinates of the axes of the five beams in the model are

Beams	θ_o	ϕ_o
t	θ_n	ϕ_n
a	$\theta_n - U$	$\phi_n - V$
b	$\theta_n - U$	$\phi_n + V$
c	$\theta_n + U$	$\phi_n - V$
d	$\theta_n + U$	$\phi_n + V$

For the small offset angle used in a monopulse we would not expect the peak gain G_I' or the beamwidth to change.

(NOTE: In the previous presentation of the monopulse model in the progress reports a rotationally symmetric beam was assumed similar to Eq. 3.3. It was then necessary to find the angle between the LOS and each of the 5 beam axes. The approximation represented by Eq. 8.6 gives the gain in terms of θ, ϕ of the LOS directly. In the vicinity of $\theta = 90^o$, $\phi = 90^o$ we can treat θ and ϕ much the same as we would treat rectangular coordinates. Thus with Eq. 8.6 as the model the geometrical problem is simplified).

In the direction θ, ϕ we obtain G_a, G_b, G_c and G_d. Since sum and difference signals must be obtained by adding and subtracting on a voltage basis, we have for the sum channel gain

$$G_s = A_s \left(\sqrt{G_a} + \sqrt{G_b} + \sqrt{G_c} + \sqrt{G_d} \right)^2 \qquad (9.1)$$

where A_s is a factor to account for the modification of the peak gain by the monopulse action.

Similarly

$$G_Q = A_s \left(\sqrt{G_a} + \sqrt{G_b} - \sqrt{G_c} - \sqrt{G_d} \right)^2 \qquad (9.2)$$

$$G_{\phi} = A_s \left(\sqrt{G_a} - \sqrt{G_b} + \sqrt{G_c} - \sqrt{G_d} \right)^2 \qquad (9.3)$$

Quadrant can be determined by the phases of the difference signals compared to the sum (on a field strength basis).

If we let

$$G_P = \exp \left[\frac{G_1' - PV^2 - TU^2}{10w} \right] \qquad (9.4)$$

where P and T are given by Eq. 8.2 and 8.3 and where

$$w = \log_{10} e = 0.434294482 \qquad (9.5)$$

and if we let

$$\phi = \phi_n + \Delta\phi \qquad (9.6)$$

$$\theta = \theta_n + \Delta\theta \qquad (9.7)$$

then

$$G_s = A_s G_p \exp \left[- \frac{P (\Delta\phi)^2 - T (\Delta\theta)^2}{10w} \right] \left[4 \cosh \frac{PV\Delta\phi}{10w} \cosh \frac{TU\Delta\theta}{10w} \right]^2 \qquad (9.8)$$

$$G_\theta = A_s G_p \exp\left[-\frac{P(\Delta\phi)^2 + T(\Delta\theta)^2}{10w}\right]\left[4\cosh\frac{PV\Delta\phi}{10w}\sinh\frac{TU\Delta\phi}{10w}\right]^2 \quad (9.9)$$

$$G_\phi = A_s G_p \exp\left[-\frac{P(\Delta\phi)^2 + T(\Delta\theta)^2}{10w}\right]\left[4\sinh\frac{PV\Delta\phi}{10w}\cosh\frac{TU\Delta\theta}{10w}\right] \quad (9.10)$$

and

$$G_T = G_1 \exp\left[-\frac{P(\Delta\phi)^2 + T(\Delta\theta)^2}{10w}\right] \quad (9.11)$$

The only actual gain value needed is G_D. The tracking system will utilize the error signals normalized with respect to the monopulse sum signal. Thus the output of the monopulse model will be G_D, G_θ/G_S, and G_ϕ/G_S (plus the quadrant information). The required error signal ratios are

$$\frac{G_\theta}{G_s} = \tanh^2\left(\frac{TU\Delta\theta}{10w}\right) \quad (9.12)$$

and

$$\frac{G_\phi}{G_s} = \tanh^2\left(\frac{PV\Delta\phi}{10w}\right) \quad (9.13)$$

For the 4-horn case the sum channel of the monopulse is the service channel. For this case it is necessary to evaluate A_S so that $G_D(\theta,\phi) = G_S(\theta,\phi)$ may be found. For the no monopulse or the 5 horn-monopulse we do not need to evaluate A_S.

The quantity A_S may be found by performing the integration

$$\int_0^{2\pi}\int_0^{\pi} G_s(\theta, \phi) \sin\theta \, d\theta \, d\phi = 4\pi \tag{9.15}$$

Unfortunately, the model for $G_S(\theta, \phi)$ is not valid for all θ, ϕ. But the model is best near θ_n, ϕ_n where its contribution to the integral is most important. A reasonably good value of A_S can be obtained by limiting the range of integration to a small region around θ_n, ϕ_n which we shall denote by τ. Specifically,

$$16 A_s G_p = \frac{4\pi}{\iint_\tau \frac{G_s(\theta, \phi)}{16 A_s G_p} \sin\theta \, d\theta \, d\phi} \tag{9.16}$$

We already know G_1, the maximum value of $G_T(\theta, \phi)$ as given by Eq. 9.11. We can find the value G_y that the above process would yield. Thus,

$$G_y = \frac{4\pi}{\iint_\tau \frac{G_T(\theta, \phi)}{G_1} \sin\theta \, d\theta \, d\phi} \tag{9.17}$$

$$= \frac{4\pi}{\iint_\tau \exp\left[-\frac{P(\Delta\phi)^2 + T(\Delta\theta)^2}{10w}\right] \sin\theta \, d\theta \, d\phi}$$

The ratio of Eq. 9.16 to Eq. 9.17 is the gain loss due to the monopulse action as compared to that that would be provided by a single horn on axis.

Thus, the maximum value of $G_S(\theta_n, \phi_n)$ is

$$G_s(\theta_n, \phi_n) = \frac{(16 A_s G_p)}{G_y} G_1 \tag{9.18}$$

If the model were perfect, then G_y would be equal to G_1 and $G_S(\theta_n, \phi_n)$ would be the value obtained from Eq. 9.16. By using the ratio 16 $A_S G_P/G_y$ to modify G_1, we obtain a better model since some of the inaccuracies in Eq. 9.16 and Eq. 9.17 tend to cancel.

Finding the peak value of G_S is only a problem in the four-horn case. When MON=4, the integrations indicated by Eq. 9.16 and Eq. 9.17 will be performed for the first set of values θ, ϕ. The peak value thus obtained for $G_S(\theta_n, \phi_n)$ from Eq. 9.18 will be retained for all subsequent LOS positions for the same case.

3.2.1 Antenna Control System Model

This section describes the mathematical model used by the simulation program for the antenna control system and has been extracted from the Task 1 Report – Math Modeling of High Gain Antenna - dated 1 March 1972.

The programming of this modeling is contained in subroutines CNTRL7 and SERVØ.

3.2.2.0 MODES OF OPERATION

3.2.2.1 REFERENCE FRAMES

In order to discuss the several modes of operation to be simulated, three of the orthogonal, righthand reference frames that will be used are described. The antenna reference frame (A) has, as two of its axes, the negative boresight axis and the inner most gimbal axis. The IMU reference frame is fixed with respect to the space station. The gimbal angles are Euler angles relating the angular position of the antenna reference frame to the IMU reference frame, assuming rigidity of all members. The outer gimbal angle (about the axis common to the boom and gimbal ring) is α and the inner gimbal angle is β . The IMU senses the angular position and angular velocity of the IMU reference frame with respect to an inertial reference frame (I).

3.2.2.2 COMPUTER COMMAND MODE

In the computer command mode the antenna angular position command is computed by the on-board digital processor as a function of the ephemeris of the relay satellite at which the antenna is to point and the position and attitude of the space station with respect to the inertial reference frame as determined by the inertial measurement unit (IMU) and the on-board space station ephemeris. A spiral search scan may be superimposed for acquisition of the relay satellite RF signal. For slewing to a relay satellite, limits will be placed on commanded angular rates commensurate with mechanical limitations. The antenna angular position command is converted from components in the IMU reference frame to gimbal (Euler) angles prior to being compared with the actual antenna position, as shown in Fig. B-1.

The rate stabilization shown as a block in Fig. B-1 and in detail in Fig. B-2 provides the rate feedback path. In order to reduce the disturbance input effect of space station attitude changes on the antenna angular position with respect to the inertial reference frame, the space station angular rate is added to the antenna angular rate in the IMU reference frame.

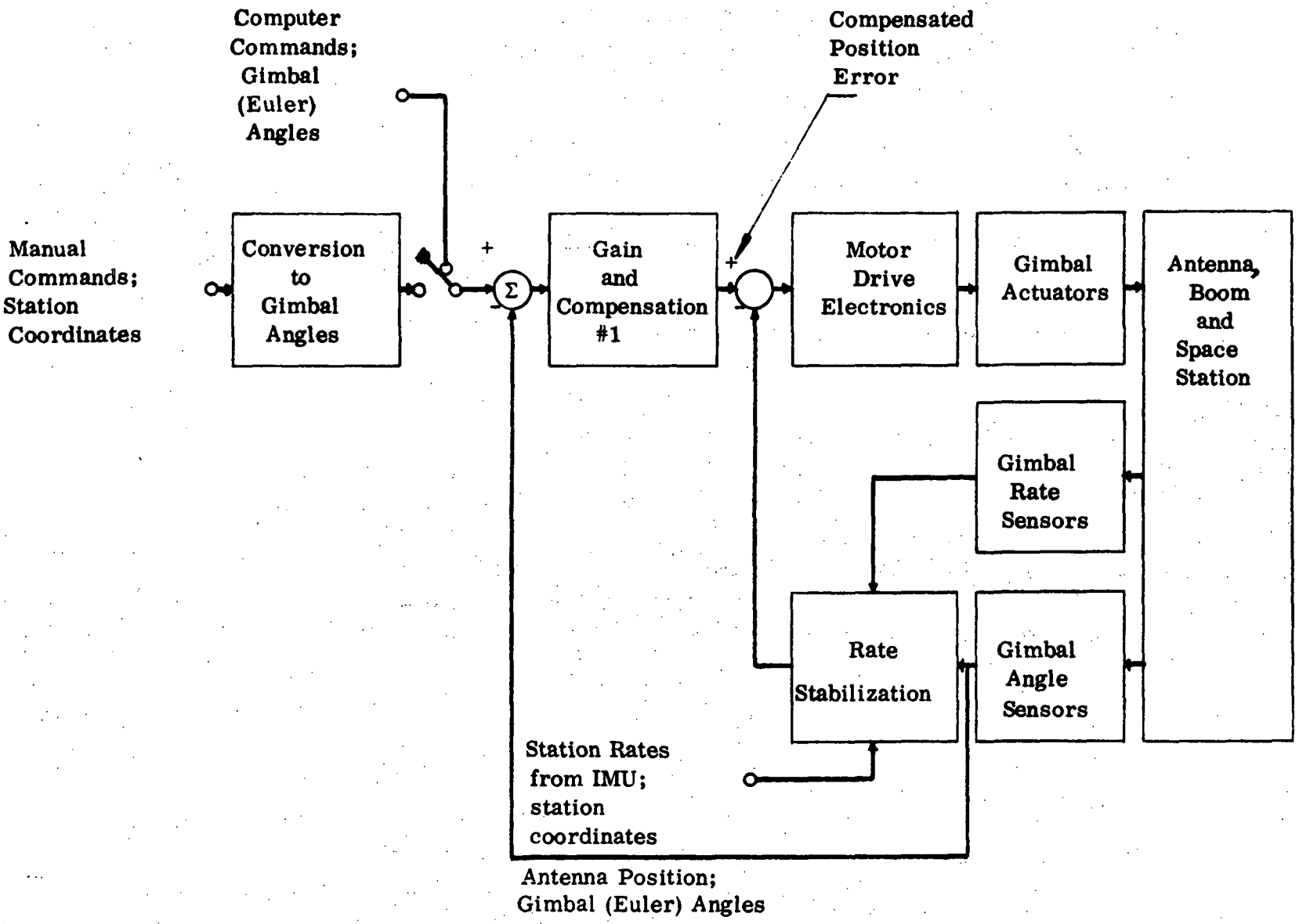

Figure B-1 MANUAL AND COMPUTER COMMAND MODES

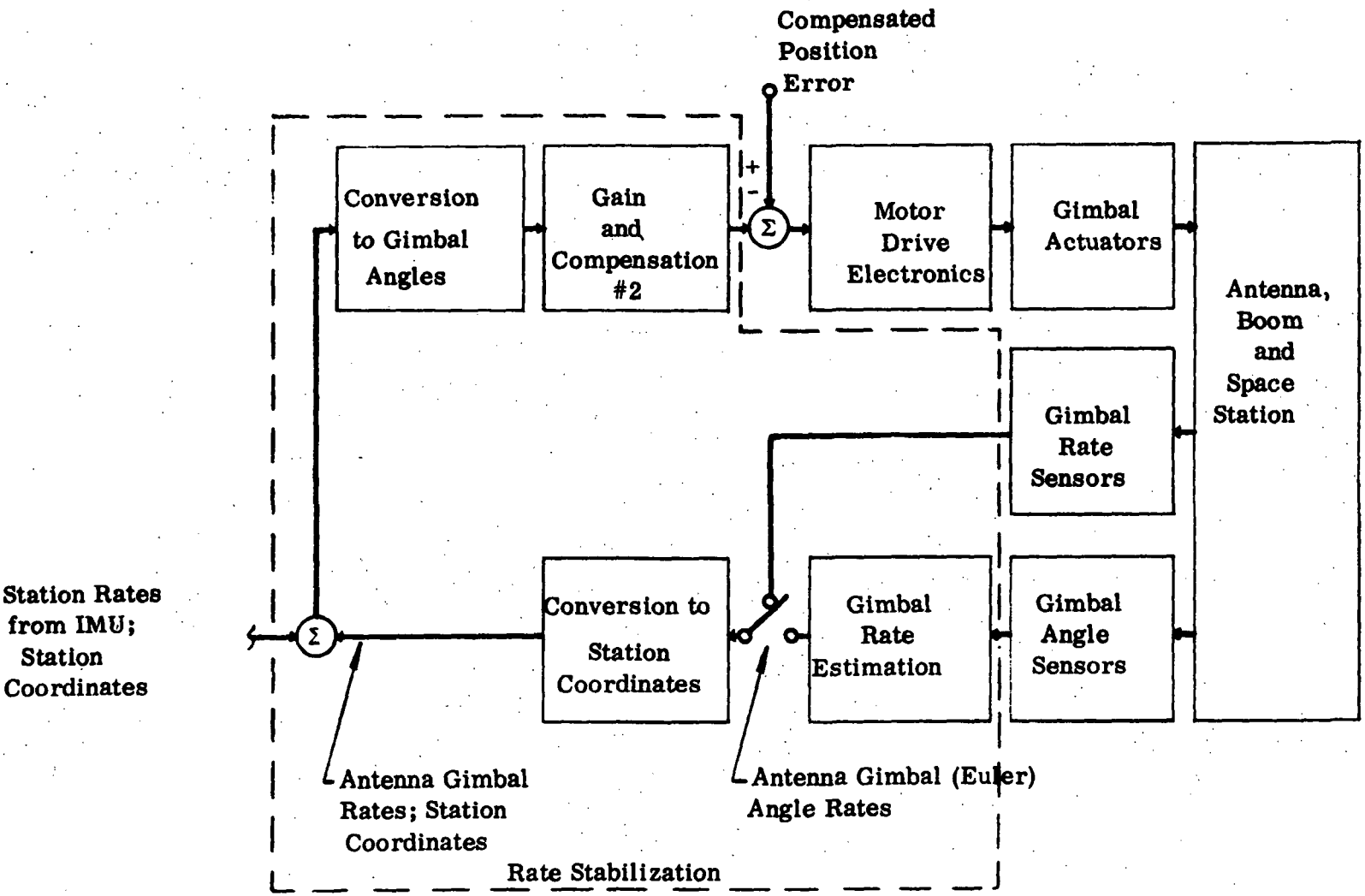

Figure B-2 RATE STABILIZATION

3.2.2.3 MANUAL COMMAND MODE

It is assumed that the manual mode is used to bring the antenna to a fixed orientation relative to the inertial reference frame and that the manual command signals originate within the space station by someone making appropriate settings of input devices and then initiating motion. Only step angular position commands relative to the inertial reference frame will be simulated. The commands will be converted to gimbal angles and then compared with the sensed gimbal angles to form the position error signal as shown in Fig. B-1.

3.2.2.4 RF AUTOTRACK MODE

In the RF autotrack mode, using a sufficiently strong RF signal being received from the relay satellite, the angular position difference between the line-of-sight to the relay satellite and the antenna boresight axis is sensed by the monopulse system. The servo is automatically switched from the search scan computer command mode to the RF autotrack mode when the received signal strength exceeds a preset threshold level. Since the receiving antenna beam shape changes as a function of carrier frequency, a corresponding error signal gain adjustment must be made as indicated in Fig. B-3. Next, the error signals are converted from the antenna reference frame (the frame in which they are sensed) to the gimbal (Euler) angles.

When in the RF autotrack mode, the gimbal angle sensor outputs may be used to correct the on-board program which computes the gimbal angle commands required to point the antenna at the relay satellite, i.e., to update the computer command mode program.

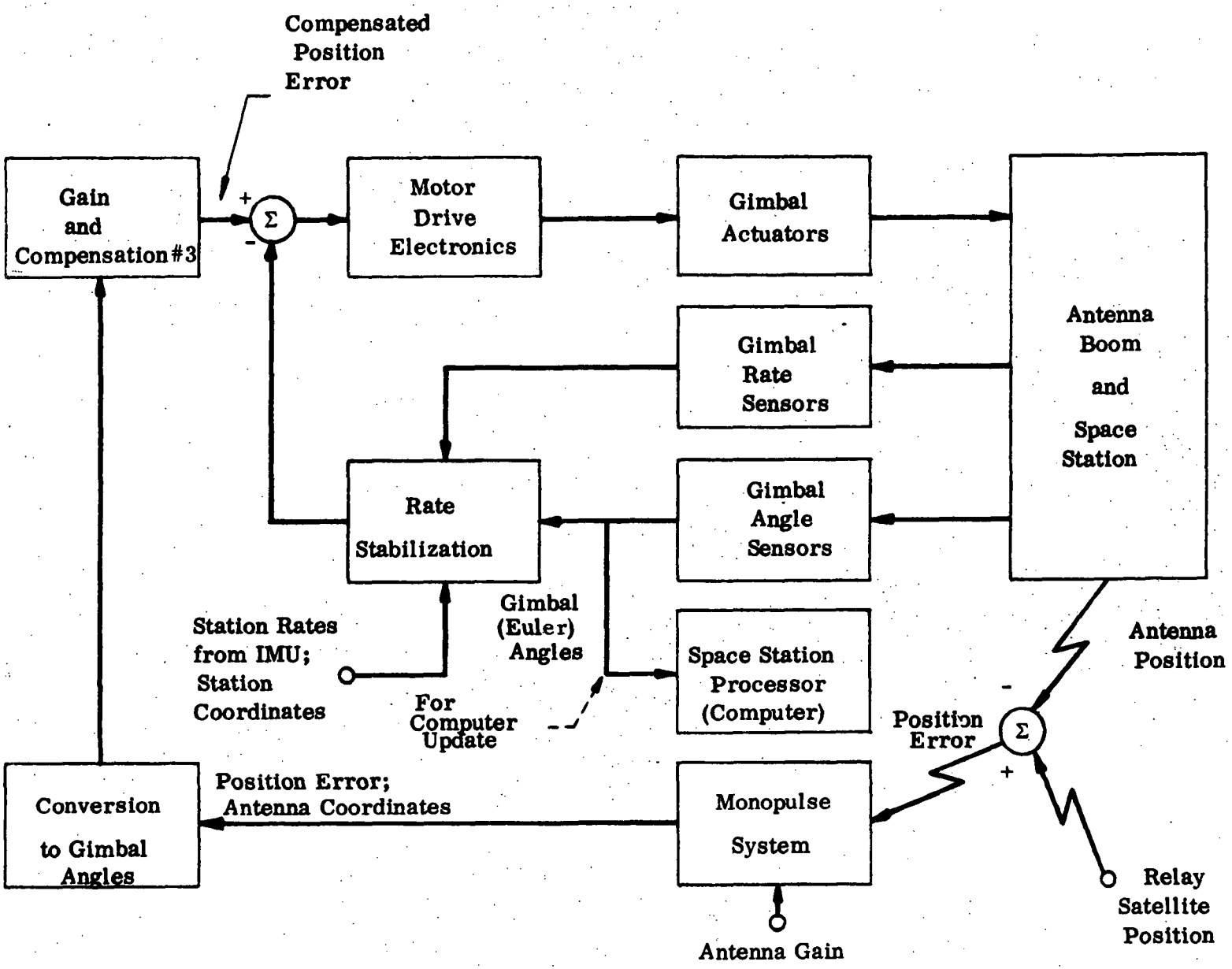

Figure B-3 R-F AUTOTRACK MODE

3.2.3.0 CONTROL LAWS

3.2.3.1 OBSERVATION OF OUTPUT STATES

The control laws (more than one will be modeled and simulated) will use the angular position and rate of the antenna about the gimbal axes when in the computer command and manual command modes. When in the RF autotrack mode, the angular position error signal is developed within the monopulse system but the gimbal rates may still be used directly. Fig. B-4 indicates several alternate sources of information for the control law. When in the computer command mode, gimbal axis angular rate information may be sensed by a rate gyro or a tachometer, or estimated from the gimbal angular position sensor output.

3.2.3.2 STRUCTURE

Control law alternatives are shown in Fig. B-5 and include integral-error compensation, derivative-error compensation, and derivative-output compensation. The control law outputs, which are the compensated error signals for each gimbal axis, are the inputs to the motor drive electronics. As is indicated in the figure, the math model includes both linear and nonlinear control law alternatives. The control law selected is implemented within the three "gain and compensation" blocks shown in Figs. B-1, B-2, and B-3.

3.2.3.3 VISIBILITY

Possible obscuration of the relay satellite by the earth or by portions of the space station is monitored using visibility discretes. If the antenna servo system is operating in the monopulse autotrack mode and the line-of-sight to the relay satellite is obscured, it will be possible to automatically switch to the computer command mode.

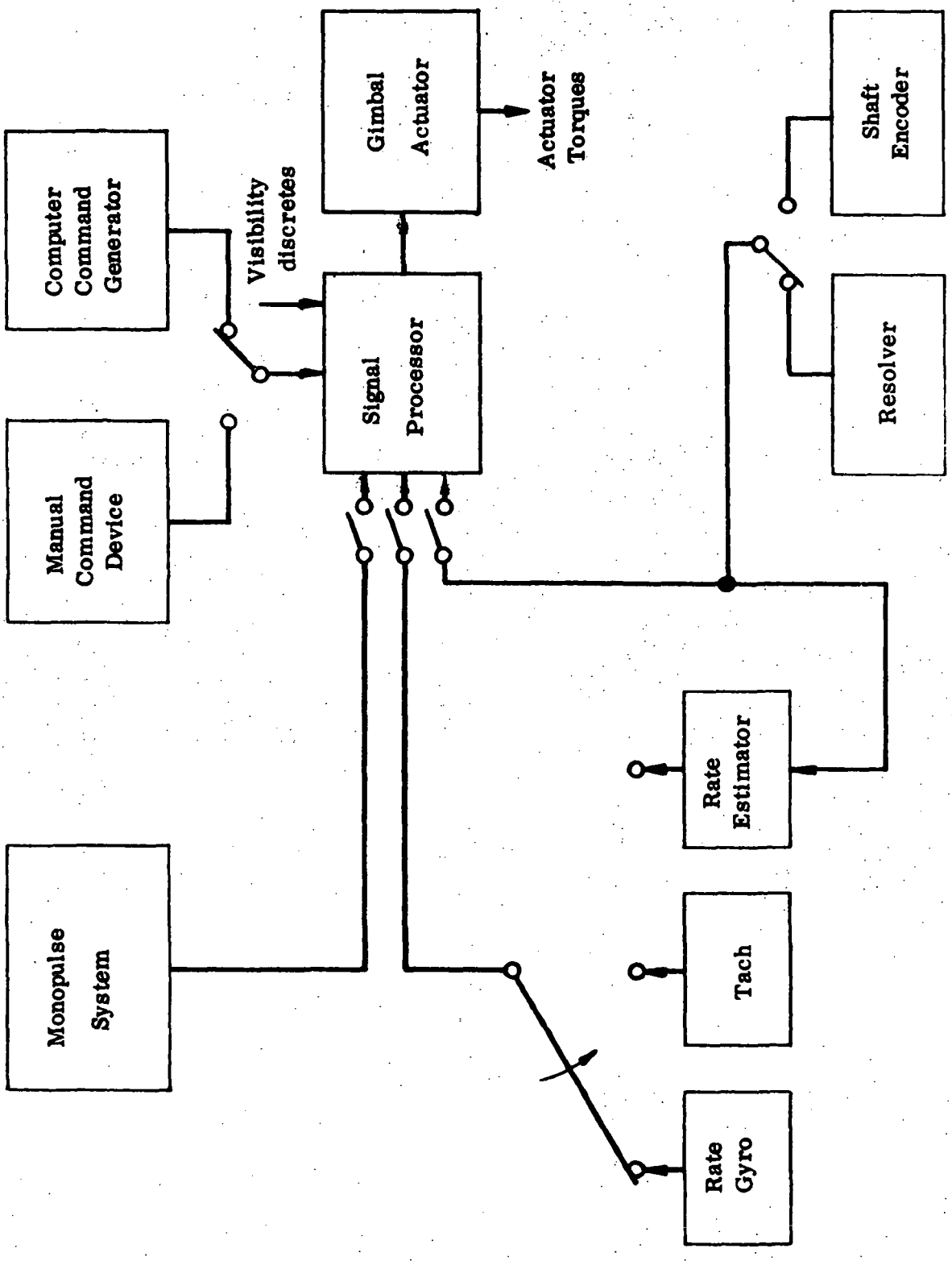

Figure B-4 CONTROL LAW INFORMATION SOURCES

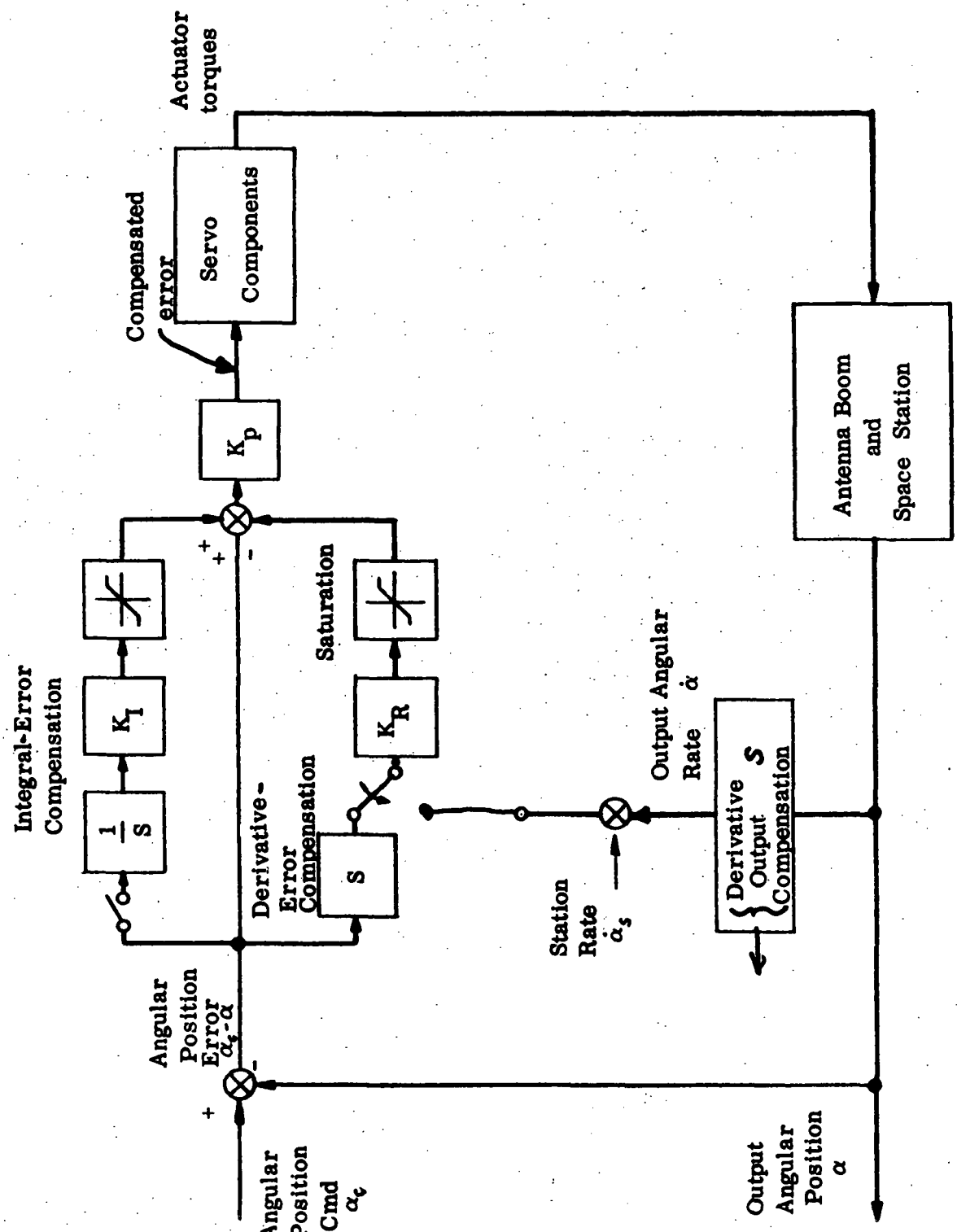

Figure B-5 CONTROL LAW ALTERNATIVES - SINGLE AXIS

3.2.4 DIGITAL PROCESSOR

The sampled-data effects of digital processing will not be simulated because the Adams-Bashforth integration package which will be used, has a variable integration step size. Simulation of a fixed sampling rate controller would introduce a discontinuity at each sampling instant which would require a re-initialization of the Adams-Bashforth integration package, thus substantially increasing the computer run time. This also precludes simulation of random effects using a random number generator. The entire servo simulation will be deterministic. All digital processing will be modeled as continuous signal processing.

3.3.1 On Board Computer Model

This section describes the mathematical model used by the simulation program for the on board computer and has been extracted from portions of the Task 2 Report – Mathematical Model for the Pointing Requirements of the Space Station High Gain Antenna – dated 28 Oct. 1972, and the Task 4 Report – Math Modeling of Interface Computer – dated 30 March 1972.

The programming of this modeling is conained in the subroutines ØBKNMT, ØBEPH3, ØBEPH1, ØBEPH2, INTSS1, INTSS2, ØBSTCL, ANTCOM, and CLBRTN which are called by SETUP to compute the antenna gimbal angle commands predicted by the on board computer.

3.3.2 Computed Space Station Kinematics

The on board kinematics computations are simulated by the subroutine ØBKNMT. The function of these computations is to determine the space station attitude relative to the orbital reference frame from the initial attitude and the time history of the space station and orbital reference frame inertial rates.

Within the subroutine the relative space station attitude is specified by the euler parameters (q_1, ..., q_4) of the rotation which would align the orbital reference frame (O) with the space station reference frame (C). When this rotation is by the angle φ about the axis $\hat{\epsilon}$, the euler parameters are defined as

$$q_1 \triangleq \epsilon_x \sin(\varphi/2)$$

$$q_2 \triangleq \epsilon_y \sin(\varphi/2)$$

$$q_3 \triangleq \epsilon_z \sin(\varphi/2)$$

$$q_4 \triangleq \cos(\varphi/2)$$

where

$$\begin{bmatrix} \epsilon_x \\ \epsilon_y \\ \epsilon_z \end{bmatrix} = [\hat{\epsilon}]_o = [\hat{\epsilon}]_c$$

The time derivatives of these euler parameters may be expressed in terms of the components of the space station and orbital reference frame angular velocities ($\vec{\omega}^{c-I}$ and $\vec{\omega}^{o-I}$ respectively) as

$$\begin{bmatrix} \dot{q}_1 \\ \dot{q}_2 \\ \dot{q}_3 \\ \dot{q}_4 \end{bmatrix} = \frac{1}{2}(\Omega_c + \bar{\Omega}_o) \begin{bmatrix} q_1 \\ q_2 \\ q_3 \\ q_4 \end{bmatrix}$$

where

$$\Omega_c \triangleq \begin{bmatrix} 0 & \omega_3^c & -\omega_2^c & \omega_1^c \\ -\omega_3^c & 0 & \omega_1^c & \omega_2^c \\ \omega_2^c & -\omega_1^c & 0 & \omega_3^c \\ -\omega_1^c & -\omega_2^c & -\omega_3^c & 0 \end{bmatrix}, \quad \left[\vec{\omega}^{c-I}\right]_c = \begin{bmatrix} \omega_1^c \\ \omega_2^c \\ \omega_3^c \end{bmatrix}$$

$$\bar{\Omega}_o \triangleq \begin{bmatrix} 0 & \omega_3^o & -\omega_2^o & -\omega_1^o \\ -\omega_3^o & 0 & \omega_1^o & -\omega_2^o \\ \omega_2^o & -\omega_1^o & 0 & -\omega_3^o \\ \omega_1^o & \omega_2^o & \omega_1^o & 0 \end{bmatrix}, \quad \left[\vec{\omega}^{o-I}\right]_o = \begin{bmatrix} \omega_1^o \\ \omega_2^o \\ \omega_3^o \end{bmatrix}$$

and the direction cosine matrix for the orbit frame to platform frame transformation may be expressed in terms of the euler parameters as

$$[T_{c/o}] = \begin{bmatrix} q_1^2 - q_2^2 - q_3^2 - q_4^2 & 2(q_1 q_2 + q_3 q_4) & 2(q_1 q_3 - q_2 q_4) \\ 2(q_1 q_2 - q_3 q_4) & -q_1^2 + q_2^2 - q_3^2 + q_4^2 & 2(q_2 q_3 + q_1 q_4) \\ 2(q_1 q_3 + q_2 q_4) & 2(q_2 q_3 - q_1 q_4) & -q_1^2 - q_2^2 + q_3^2 + q_4^2) \end{bmatrix}$$

These formulations are derived from the classical works of Euler, Rodriques, Hamilton and others and are documented in a Lockheed internal report by E. F. Weiten.[1]

The above differential equations for the four euler parameters are numerically integrated and used as indicated above to obtain the direction cosine matrix $[T_{c/o}]$ as a function of time.

[1] A Four-Vector Method of Describing the Rotational Motion of Rigid Bodies, E. F. Weiten, Feb. 1964.

3.3.3 Computed Ephemerides

The relay satellite ephemerides are computed by subroutines ØBEPH1 & ØBEPH2, and the space station ephemeris is computed by subroutine ØBEPH3. The computations are identical in all three of these routines.

The on-board ephemeris subroutine ØBEPH1 computes the position vector $\vec{R}$ and the inertial velocity vector $\vec{V}$ by means of the approximate formulae that would be used by an on-board computer. While there are several possibilities for on board ephemeris formulas this first version of ØBEPH1 (ØBEPH1/LAGRAN) uses 8 point lagrangian interpolation for each of the components of $\vec{R}$ and $\vec{V}$.

For each of the 8 time points, values are supplied at initialization for the time (t_i), the X, Y, Z components of $\vec{R}$ (Y_{i1}, Y_{i2}, Y_{i3} respectively), and the X, Y, Z components of $\vec{V}$ (Y_{i4}, Y_{i5}, Y_{i6} respectively).

The components of $\vec{R}$ and $\vec{V}$ are then computed as functions of time (t) according to

$$[\vec{R}]_E = \begin{bmatrix} Z_1 \\ Z_2 \\ Z_3 \end{bmatrix}, \quad [\vec{V}]_E = \begin{bmatrix} Z_4 \\ Z_5 \\ Z_6 \end{bmatrix}$$

$$Z_i \triangleq \sum_{j=1}^{8} Q_j Y_{ji}, \quad Q_i \triangleq \prod_{\substack{j=1 \\ j\neq i}}^{8} \frac{t - t_j}{t_i - t_j}$$

For the space station the orbital reference rate ($\vec{\omega}_r$) and the earth frame to orbit frame transformation matrix ($[T_{O/E}]$) are computed from

$$\vec{\omega}_r = \frac{1}{|\vec{R}|} (\vec{R} \times \vec{V})$$

$$\left[T_{O/E}\right] = \begin{bmatrix} \dfrac{1}{\left|\vec{\omega}_r\right|\left|\vec{R}\right|}\left[\vec{\omega}_r \times \vec{R}\right]_E^T \\ -\dfrac{1}{\left|\vec{\omega}_r\right|}\left[\vec{\omega}_r\right]_E^T \\ -\dfrac{1}{\left|\vec{R}\right|}\left[\vec{R}\right]_E^T \end{bmatrix}$$

This expression for $\vec{\omega}_r$ is an approximation which neglects the very small component along the orbital z-axis due to gravitational acceleration along the orbital y-axis (an earth oblateness effect). The expression for $[T_{O/E}]$ in terms of $\vec{R}$ and $\vec{V}$ is however exact, with $\vec{\omega}_r$ being used as an intermediate function of $\vec{R}$ and $\vec{V}$.

3.3.4 Earth Occultation of LØS (ØBSTCL)

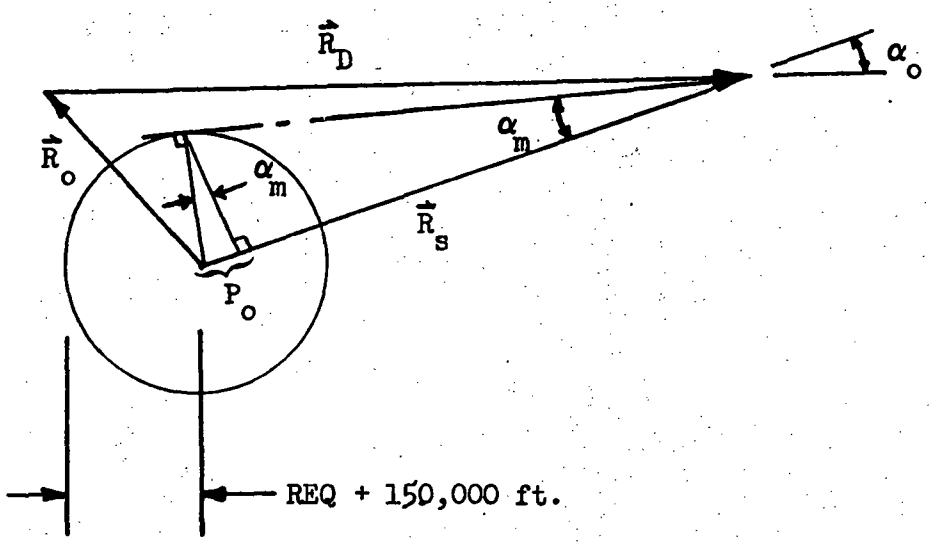

Figure 8.1 Earth Occultation Geometry

The object (relay satellite or ground station) located at $\vec{R}_s$ is considered to be visible from the station located at $\vec{R}_s$ if the line of sight between the station and the object does not pass through the sphere of radius REQ + 150000 ft centered at the center of the earth. This model neglects the oblate shape of the earth (a variation of about 70000 ft) and assumes no effect upon the line of sight above an altitude of 150000 ft.

The compulations are performed as follows: the angle (α_o) between $\vec{R}_s$ and $\vec{R}_D$ is compared with the angle (α_m) defined by

$$\alpha_m = \sin^{-1}\left(\frac{\text{REQ} + 150000}{|\vec{R}_s|}\right)$$

and if $\alpha_o > \alpha_m$ then the object must be visible and no further computations are required. If $\alpha_o < \alpha_m$ then the object will not be visible if it is on the opposite side of the horizon from the station, i.e., if the projection of $\vec{R}_o$ on $\vec{R}_s$ is less than P_o

$$\left.\begin{aligned} &\vec{R}_o \cdot \frac{\vec{R}_s}{|\vec{R}_s|} < P_o \\ &P_o = (REQ + 150000) \sin \alpha_m = \frac{(REQ + 150000)^2}{|\vec{R}_s|} \end{aligned}\right\} \Longrightarrow$$

$$\vec{R}_o \cdot \vec{R}_s < (REQ + 150000)^2$$

The condition for line of sight intersection with the earth (approximation) is then

$$\alpha_o < \alpha_m \text{ and } \vec{R}_o \cdot \vec{R}_s < (REQ + 150000)^2$$

3.3.5 Space Station Occultation of LOS (INTSS1 & 2)

Discussion

The objective of this function is to determine whether the line of sight (specified by the unit vector $\vec{S}$) orginating from the antenna gimbal point (specified by the position vector $\vec{R}$) passes through the space station ellipsoid envelope (specified by the relation $x^2/a^2 + y^2/b^2 + z^2/c^2 = 1$).

The method used is to analytically determine the minimum value of the quantity

$$Q \triangleq x^2/a^2 + y^2/b^2 + z^2/c^2$$

along the line

$$x = R_x + S_x d$$

$$y = R_y + S_y d$$

$$z = R_z + S_z d$$

(where d is the forward distance along the line of sight from the antenna gimbal point), and then to observe whether or not the minimum is less than 1 and occurs at a positive value of d. Both of these conditions being met indicates an intersection.

Setting the derivative of Q with respect to d equal to zero indicates that Q is minimum when d has the value

$$d_o = -\frac{S_x R_x/a^2 + S_y R_y/b^2 + S_z R_z/c^2}{(S_x/a)^2 + (S_y/b)^2 + (S_z/c)^2}$$

and the minimum value of Q is

$$Q_o = \left(\frac{R_x + S_x d_o}{a}\right)^2 + \left(\frac{R_y + S_y d_o}{b}\right)^2 + \left(\frac{R_z + S_z d_o}{c}\right)^2$$

In terms of these quantities the consition for line of sight intersection with the space station envelope is

$$d_o > 0 \text{ and } Q_o < 1$$

3.3.6 Gimbal Angles and Rates (ANTCØM)

Discussion

The equations which form the basis for ANTCØM are given below. The gimbal angles are obtained from the line of sight (LØS) vector coordinatized in the earth frame (E) assuming a roll, pitch (R/P) rotation from the platform frame (C) to the antenna frame (H). The object is to find the gimbal angles (α and β) which cause the LØS to align with the negative z axis of the antenna frame.

$$\underset{E}{L} = \underset{E}{RR} - \underset{E}{RA} \triangleq \text{LØS vector coordinatized in E frame}$$

$$\ell = \langle \underset{E}{L}, \underset{E}{L} \rangle^{\Delta} \text{ Magnitude of the LØS vector}$$

$$\underset{C}{L} = T_{C/E} \underset{E}{L} \triangleq \text{LØS vector coordinatized in C frame}$$

$$T_{H/C} = [\beta]_2 [\alpha]_1 \triangleq \text{Transformation from C frame to H frame}$$

$$[\alpha]_1 = \begin{bmatrix} 1 & 0 & 0 \\ 0 & C\alpha & S\alpha \\ 0 & -S\alpha & C\alpha \end{bmatrix} \triangleq \text{a rotation by } \alpha \text{ about the x axis } \left(\begin{matrix} S\alpha \triangleq \sin\alpha \\ C\alpha \triangleq \cos\alpha \end{matrix} \right)$$

$$[\beta]_2 = \begin{bmatrix} C\beta & 0 & -S\beta \\ 0 & 1 & 0 \\ S\beta & 0 & C\beta \end{bmatrix} \triangleq \text{a rotation by } \beta \text{ about the y axis}$$

$$\underset{H}{L} = \begin{bmatrix} 0 \\ 0 \\ -\ell \end{bmatrix} = \text{LØS vector in H frame after the gimbal rotations}$$

$$\text{Defining } \underset{C}{L} = \begin{bmatrix} \ell_1 \\ \ell_2 \\ \ell_3 \end{bmatrix}$$

$$\begin{bmatrix} 0 \\ 0 \\ -\ell \end{bmatrix} = \begin{bmatrix} C\beta & S\beta\, S\alpha & -S\beta\, C\alpha \\ 0 & C\alpha & S\alpha \\ S\beta & -C\beta\, S\alpha & C\beta\, C\alpha \end{bmatrix} \begin{bmatrix} \ell_1 \\ \ell_2 \\ \ell_3 \end{bmatrix}$$

Solving the above equations for α and β results in

$$\alpha = \tan^{-1}\left(\frac{\ell_2}{-\ell_3}\right)$$

$$\beta = \tan^{-1}\left(\frac{-\ell_1}{-\ell_3/C\alpha}\right)$$

i.e. $$(C\alpha)\,\ell_2 = -(S\alpha)\,\ell_3$$

$$\tan\alpha = \left(\frac{\ell_2}{-\ell_3}\right)$$

Where the signs are chosen to align the negative z_H axis with the LØS vector for $\beta = 0$.

Similarly

$$(C\beta)\,\ell_1 + (S\alpha\, S\beta)\,\ell_2 - (S\beta\, C\alpha)\,\ell_3 = 0$$

and $$-\ell_1 = [(S\alpha)\,\ell_2 - (C\alpha)\,\ell_3]\tan\beta$$

Noting that $(S\alpha)\,\ell_2 - (C\alpha)\,\ell_3 = \dfrac{(S\alpha)\,(C\alpha)\,\ell_2 - (C\alpha)^2\,\ell_3}{C\alpha}$

$$= -\frac{(S\alpha)^2\,\ell_3 - (C\alpha)^2\,\ell_3}{C\alpha} = -\frac{\ell_3}{C\alpha}$$

Hence

$$-\ell_1 = \left(\frac{-\ell_3}{C\alpha}\right) \tan \beta$$

or

$$\beta = \tan^{-1}\left(\frac{-\ell_1}{-\ell_3/C\alpha}\right)$$

where the signs were chosen (for $\alpha = 0$) to align the negative z_H axis with the LØS vector.

The determination of signs in this equation can also be arrived at from consideration of the third equation:

$$-\ell = \ell_1 \cdot S\beta - \ell_2\, C\beta\, S\alpha + \ell_3\, C\beta\, C\alpha$$

The expressions for the gimbal angle rates ($\dot{\alpha}$, $\dot{\beta}$) can be derived from the following starting point.

Assume that the following variables are known

ω^{C-I} = angular rate of the platform frame (C) with respect to an inertial frame (I)

$\overset{I}{RR}$ = time derivative of the relay orbit radius vector with respect to an inertial frame

$\overset{I}{RA}$ = time derivative of the platform orbit radius vector with respect to an inertial frame

$T_{C/E}$ = transformation from earth frame (E) to plaform frame (C)

α, β, $T_{H/C}$ – as defined previously

Since $\underset{L}{}\ = (RR - RA)$

$$\underset{L}{I} = \left(\underset{RR}{I} - \underset{RA}{I}\right)$$

then $\underset{L}{C} = -\left(\omega^{C-I} \times \underset{L}{}\right) + \underset{L}{I}$

and $\underset{L}{H} = \underset{L}{C} + \left(\omega^{C-H} \times , \underset{L}{}\right)$

$$= \underset{L}{C} - \left(\omega^{H-C} \times \underset{L}{}\right)$$

It is desirable to coordinatize the above equation in the antenna frame (H) since both L and $\underset{H}{L}$ have simple representations in that frame. Assuming the antenna to be tracking the LØS perfectly

$$\underset{H}{L} = \begin{bmatrix} 0 \\ 0 \\ -\ell \end{bmatrix} \quad \ell = \text{range}$$

$$\underset{H}{\overset{H}{L}} = \begin{bmatrix} 0 \\ 0 \\ -\dot{\ell} \end{bmatrix} \quad \dot{\ell} = \text{range rate}$$

Hence

$$\underset{H}{\overset{H}{L}} = \underset{H}{\overset{C}{L}} - \left(\underset{H}{\omega^{H-C}} \times \underset{H}{L}\right)$$

where

$$\underset{H}{\overset{C}{L}} = \begin{bmatrix} d_1 \\ d_2 \\ d_3 \end{bmatrix} \quad \text{(for convenience)}$$

$$\overset{H}{\omega}^{H-C} = \begin{bmatrix} 0 \\ \dot{\beta} \\ 0 \end{bmatrix} + \begin{bmatrix} C\beta & 0 & -S\beta \\ 0 & 1 & 0 \\ S\beta & 0 & C\beta \end{bmatrix} \begin{bmatrix} \dot{\alpha} \\ 0 \\ 0 \end{bmatrix} = \begin{bmatrix} C\beta\,\dot{\alpha} \\ \dot{\beta} \\ S\beta\,\dot{\alpha} \end{bmatrix}$$

$$\left(\overset{H}{\omega}^{H-C}{}_{x}\right) \triangleq \begin{bmatrix} 0 & -S\beta\,\dot{\alpha} & \dot{\beta} \\ S\beta\,\dot{\alpha} & 0 & -C\beta\,\dot{\alpha} \\ -\beta & C\beta\,\dot{\alpha} & 0 \end{bmatrix}$$

Combining the above

$$\begin{bmatrix} 0 \\ 0 \\ -\dot{\ell} \end{bmatrix} = \begin{bmatrix} d_1 \\ d_2 \\ d_3 \end{bmatrix} + \begin{bmatrix} \dot{\beta} \\ -C\beta\,\dot{\alpha} \\ 0 \end{bmatrix} \ell$$

Solving for $\dot{\alpha}$ and $\dot{\beta}$

$$\dot{\beta} = -\frac{d_1}{\ell}$$

$$\alpha = \frac{+d_2}{\ell \cdot C\beta}$$

range rate $\dot{\ell} = -d_3$

3.3.7 Calibration Model (CLBRTN)

The calibration model is a "best fit" of the error between the open loop generated gimbal angles and those gimble angle profiles which exist when the antenna is tracking via the monopulse RF link. The term "best fit" will be used in the sense of least square. The procedure for obtaining the best fit is described in the sequel.

When the antenna is tracking via the RF monopulse link the actual gimbal angles will be used as a reference. If the computer generated gimble angle commands were exactly correct there would be no difference between the generated command and the actual gimbal angles of the autotrack mode. However, due to misalignments, thermal distortions of the beam and other error sources, the computer generated commands will not be exactly correct. Hence, while in the autotrack mode the actual gimbal angles can be compared with the commanded to produce error data. This data can then be fitted to some selected model. See Figure 5.0-1.

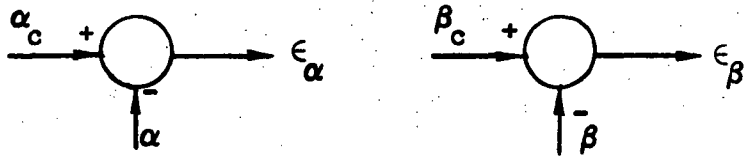

Figure 5.0-1 Comparison of Actual and Commanded Gimbal Angles During Autotrack Mode

The model which will be used in the simulation to represent the gimbal angle error is

$$\epsilon_\alpha = A_\alpha + B_\alpha \sin \omega_o(t-t_o) + C_\alpha \cos \omega_o(t-t_o)$$

$$\epsilon_\beta = A_\beta + B_\beta \sin \omega_o(t-t_o) + C_\beta \cos \omega_o(t-t_o)$$

where ω_o is the average orbit rate $\left(\frac{2\pi}{T}\right)$.

However, in order to illustrate the fitting procedure the following simple model will be used

$$\epsilon_\alpha = A_\alpha + B_\alpha \sin \omega_o(t-t_o)$$

$$\epsilon_\beta = A_\beta + B_\beta \sin \omega_o(t-t_o)$$

Defining $\underline{x} \triangleq \begin{bmatrix} A_\alpha \\ B_\alpha \end{bmatrix}$ (treating the axes independently)

$$\underline{Y} \triangleq \begin{bmatrix} \epsilon_\alpha(t_1) \\ \epsilon_\alpha(t_2) \\ \vdots \\ \epsilon_\alpha(t_n) \end{bmatrix} \triangleq \begin{bmatrix} \epsilon_{\alpha_1} \\ \epsilon_{\alpha_2} \\ \vdots \\ \epsilon_{\alpha_n} \end{bmatrix}$$

$$\underline{Y} = \begin{bmatrix} 1 & \sin \omega_o(t_1-t_o) \\ 1 & \sin \omega_o(t_2-t_o) \\ \vdots & \\ 1 & \sin \omega_o(t_n-t_o) \end{bmatrix} \underline{x} \triangleq \underline{\underline{H}}\, \underline{X}$$

The object is to find an $\underline{X} = \hat{\underline{X}}$ such that

$$\frac{1}{2} \langle \underline{Y} - \underline{\underline{H}}\, \hat{\underline{X}} , \underline{Y} - \underline{\underline{H}}\, \hat{\underline{X}} \rangle \triangleq \frac{1}{2} \langle \underline{z} , \underline{z} \rangle \triangleq J$$

is a minimum.

i.e. $$\frac{\partial J}{\partial \hat{\underline{x}}} = \underline{z}^T \frac{\partial \underline{z}}{\partial \hat{\underline{X}}} = (\underline{Y} - \underline{\underline{H}}\, \hat{\underline{X}})^T (-\underline{\underline{H}}) = \underline{0}^T$$

The above equation implies

$$+ \underline{\underline{H}}^T y = \underline{\underline{H}}^T \underline{\underline{H}} \hat{X}$$

Therefore if $[\underline{\underline{H}}^T \underline{\underline{H}}]$ has rank two $[\underline{\underline{H}}^T \underline{\underline{H}}]^{-1}$ exists and

$$\hat{\underline{X}} = [\underline{\underline{H}}^T \underline{\underline{H}}]^{-1} \underline{\underline{H}}^T \underline{y}$$

It is suggested that during the actual calibration that the data vector $\underline{y}$ be filled by taking points equally spaced around the orbit.

The simulation will contain the capability of adding in the error model specified previously, but it will be up to the user to generate the coefficients for the best fit. The simulation can be used to generate the data from which the fit can be made once all the important error sources have been added to the program. Bias and thermal errors will be the error sources which will be mainly compensated.

By doing this type of calibration it should be possible to reduce the overall pointing errors of the computer steering mode of operation. It will also reduce down times, i.e., if the monopulse momentarily looses track and the computer steering is immediately initiated, a reacquisition search mode requirement will be less likely.

3.4.1 Actual Dynamics, Kinematics, and Geometry Model

This section describes the mathematical model used by the simulation program for the environment in which the antenna system is to operate. Portions have been extracted from the Task 2 Report – Mathematical Model for the Pointing Requirements of the Space Station High Gain Antenna – dated 28 Oct. 1972, and the Task 3 Report – Math Modeling of Influence Factors – dated 22 May 1972.

The programming of this modeling is contained in subroutines KINMAT, ANTDYN, EPHEM1, EPHEM2, EPHEM3, SUN, and MØØN which are called by SETUP to determine the actual line of sight and sun vector directions.

3.4.2.0 Antenna Mounting Dynamics and Deflections (ANTDYN)

The antenna dynamics model has its origins in some work performed by G. Margulies*. This model was modified for further work at LMSC. The model at that stage was present in Appendix D of the original proposal for the "Computer Simulation of Space Station Computer Steered High Gain Antenna". The model contained within this section is a modification of those equations to meet the purpose and assumptions of this study. The resulting model is described in Section 3.1 of the Task 3 Report.

In order to include the effects of the antenna boom flexibility (and space station flexibility in general), the dynamics equations could not be separated from the flexibility equations. Hence a great deal of effort was required to obtain the equations describing the overall rigid body and flexibility model. To accomplish this most efficiently, the aid of G. Margulies and his associate J. Ho (of the R and D division of LMSC) was enlisted. The work presented is a condensation of the work done by J. Ho in May of 1972. It is felt that this resulting model correctly models the configuration of the space station gimballed antenna. However, there may be some difficulty in actually arriving at the required parameters associated with the flexibility model.

*G. Margulies, "Mathematical Model for the Attitude Dynamics of the Apollo Telescope Mount Satellite, LMSC/T-50-66-1, 12 December 1966.

3.4.2.1 Notations and Definitions

Square brackets ([ ]) are used here to indicate matrices with the symbol or symbols inside labelling the whole matrix (one symbol) or the individual elements (appropriate number of symbols) or partitioned submatrices (appropriate number of symbols spearated by dashed lines). Vectors and diadics (operators) are indicated by symbols with one or two (respectively) bars over them. When a vector or diadic symbol appears inside of a set of square brackets with a subscript P, or A this indicates the matrix of coordinates of the vector or diadic in the space station (P for platform) or antenna (A) reference frame.

The symbols used here are defined in the following lists.

Antenna Characteristics

$\bar{\bar{I}}_A \triangleq$ inertia diadic of antenna

$m_A \triangleq$ mass of antenna

$\bar{R}_2 \triangleq$ displacement vector, antenna center of mass to hinge point

$\bar{e}_\beta \triangleq$ unit vector in direction of antenna fixed gimbal axis

Space Station Characteristics

$m_P \triangleq$ space station mass

$\bar{R}_1 \triangleq$ displacement vector, undeformed space station center of mass to hinge point

$\bar{e}_\alpha \triangleq$ unit vector in direction of space station fixed gimbal axis

$\omega_q \triangleq$ bending mode frequency for free vibration of non-spinning space station in mode described by $\bar{\varphi}$ (below)

$\bar{\varphi} \triangleq$ bending deformation mode shape, a vector function of spatial coordinates which is analytic, has zero value and zero curl at the hinge point.

In the following definitions $\int_P (\ )\, dm$ indicates integration over the mass distribution of the space station, and $\bar{r}_1$ is the displacement vector from the hinge point to the element dm.

$$m_\varphi \triangleq \int_P \varphi^2 \, dm$$

$$\bar{\Phi} \triangleq \frac{1}{m_P} \int_P \bar{\varphi} \, dm$$

$$\bar{Y} \triangleq \frac{1}{m_P} \int_P (\bar{r}_1 \times \bar{\varphi}) \, dm$$

$$\bar{\bar{E}}_o \triangleq \frac{1}{m_P} \int_P \left\{ \varphi^2 \bar{\bar{E}} - \bar{\varphi}\,\bar{\varphi} \right\} dm \text{ , } \bar{\bar{E}} \text{ is unit diadic}$$

$$\bar{\bar{N}}^* \triangleq \frac{1}{m_P} \int_P \left\{ (\bar{\varphi} \cdot \bar{r}_1)\, \bar{\bar{E}} - \ddot{\bar{\varphi}}\, \bar{r}_1 \right\} dm$$

$\bar{\psi}_c \triangleq$ bending mode slope $\frac{1}{2} \bar{\nabla} \times \bar{\varphi}$ at control position

Variables

$\bar{\omega} \triangleq$ angular velocity of space station at hinge point

$\bar{\omega}_c \triangleq$ angular velocity of space station at control position

$\alpha \triangleq$ gimbal angle about $\bar{e}_\alpha$

$\beta \triangleq$ gimbal angle about $\bar{e}_\beta$

$q \triangleq$ bending coordinate in terms of which the translational and angular displacements of the space station due to bending are given respectively by $q\,\bar{\varphi}$ and $q\,\frac{1}{2} \bar{\nabla} \times \bar{\varphi}$

Forces

$T_\alpha \triangleq$ torque about gimbal axis $\bar{e}_\alpha$

$T_\beta \triangleq$ torque about gimbal axis $\bar{e}_\beta$

Derived Quantities

$$[G]_P \triangleq [\, [\bar{e}_\alpha]_P \;\vdots\; [\bar{e}_\beta]_P \,]$$

$$m_T \triangleq m_A + m_P$$

$$m_B \triangleq m_A\, m_P/m_T$$

$$\bar{\bar{R}}_{22} \triangleq m_B \left\{ (\bar{R}_2 \cdot \bar{R}_2)\, \bar{\bar{E}} - \bar{R}_2\, \bar{R}_2 \right\}$$

$$\bar{\bar{L}} \triangleq \bar{\bar{I}}_A + \bar{\bar{R}}_{22}$$

$$\bar{\eta} \triangleq \dot{\alpha}\, \bar{e}_\alpha + \dot{\beta}\, \bar{e}_\beta$$

$$\bar{\varepsilon} \triangleq \dot{\alpha}\, \dot{\beta}\, (\bar{e}_\alpha \times \bar{e}_\beta) + (\bar{\omega} \times \bar{\eta})$$

$$\bar{R}_1' \triangleq \bar{R}_1 - q\, \bar{\Phi}$$

$$\bar{b} \triangleq 2\, q\, \bar{\Phi} - \bar{\omega} \times \bar{R}_1'$$

$$\bar{Q}' \triangleq -(\bar{\omega} + \bar{\eta}) \times \bar{\bar{L}} \cdot (\bar{\omega} + \bar{\eta}) - \bar{\bar{L}} \cdot \bar{a} - m_B\, \bar{R}_2 \times (\bar{\omega} \times \bar{b})$$

$$\bar{\bar{R}}_{12}' \triangleq m_B \left\{ (\bar{R}_1' \cdot \bar{R}_2)\, \bar{\bar{E}} - \bar{R}_1'\, \bar{R}_2 \right\}$$

$$\bar{\bar{N}}' \triangleq \bar{\bar{L}} - \bar{\bar{R}}_{12}'$$

$$[\mathcal{L}]_P \triangleq m_B\, [\bar{R}_2 \times \bar{\Phi}\,]_P$$

$$M \triangleq m_\varphi - m_P^2 \bar{\Phi}^2/m_T$$

$$[\psi]_P \triangleq m_B \left[\bar{Y} + \left(\frac{m_P}{m_T} \bar{R}_1 - \frac{m_A}{m_T} \bar{R}_2 \right) \times \bar{\Phi} \right]_P$$

$$K \triangleq (m_\varphi - m_P \bar{\Phi}^2)\, \omega_q^2$$

$$\mathcal{F} \triangleq -K\, q + m_P\, \bar{\omega} \cdot (\bar{\bar{N}}^* + q\, \bar{\bar{E}}_o) \cdot \bar{\omega}$$

$$+ (m_P^2/m_T)\, \bar{\Phi} \cdot (\bar{\omega} \times \bar{b}) + m_B\, \bar{\Phi} \cdot \left\{ \bar{R}_1 \times \bar{a} - \bar{\omega} \times (\bar{\omega} \times \bar{R}_1) \right\}$$

3.4.2.2 Antenna Dynamics Equations

For the special case in which the space station dynamics are not considered and the space station rate $\bar{\omega}$, and acceleration $\dot{\bar{\omega}}$ are treated as known inputs the antenna dynamics equations may be expressed as

$$\left[\begin{array}{c|c} [G]^T\,[\bar{\bar{L}}]\,[G] & [G]^T\,[\mathscr{L}] \\ \hline [\mathscr{L}]^T\,[G] & M \end{array}\right] \left[\begin{array}{c} \ddot{\alpha} \\ \ddot{\beta} \\ \hline \ddot{q} \end{array}\right] =$$

$$\left[\begin{array}{c} [G]^T\,[\bar{Q}'] + \begin{bmatrix} T_\alpha \\ T_\beta \end{bmatrix} - [G]^T\,[\bar{\bar{N}}']\,[\dot{\bar{\omega}}] \\ \hline \mathscr{L} - [\psi]^T\,[\dot{\bar{\omega}}] \end{array}\right] \qquad \text{Eq. 3.0.1}$$

where the subscript P has been dropped from $[G]_P$, $[\bar{\bar{L}}]_P$, $[\mathscr{L}]_P$, $[\bar{Q}']_P$, $[\bar{\bar{N}}']_P$, $[\psi]_P$, and $[\dot{\bar{\omega}}]_P$ both for clarity and to emphasize the fact that the equations are independent of the reference frame chosen for coordinatization.

Equation 3.0.1 was obtained from Ref. 2 by straightforward translation to the notation of Ref. 1 followed by specialization to the antenna dynamics only case considered here.

Since the space station is not rigid its angular velocity is not unique. The $\bar{\omega}$ which appears in Equation 3.0.1 is the space station angular velocity at the hinge point which is not in general the controlled part of the space station for which the angular velocity $\bar{\omega}_c$ and acceleration $\dot{\bar{\omega}}_c$ are known. These quantities are related by characteristics of the bending mode shape:

$$\bar{\omega}_c = \bar{\omega} + \dot{q}\,\bar{\psi}_c \qquad \text{Eq. 3.0.2}$$

$$\dot{\bar{\omega}}_c = \dot{\bar{\omega}} + \ddot{q}\,\bar{\psi}_c \qquad \text{Eq. 3.0.3}$$

Since $\ddot{q}$ is a state variable Eq. 3.0.2 may be used to compute $\bar{\omega}$ from the input $\bar{\omega}_c$. However $\ddot{q}$ is not a state variable and is not available for the analogous computation of $\dot{\bar{\omega}}$, hence Eq. 3.0.3 is combined with Eq. 3.0.1 to obtain

$$\left[\begin{array}{c|c} [G]^T [\bar{\bar{L}}] [G] & [G]^T \left([\bar{\mathcal{L}}] - [\bar{\bar{N}}'] [\bar{\Psi}_c]\right) \\ \hline [\bar{\mathcal{L}}]^T [G] & M - [\psi]^T [\bar{\Psi}_c] \end{array}\right] \left[\begin{array}{c} \ddot{\alpha} \\ \ddot{\beta} \\ \hline \ddot{q} \end{array}\right] =$$

$$\left[\begin{array}{c} [G]^T [\bar{Q}'] + \left[\begin{array}{c} T_\alpha \\ T_\beta \end{array}\right] - [G]^T [\bar{\bar{N}}'] [\dot{\bar{\omega}}_c] \\ \hline \mathcal{L} - [\psi]^T [\dot{\bar{\omega}}_c] \end{array}\right] \qquad \text{Eq. 3.0.4}$$

These equations are used in the simulation program to compute the derivatives $\ddot{\alpha}$, $\ddot{\beta}$, and $\ddot{q}$ of the state variables $\dot{\alpha}$, $\dot{\beta}$, and $\dot{q}$ respectively from the state variables and the driving quantities T_α, T_β, $\bar{\omega}_c$, and $\dot{\bar{\omega}}_c$ supplied by other elements in the program.

3.4.2.3 Bending Inputs for Sample Mode Shape

As an example of a flexible S/S model consider the simple case of a rigid main body with a flexible antenna mounting boom depicted below.

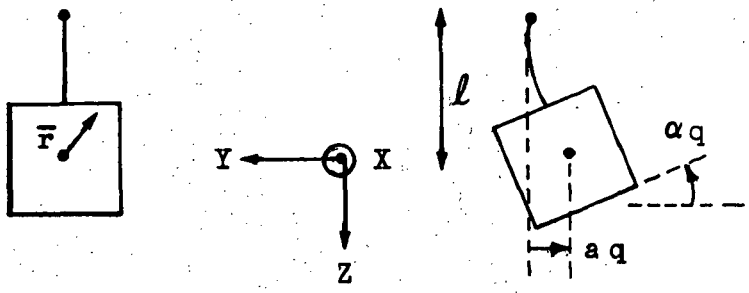

If the flexible boom is taken to be of negligible mass then the modal displacement $\bar{\varphi}$ is only important for the main body, where it may be expressed as

$$\bar{\varphi}(\bar{r}) = -a\hat{j} - \alpha Z\hat{j} + \alpha Y\hat{k} \Rightarrow$$

$$[\bar{\varphi}]_P = \begin{bmatrix} 0 \\ -a - \alpha Z \\ \alpha Y \end{bmatrix}$$

The bending inputs for this mode shape are evaluated as follows:

$$m_\varphi \triangleq \int_P \varphi^2 dm = \int_P \left\{ (a + \alpha Z)^2 + (\alpha Y)^2 \right\} dm \equiv \ldots$$

$$\equiv m_P a^2 + \alpha^2 I_{XX}^P$$

$$[\bar{\Phi}]_P \triangleq \frac{1}{m_P}\int_P [\bar{\varphi}]_P \, dm = \frac{1}{m_P}\int_P \begin{bmatrix} 0 \\ -a-\alpha Z \\ \alpha Y \end{bmatrix} dm$$

$$= \begin{bmatrix} 0 \\ -a \\ 0 \end{bmatrix}$$

$$[\bar{\bar{E}}_o]_P \triangleq \frac{m_\varphi}{m_P}\mathbb{1} - \frac{1}{m_P}\int_P [\bar{\varphi}\,\bar{\varphi}]_P \, dm =$$

$$\frac{m_\varphi}{m_P}\mathbb{1} - \frac{1}{m_P}\begin{bmatrix} 0 & 0 & 0 \\ 0 & a^2 m_P + \alpha^2 I_Z^P & \alpha^2 I_{YZ}^2 \\ 0 & \alpha^2 I_{YZ}^P & \alpha^2 I_Y^P \end{bmatrix} \equiv \ldots$$

$$\equiv \frac{\alpha^2}{m_P}\begin{bmatrix} \frac{1}{\alpha^2} m_P a^2 + I_{XX}^P & 0 & 0 \\ 0 & I_Y^P & -I_{YZ}^P \\ 0 & -I_{YZ}^P & \frac{1}{\alpha^2} m_P a^2 + I_Z^P \end{bmatrix}$$

$$[\bar{\bar{N}}^*]_P \triangleq \frac{1}{m_P}\int \left\{(\bar{\varphi}\cdot\bar{r}_1)\mathbb{1} - [\bar{\varphi}\,\bar{r}_1]_P\right\} dm \equiv \ldots$$

$$\equiv \frac{\alpha}{m_P}\begin{bmatrix} 0 & 0 & 0 \\ -I_{XZ}^P & -I_{YZ}^P & I_Z^P + m_P\frac{a\ell}{\alpha} \\ I_{XY}^P & I_Y^P & I_{YZ}^P \end{bmatrix}$$

$$[\bar{\gamma}]_P \triangleq \frac{1}{m_P}\int_P [\bar{r}_1 \times \bar{\varphi}]_P \, dm \equiv \ldots$$

$$\equiv \frac{\alpha}{m_P}\begin{bmatrix} I_{XX}^P + m_P \frac{a\ell}{\alpha} \\ I_{XY}^P \\ I_{XZ}^P \end{bmatrix}$$

$$[\bar{\gamma}_c]_P \equiv \begin{bmatrix} \alpha \\ 0 \\ 0 \end{bmatrix} \text{ for control system on main body.}$$

The mass distribution parameters (inertias) used in the above results are defined as:

$$I_X^P \triangleq \int_P X^2 \, dm, \text{ similarly for Y \& Z}$$

$$I_{XY}^P \triangleq \int_P XY \, dm, \text{ similarly for XZ \& YZ}$$

$$I_{XX}^P \triangleq I_Y^P + I_Z^P, \text{ similarly for YY \& ZZ}$$

3.4.3 Actual Kinematics (KINMAT)

The mathematical model for obtaining the space station attitude from the space station angular rate and the orbital rate is identical to that used by the on board kinematics computations (Section 3.3.2).

3.4.4 Vehicle Ephemerides

Mathematical Discussion

The equations used by subroutine EPHEM1 to compute the satellite ephemeris information are derived in the LMSC document The Motion of a Satellite About an Oblate Earth, H. W. Small, Nov. 10, 1961, LMSC/A086756, and are more clearly presented in the LMSC document The Motion of a Satellite About an Oblate Earth – A Guide to the use of the Solution, P. Norov, Nov. 29, 1962, LMSC/A340246. The statement of these equations without the derivation is presented here.

The position vector $\vec{R}$ and the inertial velocity vector $\vec{V}$ coordinatized in the earth reference frame are obtained from the instantaneous orbit elements P, A, B, i, Ω, u by the relations

$$\vec{R} = \frac{P}{1 + A \cos u + B \sin u}\,\hat{e}_R$$

$$\vec{V} = \sqrt{\frac{\mu}{P}}\left[\left(1 + A \cos u + B \sin u\right)\hat{e}_L + \left(A \sin u - B \cos u\right)\hat{e}_R\right]$$

where $\mu = 1.407645 \times 10^{16}\ ft^3/sec^2$,

$$\hat{e}_R = \begin{bmatrix} \cos u \cos \Omega - \sin u \cos i \sin \Omega \\ \cos u \sin \Omega + \sin u \cos i \cos \Omega \\ \sin u \sin i \end{bmatrix}, \text{ and}$$

$$\hat{e}_L = \begin{bmatrix} -\sin u \cos \Omega - \cos u \cos i \sin \Omega \\ -\sin u \sin \Omega + \cos u \cos i \cos \Omega \\ \cos u \sin i \end{bmatrix}$$

The first five of these instantaneous orbit elements are obtained from the mean orbit elements P_B, e_B, ω_B, i_B, Ω_B (which are constants) and u by the relations

$$P = P_B (1 + \bar{J}_2 \alpha_1 \sin^2 i_B)$$

$$A = A_o + B_o G - \bar{J}_2 [(1 - e_B^2) \cos u (P_2 + \sin^2 i_B \cos^2 u) + P_2 \psi_o (A_o + (1 + \psi_o) \cos u]$$

$$B = B_o - A_o G - \bar{J}_2 [(1 - e_B^2) \sin u (P_2 - \sin^2 i_B \sin^2 u) + P_2 \psi_o (B_o + (1 + \psi_o) \sin u]$$

$$i = i_B + \frac{1}{2} \bar{J}_2 \alpha_1 \sin i_B \cos i_B$$

$$\Omega = \Omega_B - (\frac{3}{2} \bar{J}_2 \cos i_B) u + \bar{J}_2 \alpha_2 \cos i_B$$

where

$$\bar{J}_2 \triangleq J_2 \left(\frac{R_{EQ}}{P}\right)^2 = .0010827 \left(\frac{20925741}{P}\right)^2$$

$$\alpha_1 \triangleq \frac{3}{2} (\cos^2 u - \sin^2 u) + 2 (A_o \cos^3 u - B_o \sin^3 u)$$

$$\alpha_2 \triangleq \frac{3}{2} \sin u \cos u + 3 B_o \cos u - A_o \sin^3 u - B_o \cos^3 u$$

$$A_o \triangleq e_B \cos [\omega_B + \frac{3}{2} \bar{J}_2 (2 - \frac{5}{2} \sin^2 i_B) u]$$

$$B_o \triangleq e_B \sin [\omega_B + \frac{3}{2} \bar{J}_2 (2 - \frac{5}{2} \sin^2 i_B) u]$$

$$G \triangleq \bar{J}_2 \alpha_2 (1 - \frac{5}{2} \sin^2 i_B) - \frac{3}{2} \bar{J}_2 (A_o \sin u - B_o \cos u)$$

$$P_2 \triangleq \frac{3}{2} \sin^2 i_B \sin^2 u - \frac{1}{2}$$

$$\psi_o \triangleq 1 + A_o \cos u + B_o \sin u$$

while u is obtained by numerically integrating the equation

$$\dot{u} = \sqrt{\frac{\mu}{p^3}} \left(1 + A \cos u + B \sin u\right)^2 \left[1 + 3 \bar{J}_2 \left(\frac{P_B}{P}\right)^2 \cos^2 i \sin^2 u \; x \left(1 + A \cos u + B \sin u\right)\right]$$

The transformation $T_{O/E}$ from the earth reference frame to the orbit reference frame and the inertial angular velocity of the orbit reference frame ω^{O-I} are obtained from a 313 euler angle transformation with angles Ω_E, i, u_m and rates $\dot{\Omega}$, $\dot{i}$, $\dot{u}$ where

$\Omega_E = \Omega - \omega_E t$, $\omega_E \triangleq$ angular velocity of earth $= .72921321 \times 10^{-4}$ sec^{-1}

i = i defined above

u_m = u modulo 2π

$$\dot{\Omega} = \left[-3 \bar{J}_2 \left(\frac{P_a}{P}\right)^2 \sqrt{\frac{\mu}{p^3}} \left(1 + A \cos u + B \sin u\right)^3 \cos i\right] \sin^2 u$$

$$\dot{i} = \left[-3 J_2 \left(\frac{P_a}{P}\right)^2 \sqrt{\frac{\mu}{p^3}} \left(1 + A \cos u + B \sin u\right)^3 \cos i\right] \cos u \sin i$$

$\dot{u}$ = u defined above

followed by the interchange of axes given by the transformation

$$T_x = \begin{bmatrix} 0 & 1 & 0 \\ 0 & 0 & -1 \\ -1 & 0 & 0 \end{bmatrix}$$

3.4.5 Sun Ephemeris

Mathematical Discussion

In the initialization section, Subroutine SUN first converts the input date (e.g., 062767 for June 27, 1967) to Modified Julian Date (MJD), which is defined as

$$\text{Modified Julian Date} = \text{Julian Day Number} - 2{,}400{,}000.5,$$

where the Julian Day Number is the number of days which have elapsed from Greenwich mean noon on January 1, 4713 B.C. (Julian proleptic calendar), to Greenwich mean noon on the calendar date in question. (Thus, at noon June 27, 1967, JD = 2,439,662, and MJD = 39,661.5.) The MJD is thus a measure of the JD in which the "24" is dropped and the day advances one unit at midnight rather than at noon.

The mean orbit elements of the sun at midnight (o^h GMT) beginning the input date (or the following day if the seconds part of the base time is greater than 86,400) are computed from formulas referred to an epoch date of January 1.0, 1900 (midnight beginning January 1, 1900, MJD 15020) rather than January 0.5, 1900 (noon on December 31, 1899) as in Ref. 1, the Explanatory Supplement to the American Ephemeris and Nautical Almanac. The distinction between Greenwich Mean Time (or UT, Universal Time) and ephemeris time ET is ignored for these purposes. Let d be the number of ephemeris days which have elapsed from the epoch date to the base midnight date:

$$d = \text{MJD} - 15{,}020. \qquad \text{(NDAY (3))}$$

also, let T be this time period measured in Julian centuries of 36525 ephemeris days:

$$T = \frac{d}{36525} \qquad \text{(TCNTRY)}$$

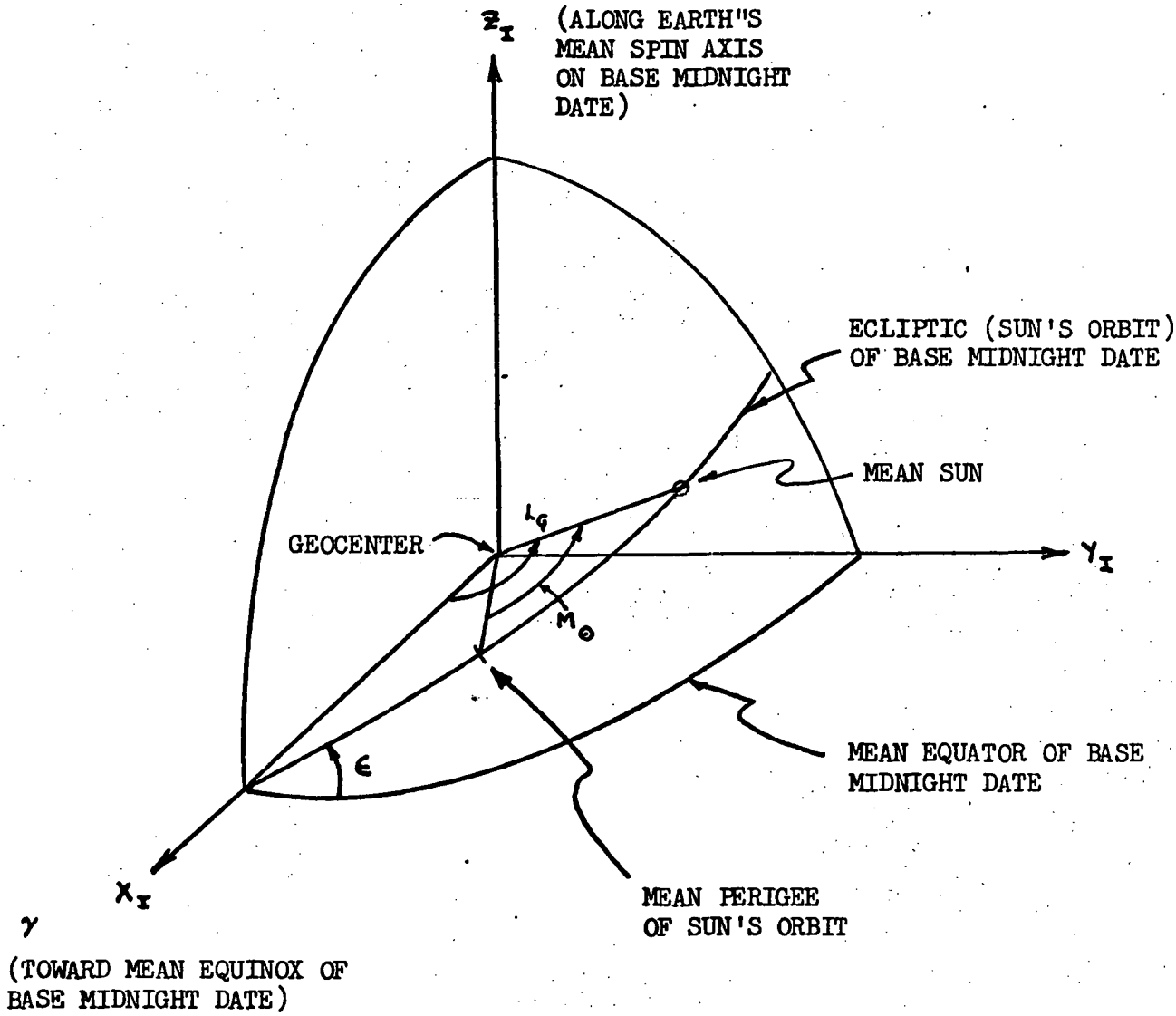

Figure 6.1 The Inertial Coordinate System and Solar Angular Orbit Elements

Then the mean elements of the sun with respect to an inertial coordinate frame (Fig. 1) referred to the mean equator and equinox of the base midnight date are given by the following expressions (cf. Ref. 1, p. 98):

Mean anomaly $M_\odot$, measured from mean perigee of the sun's orbit, along the ecliptic to the mean sun:

$$M_{\odot,\,B} = 358^\circ.96863013 + (1^\circ - ^\circ.014399733)\,d - ^\circ.00015\,T^2 - ^\circ.000003\,T^3 \quad . \qquad (CM)$$

Mean eccentricity $e_\odot$:

$$e_{\odot,B} = .0167510394 - .00004180\,T - .000000126\,T^2 \qquad (ECC)$$

Mean obliquity of the ecliptic ϵ:

$$\epsilon_B = 23^\circ.45229382 - ^\circ.0130125\,T - ^\circ.00000164\,T^2 + ^\circ.000000503\,T^3. \qquad (OBL)$$

Geometric mean longitude $L_\odot$, measured from the mean equinox of the base midnight date, along the ecliptic to the mean sun:

$$L_{\odot,B} = 280^\circ.18950367 + (1^\circ - ^\circ.0143526646)\,d + ^\circ.000303\,T^2. \qquad (CL)$$

All of the angles are taken modulo 360° and converted to radians.

In addition to the base solar elements, the Greenwich mean sidereal time (GMST), also referred to as the right ascension of Greenwich α_G or (imprecisely) the Greenwich hour angle GHA is computed at the base midnight date:

$$\alpha_{G,B} = 100^\circ.1811849 + (1^\circ - ^\circ.0143526646)\,d. \qquad (COMG)$$

$\alpha_{G,B}$ is also taken modulo 360° and converted to radians.

On subsequent calls, Subroutine SUN computes the inertial and earth-referenced direction cosines of the true sun at any time T (in seconds) after the input base time of the run, or TIME = TIMERF + T seconds after the base midnight date: starting from the mean angular elements at this time,

$$M_\odot = M_{\odot,B} + 1.9909687222 \times 10^{-7} \cdot \text{TIME} \quad \text{rad.} \qquad \text{(AM)}$$

$$L_\odot = L_{\odot,B} + 1.99106380\text{4} \times 10^{-7} \cdot \text{TIME} \quad \text{rad.,} \qquad \text{(AL)}$$

the true longitude of the sun $\Lambda_\odot$ is found by computing the equation of the center $\epsilon_\odot$ from a series expansion in the mean anomaly (Ref. 2, p. 77):

$$\Lambda_\odot = L_\odot + \dot{\epsilon}_\odot, \qquad \text{rad,} \qquad \text{(ARGS)}$$

where

$$\dot{\epsilon}_\odot = (2e - \tfrac{1}{4}e^3)\sin M + (\tfrac{5}{4}e^2 - \tfrac{11}{24}e^4)\sin 2M + \tfrac{13}{12}e^3 \sin 3M + \tfrac{103}{96}e^4 \sin 4M \qquad \text{(DARG)}$$

$$= [(\tfrac{5}{2} + \tfrac{27}{8}e^2\cos^2 M - \tfrac{125}{24}e^2\sin^2 M)\, e\cos M + (2 + 3e^2\cos^2 M - \tfrac{4}{3}e^2\sin^2 M)]\, e\sin M,$$

and e is written for $e_{\odot,B}$.

The error in truncating this series expansion at the e^4 term is of order e^5, or 1×10^{-9} radians. The inertial direction cosines of the true sun are then

$$\begin{bmatrix} \ell_{\odot,I} \\ m_{\odot,I} \\ n_{\odot,I} \end{bmatrix} = \begin{bmatrix} \cos\Lambda_\odot & \\ \sin\Lambda_\odot & \cos\epsilon_B \\ \cos\Lambda_\odot & \sin\epsilon_B \end{bmatrix} . \qquad \text{(SI)}$$

To find the direction cosines in the earth-fixed coordinate system, the earth-to-inertial transformation matrix T_{EI} is used: At TIME seconds after the base midnight date, the GMST is

$$\alpha_G = \alpha_{G,B} + \Omega_{EI} \cdot \text{TIME} \qquad \text{rad.}, \tag{OMG}$$

where Ω_{EI} is the inertial rotation rate of the earth,

$$\Omega_{EI} = 7.29211514\overline{7} \times 10^{-5} \text{ rad/sec.} \tag{OMGE}$$

Neglecting precession and nutation effects, T_{EI} may be written

$$T_{EI} = \begin{bmatrix} \cos \alpha_G & -\sin \alpha_G & 0 \\ \sin \alpha_G & \cos \alpha_G & 0 \\ 0 & 0 & 1 \end{bmatrix}, \tag{ETI}$$

so that the earth-referenced direction cosines of the true sun are

$$\begin{bmatrix} \ell_{\odot,E} \\ m_{\odot,E} \\ n_{\odot,E} \end{bmatrix} = (T_{EI})^T \begin{bmatrix} \ell_{\odot,I} \\ m_{\odot,I} \\ n_{\odot,I} \end{bmatrix} . \tag{SE}$$

The magnitude of the radius vector from the earth to the sun is then calculated. In astronomical units, it is given by

$$R_\odot = \frac{(1 - e^2)}{1 + e \cos (M_\odot + \xi_\odot)} . \tag{PAU}$$

Subroutine SUN also determines whether the satellite is in sunlight or not. The conditions which must be satisfied for the satellite to lie in the (cylindrical) shadow of the earth are (Fig. 2)

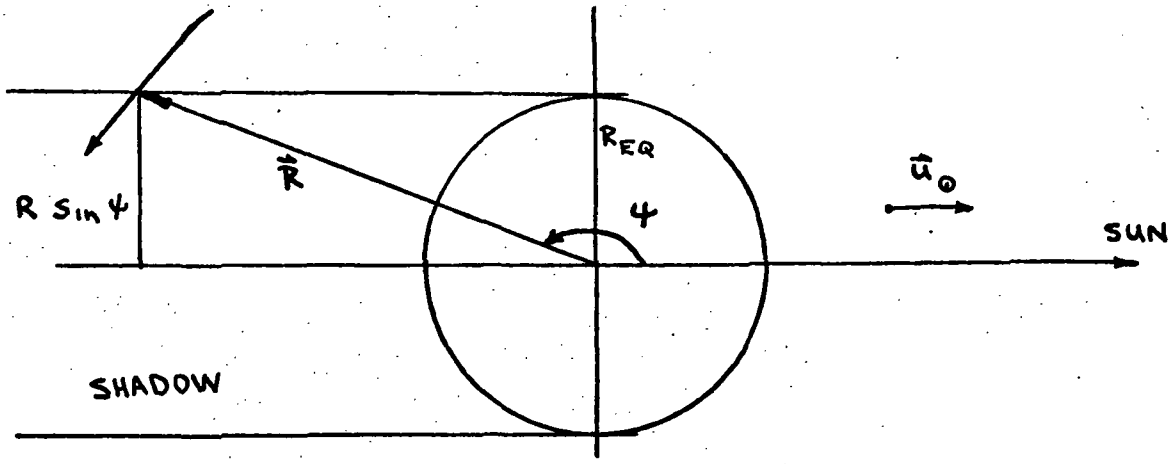

Figure 6.2 Geometry for Satellite in Earth's Shadow

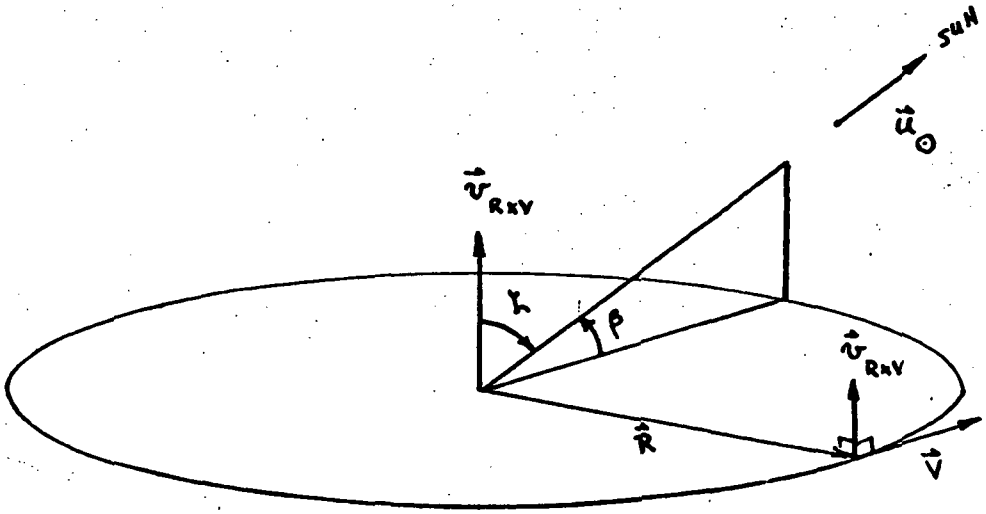

Figure 6.3 Orbit Beta Angle

$$\cos \psi < 0$$

$$R \sin \psi < R_{EQ} ,$$

where R_{EQ} is the earth's equatorial radius, R is the satellite radial distance, and ψ is the geocentric angle between the sun and the satellite. If $\vec{u}_\odot$ is the earth-frame unit vector in the solar direction, then the above conditions can be written in the vector form

$$\vec{R} \cdot \vec{u}_\odot < 0$$

$$\left| \vec{R} \times \vec{u}_\odot \right| < R_{EQ} .$$

The integer NIGHT is set to 1 if the satellite is in shadow and 0 if it is in sunlight.

Finally, SUN calculates the "orbit beta angle" β (Fig. 3), which is the angle between the solar direction unit vector $\vec{u}_\odot$ and its projection on the satellite orbital plane. If ζ is the angle between $\vec{u}_\odot$ and a vector normal to the orbit plane,

$$\sin \zeta = \left| \vec{u}_\odot \times \vec{v}_{RXV} \right| , \qquad \text{(SBETA)}$$

then

$$\beta = 90° - \zeta . \qquad \text{(BETA)}$$

REFERENCES (For Section 3.4.5)

1. Explanatory Supplement to the American Ephemeris and Nautical Almanac, H. M. Stationery Office, London, 1961.

2. Methods of Celestial Mechanics, D. Brouwer and G. M. Clemence, Academic Press, New York, 1961.

3.4.6 Moon Ephemeris

Mathematical Discussion

In the Initialization Section, Subroutine MOON computes the mean orbit elements of the moon at the base midnight date (see SUN Mathematics Section). If T is the time elapsed from an epoch date of January 0.5, 1900 (noon on December 31, 1899),

$$T = \frac{MJD - 15,019.5}{36525} , \qquad \text{(TCNTRY)}$$

then the mean elements with respect to the inertial coordinate system described earlier (Fig. 1 of Subroutine SUN section) are given by the following expressions (Ref.: Explanatory Supplement to the American Ephemeris and Nautical Almanac):

Mean anomaly $M_{\mathbb{C}}$, measured from the mean lunar perigee along the orbit to the mean moon: $M_{\mathbb{C}} = \mathbb{C} - \Gamma'$,

$$M_{\mathbb{C},B} = 296.^{\circ}104608 + 477,198.^{\circ}849108\ T + .^{\circ}009190\ T^2 + .^{\circ}0000032\ T^3 . \qquad \text{(AM1)}$$

Longitude of the mean ascending node $\Omega_{\mathbb{C}}$, measured from the mean equinox of date along the ecliptic:

$$\Omega_{\mathbb{C},B} = 259.^{\circ}183275 - 1934.^{\circ}14201\ T + .^{\circ}002077\ T^2 + .000002\ T^3 . \qquad \text{(ØM1)}$$

Mean argument of perigee $\omega_{\mathbb{C}}$, measured from the mean ascending node along the lunar orbit: $\omega_{\mathbb{C}} = \Gamma' - \Omega_{\mathbb{C}}$,

$$\omega_{\mathbb{C},B} = 75.^{\circ}146281 + 6003.^{\circ}176041\ T - .^{\circ}012402\ T^2 - .^{\circ}000015\ T^3 . \qquad \text{(WM1)}$$

These angles are all taken modulo 360° and converted to radians. In addition, the following mean elements are considered as constants:

Mean eccentricity $e_{\mathbb{C}}$:

$$e_{\mathbb{C},B} = .054900489 \qquad \text{(ECCM)}$$

Mean inclination $i_{\mathbb{C}}$:

$$\sin i_{\mathbb{C},B} = .089683448 \qquad \text{(SINI)}$$

$$\cos i_{\mathbb{C},B} = .99597032 \qquad \text{(COSI)}$$

Mean semi-latus rectum, $P_{\mathbb{C}} = a_{\mathbb{C}} (1 - e_{\mathbb{C}}^2)$:

$$P_{\mathbb{C},B} = 1.257355 \times 10^9 \text{ ft.} \qquad \text{(PM)}$$

On subsequent calls, Subroutine MOON computes the distance and inertial coordinate frame conponents of the true moon at any time T (in seconds) after the input base time of the run, or TIME = TIMERF + T seconds after the base midnight date: starting from the mean angular elements at this time,

$$M_{\mathbb{C}} = M_{\mathbb{C},B} + .228027135 \cdot \tau \text{ rad.} \qquad \text{(AM)}$$

$$\Omega_{\mathbb{C}} = \Omega_{\mathbb{C},B} - .00092422029 \cdot \tau \text{ rad.} \qquad \text{(ØM)}$$

$$\omega_{\mathbb{C}} = \omega_{\mathbb{C},B} + .0028685883 \cdot \tau \text{ rad.} ,$$

where

$$\tau = \text{TIME}/86{,}400, \qquad \text{(TIME)}$$

The true anomaly of the moon $\theta_{\mathbb{C}}$ is found by computing the equation of the center $\dot{\epsilon}_{\mathbb{C}}$ from a series expansion in the mean anomaly (see SUN Mathematics Section):

$$\theta_{\mathbb{C}} = M_{\mathbb{C}} + \dot{\epsilon}_{\mathbb{C}}, \qquad \text{rad} \qquad \text{(THM)}$$

where

$$\epsilon_{\mathbb{C}} = 2e_{\mathbb{C},B} \sin M_{\mathbb{C}} + \frac{5}{4} e^2_{\mathbb{C},B} \sin 2M_{\mathbb{C}} .$$

The error in truncating this series expansion at the e^2 term is of order e^3, or .0002 radians.

The magnitude of the geocentric radius vector is then

$$R_{\mathbb{C}} = \frac{P_{\mathbb{C},B}}{1 + e_{\mathbb{C},B} \cos \theta_{\mathbb{C}}} , \qquad \text{(RMS)}$$

and its components in the inertial coordinate system are

$$\begin{bmatrix} x_{\mathbb{C},I} \\ y_{\mathbb{C},I} \\ z_{\mathbb{C},I} \end{bmatrix} = \begin{bmatrix} \cos \Omega_{\mathbb{C}} \cos u_{\mathbb{C}} - \cos i_{\mathbb{C},B} \sin \Omega_{\mathbb{C}} \sin u_{\mathbb{C}} \\ (\sin \Omega_{\mathbb{C}} \cos u_{\mathbb{C}} + \cos i_{\mathbb{C},B} \cos \Omega_{\mathbb{C}} \sin u_{\mathbb{C}}) \cos \epsilon_B \\ \qquad - \sin i_{\mathbb{C},B} \sin u_{\mathbb{C}} \sin \epsilon_B \\ (\sin \Omega_{\mathbb{C}} \cos u_{\mathbb{C}} + \cos i_{\mathbb{C},B} \cos \Omega_{\mathbb{C}} \sin u_{\mathbb{C}}) \sin \epsilon_B \\ \qquad + \sin i_{\mathbb{C},B} \sin u_{\mathbb{C}} \cos \epsilon_B \end{bmatrix}$$

where

$$u_{\mathbb{C}} = \theta_{\mathbb{C}} + \omega_{\mathbb{C}} \qquad \text{(UM)}$$

and ϵ_B is the mean obliquity of the ecliptic, calculated in Subroutine SUN.

APPENDIX A

DECK SETUP AND INPUT LISTS

This appendix describes the format and ordering of the data cards which are read by the program to enter the input data.

Data cards are placed in the deck immediately after the program execution card (∇ XQT LØØP for the complete simulation program or ∇ XQT PØINT for the pointing requirements program) and are arranged as follows:

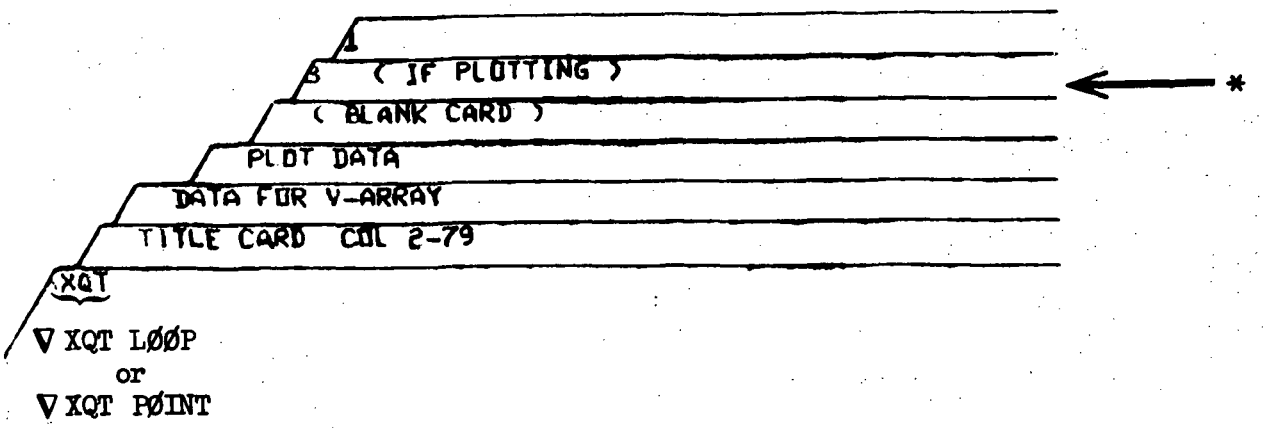

If more than one case is to be run, one or more blocks of the following might be inserted between the blank card and the "3" card (at *).

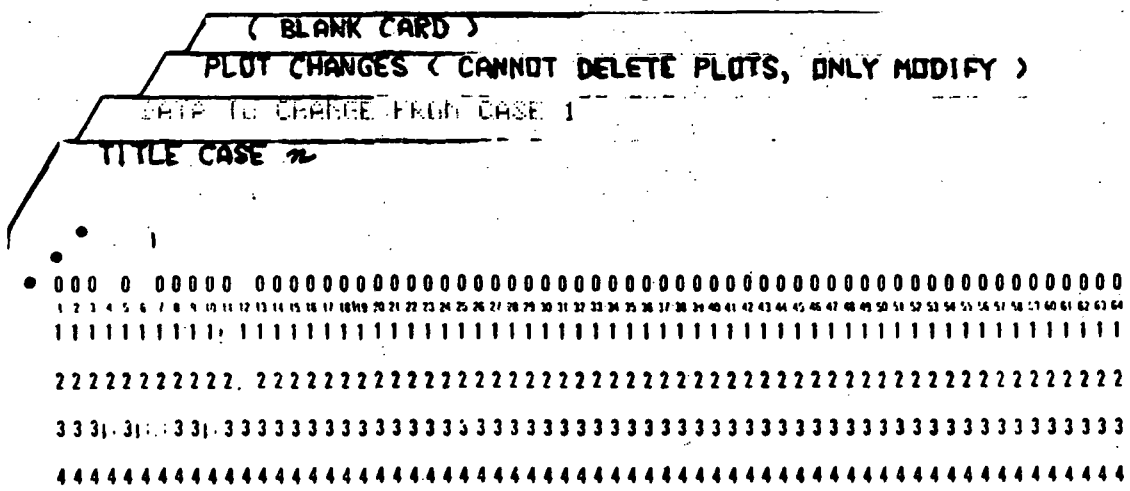

To change the "nominal" data, i.e. clear V-ARRAY and PREAD information before inputing the next set, place a "2" card, (a 2 in column one) before the desired title card.

CARD FORMATS

Title

Column 1 must be blank (see General Comments at end for extended feature)

Data for V-array

The data for the V-array is input in free field format:

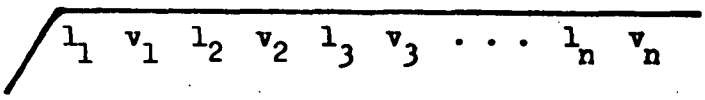

where l_i is a V-array position index and v_i is the data value associated with $V(l_i)$. Blank(s) (at least one) must separate the l_i and v_i, and l_1 need not start in column one.

The l_i are in integer format with no included blank(s) allowed since blank(s) are separators.

The v_i may use any of the following formats:

Integer - no decimal point in number

Fixed point - value has a decimal point

Exponential - number followed by the exponent as in floating point number.

All the following are valid and equivalent.

42.5, 4.25 + 1, 4.25E1, 425E-1

Example:

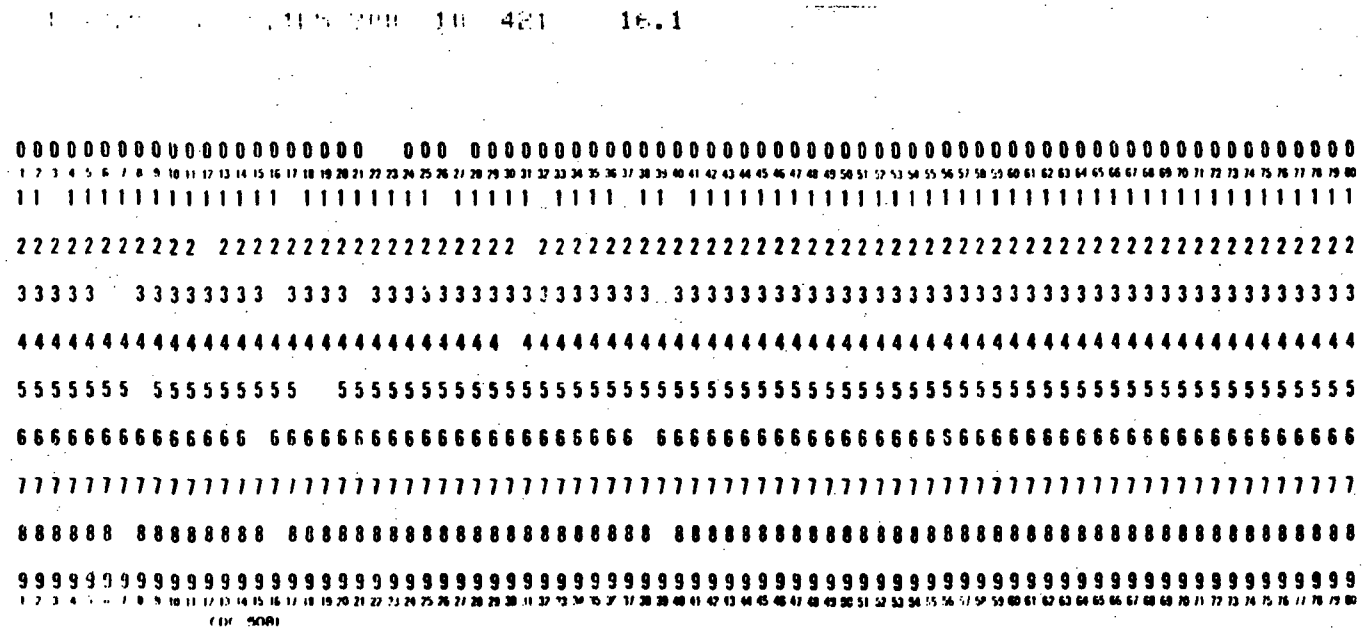

**** DATA MUST BE PAIRED, i.e., EVERY l_i MUST HAVE A v_i ****

PLOT DATA

Plots from the DEADAM package are available in four forms (see Appendix A).

The first three are closely related since their formats are derived from the same array (PREAD). For discussion, they will be referred to as Full frame, 1/3 frame, both produced on the FR-80, and printer plots plotted on the high speed printer.

These three plot forms are specified in the following manner.

Full and 1/3 frame -

P p_1 d_1 p_2 d_2 . . . p_i d_i ; i - 1, 10

p_i is the plot number

d_i is the channel information for plotting on plot p_i

d_i may be any one of the following

00Y or Y	will plot output channel Y vs time
X00	will plot time vs output channel X
XY	will plot X vs Y

X and Y must be 2 digits (i.e., 21, 02, etc.)

To designate that the <u>first group</u> of plots requested are to be 1/3 frame (three plots per frame) use

P 1000 n

where n is the number of plots to be plotted three to a frame. All plots numbered greater than n will be full frame. If n is not an integral multiple of 3, there will be blank 1/3 frame plots on the $([\frac{n}{3}] + 1)^{th}$ frame.

<u>Printer plots</u> are rough plots received as part of DEADAM printed output. To get printer plots in addition to FR80 plots, use the following data card:

L n_i n_2 n_3 . . . n_i

where n_i is a plot number specified on a "P" card that is to be print-plotted; the n_i need not be sequential.

Plot Scale Card

These cards are again associated with the plots specified on a "P" card and will therefore affect both FR80 and printer plots. They allow scaling to specified limits for these plots.

Format

/ S n 0 l_i v_i . . . l_i v_i

Where S — specifies Plot scale card

n — number of plot to be scaled (corresponds to a "P" card specification)

0 — dummy (not used)

l_i — limit being set (must be grouped: if X min set, X max must be set) according to following table.

l_i	limit
3	X min
4	X max
5	Y min
6	Y max

Data generated outside of specified limits will not be plotted.

v_i — limit value. Pairs (l_i, v_i) have the same format as (V-array position, data value) pairs.

Multiplot card

Multiplot allows the plotting of up to 10 channels vs the same abscissa; the plot is full frame. The multiplot card has the form

/ M n k l_1 l_2 . . . l_k l_{k+1}

where	M	specifies multiplot card
	n	multiplot #
	k	number of ordinate channels
	l_i	channels to be plotted on ordinate, l = 1, . . ., k
	l_{k+1}	channel to be used as abscissa
		(If l_{k+1} is 0 or blank, l_{k+1} is assumed to be time.)

Scaling is automatically set.

General Comments:

A (@) punch on a Data or Plot cards will cause the program to ignore those columns following the (@) punch on that card. At least one set of data information must have been set before the (@) punch.

Title card extension: If there is an "*" in column 80, that card will be listed immediately; and the program will read the next card to get the heading information. This will continue until the last Title card read has no "*" in column 80. This allows the user to append some comments before his V-ARRAY list out.

Entries in the V-ARRAY (entered via the above described data cards) are interpreted by the individual subroutines of the program according to the following input lists. The absolute location of an input variable is its V-ARRAY index. Relative locations are also given since the starting index for the input data of each routine (except ADAMS and ANTIN) may be changed (see input list for subroutine SETUP).

Input List For Subroutine SETUP/LØØP and SETUP/PØINT

Variable Name	Relative Location	Absolute Location	Description	Units	Nominal Value
NSSØRB	–	1	input index for EPHEM3	–	50
NRØRB1	–	2	input index for EPHEM1	–	60
NRØRB2	–	3	input index for EPHEM2	–	70
NVSUN	–	4	input index for SUN	–	80
NVSS1	–	5	input index for INTSS1	–	90
NADYN *	–	6	input index for ANTDYN	–	600
NCNTL7 *	–	7	input index for CNTRL7	–	141
NSERVØ *	–	8	input index for SERVØ	–	181
NMNPLS *	–	9	input index for MØNPLS	–	201
NØBR1Ø *	–	10	input index for ØBEPH1	–	560
NØBR2Ø *	–	11	input index for ØBEPH2	–	580
NØBSSØ	–	12	input index for ØBEPH3	–	500
NTDEF *	–	13	input index for THERMD	–	250
NKNMT *	–	14	input index for KINMAT	–	300
NØBKMT *	–	15	input index for ØBKNMT	–	325
NSSRTE *	–	16	input index for SSRATE	–	330
NCLBRT *	–	17	input index for CLBRTN	–	340
GSLAT **	–	21	ground station latitude	deg	
GSLØN **	–	22	ground station longitude	deg	
GSALT **	–	23	ground station altitude	N.M.	
KPRINT	–	41	output option index (not used)	–	1
KDEBUG	–	42	≠ 0 → debug outputs each page	–	0
KRELAY	–	43	relay to be tracked	–	1
KØPT2		44	option index (not used)	–	–
KOPT3		45	option index (not used)	–	–

* → SETUP/LØØP only

** → SETUP/PØINT only

Input List For Subroutine ADAMS (internal integration routine)

Variable Name	Relative Location	Absolute Location	Description	Units	Nominal Value
	INPADM	400	not used	-	-
IØIN	INPADM + 1	401	discontinuities at TDISC(I)	-	0
IØMAX	INPADM + 2	402	I = IØIN, ... IØMAX	-	0
TIGN	INPADM + 3	403	initial on time (periodic time)	-	0
TINC	INPADM + 4	404	period (discontinuities)	-	0
TCØMAN	INPADM + 5	405	on duration (discontinuities)		
IGUESS	INPADM + 6	406	- 1 to suppress output at disc.	-	0
	INPADM + 7	407	> 0 to suppress output at disc. except for V(406) <T< V(407)	sec.	0
TL	INPADM + 8	408	initial value of time	sec.	0
TINT	INPADM + 9	409	output interval	sec.	1
TMAX	INPADM + 10	410	maximum value of time	sec.	150
NIMAX	INPADM + 11	411	maximum # integration steps	-	131071*
IØUTM	INPADM + 12	412	maximum # output lines	-	
DTIN	INPADM + 13	413	initial integration step size	sec.	2^{-9} *
DTMIN	INPADM + 14	414	minimum integration step size	sec.	2^{-9} *
DTMAX	INPADM + 15	415	maximum integration step size	sec.	2^{+5} *
ADLL	INPADM + 16	416	error test limits	-	$.23\backslash^{-6}$ *
ADUL	INPADM + 17	417		-	$.46\backslash^{-5}$ *
EPCØN	INPADM + 18	418	predictor error limit	-	10^{-5} *
IDEBIN	INPADM + 19	419	print debug outputs for	-	0
IDEBF	INPADM + 20	420	IDEBIN < NI < IDEBF	-	0

* values set internally if input is 0

Input List For Subroutine ADAMS (internal integration routine) Continued

Variable Name	Relative Location	Absolute Location	Description	Units	Nominal Value
IERR	INPADM + 21	421	1 to make predictor error test	-	0
LØUTA	INPADM + 22	422	1 to suppress plot output at disc.	-	0
IITMAX	INPADM + 23	423	# variable output increments	-	0
NXL	INPADM + 24	424	initial output channel	-	1
NXH	INPADM + 25	425	final output channel	-	24
TIØ(1)	INPADM + 26	426	1st interval output spacing	sec.	-
TIØ(2)	INPADM + 27	427	2nd interval output spacing	sec.	-
TIØ(3)	INPADM + 28	428	3rd interval output spacing	sec.	-
TIØ(4)	INPADM + 29	429	4th interval output spacing	sec.	-
TIØ(5)	INPADM + 30	430	5th interval output spacing	sec.	-
TØU(1)	INPADM + 31	431	max. time for 1st interval	sec.	-
TØU(2)	INPADM + 32	432	max. time for 2nd interval	sec.	-
TØU(3)	INPADM + 33	433	max. time for 3rd interval	sec.	-
TØU(4)	INPADM + 34	434	max. time for 4th interval	sec.	-
TØU(5)	INPADM + 35	435	max. time for 5th interval	sec.	-
TDISC(1)	INPADM + 36	436	discontinuity time	sec.	-
.	.	.	.	.	
.	.	.	.	.	
.	.	.	.	.	
TDISC(29)	INPADM + 64	464	discontinuity time	sec.	-
ADDCØN(1)	INPADM + 65	465	additive constant 1	-	10
ADDCØN(2)	INPADM + 66	466	additive constant 2	-	10
ADDCØN(3)	INPADM + 67	467	additive constant 3	-	10
ADDCØN(4)	INPADM + 68	468	additive constant 4	-	4
ADDCØN(5)	INPADM + 69	469	additive constant 5	-	4

Input List For Subroutine ADAMS (internal integration routine) Continued

Variable Name	Relative Location	Absolute Location	Description	Units	Nominal Value
ADDCØN(6)	INPADM + 70	470	additive constant 6	-	4
ADDCØN(7)	INPADM + 71	471	additive constant 7	-	4
ADDCØN(8)	INPADM + 72	472	additive constant 8	-	4
ADDCØN(9)	INPADM + 73	473	additive constant 9	-	4
ADDCØN(10)	INPADM + 74	474	additive constant 10	-	4
ADDCØN(11)	INPADM + 75	475	additive constant 11	-	4
ADDCØN(12)	INPADM + 76	476	additive constant 12	-	.5
ADDCØN(13)	INPADM + 77	477	additive constant 13	-	.5
ADDCØN(14)	INPADM + 78	478	additive constant 14	-	10
ADDCØN(15)	INPADM + 79	479	additive constant 15	-	1
ADDCØN(16)	INPADM + 80	480	additive constant 16	-	10
ADDCØN(17)	INPADM + 81	481	additive constant 17	-	1
ADDCØN(18)	INPADM + 82	482	additive constant 18	-	.005
ADDCØN(19)	INPADM + 83	483	additive constant 19	-	.005

Input List For Subroutine ANTIN

Variable Name	Relative Location	Absolute Location	Description	Units	Nominal Value
FLAG	IDXV	110	flag: if 0 ANTIN not called	-	0
BMW	IDXV + 1	111	beam width factor	deg	70
CSN	IDXV + 2	112	feed option parameter	-	2.5
DBK	IDXV + 3	113	dia. of aperture blockage	in	0
DIA	IDXV + 4	114	reflector diameter	in	60
EFF	IDXV + 5	115	aperture efficiency	%	55
FTV	IDXV + 6	116	distance feed to vertex	in	0
FVD	IDXV + 7	117			.4
GFE	IDXV + 8	118	peak gain of feed	-	0
GHZ	IDXV + 9	119	operating frequency	G hz	4
HUB	IDXV + 10	120	radius of reflector "hub"	in	0
MØN	IDXV + 11	121	not used	-	-
PAN	IDXV + 12	122	# of reflector panels	-	0
PPW	IDXV + 13	123	integration step(pts/ wavelength)	-	2
SIM	IDXV + 14	124	flag: 0 for antenna study only	-	1
SMP	IDXV + 15	125	flag: 1 for simple model	-	0
XAP	IDXV + 16	126	not used		-
XAT	IDXV + 17	127			-
XVP	IDXV + 18	128			-
XVT	IDXV + 19	129			-
PØL	IDXV + 20	130	polarization flag: 1 for linear dipole, 2 for linear slot mode, 3 for right hand circular, and 4 for left hand circular		1

Input List For Subroutine ANTIN Continued

Variable Name	Relative Location	Absolute Location	Description	Units	Nominal Value
			For SIM = 0		
PHC	IDXV + 21	131	constant φ	deg	-
THS	IDXV + 22	132	initial θ	deg	-
THD	IDXV + 23	133	θ increment (for θ scan)	deg	-
THF	IDXV + 24	134	final θ	deg	-
THC	IDXV + 25	135	constant θ	deg	-
PHS	IDXV + 26	136	initial φ	deg	-
PHD	IDXV + 27	137	φ increment (for φ scan)	deg	-
PHF	IDXV + 28	138	final φ	deg	-

Input List For Subroutine MØNPLS

Variable Name	Relative Location	Absolute Location	Description	Units	Nominal Value
MØN	INDEXV	201	option index: 0 → no monopulse error signals, 4 → four horn system, 5 → five horn system	-	4
GDB	INDEXV + 1	202	peak antenna gain	db	0 *
P	INDEXV + 2	203	beam shape parameters	db/deg^2	3.0*
T	INDEXV + 3	204		db/deg^2	3.0*
US	INDEXV + 4	205	horn spacing	deg	.5
VS	INDEXV + 5	206	horn spacing	deg	.5
AS	INDEXV + 6	207	monopulse gain factor	-	.16
THRESH	INDEXV + 7	208	monopulse threshold gain	-	.5
K1	INDEXV + 8	209	error signal gains	-	.16
K2	INDEXV + 9	210		-	.16
THETAS	INDEXV + 10	211	monopulse activation cone angle	deg	1.0

*indicates values that may be computed by ANTIN

Input List For Subroutine THERMD

Variable Name	Relative Location	Absolute Location	Description	Units	Nominal Value
KØPT	IDXV	250	option index (not used)	-	-
DIAM	IDXV + 1	251	antenna diameter	ft	30.
FREQ	IDXV + 2	252	antenna operating frequency	G Hz	8.25
AO	IDXV + 3	253		-	1
A1	IDXV + 4	254		-	0
A2	IDXV + 5	255		-	0
BO	IDXV + 6	256		-	1
B1	IDXV + 7	257		-	0
B2	IDXV + 8	258		-	0
CO	IDXV + 9	259		-	1
C1	IDXV + 10	260		-	0
C2	IDXV + 11	261		-	0
DO	IDXV + 12	262		-	1
D1	IDXV + 13	263		-	0
D2	IDXV + 14	264		-	0
EO	IDXV + 15	265		-	1
E1	IDXV + 16	266		-	0
E2	IDXV + 17	267		-	0
GO	IDXV + 18	268		-	1
G1	IDXV + 19	269		-	0
G2	IDXV + 20	270		-	0
CDPHI	IDXV + 21	271	constant (indep. of sun	deg	0*
CDTHA	IDXV + 22	272	vector) beam shift angles	deg	0*

*indicates values that may be computed by ANTIN

Input List For Subroutine SSRATE

Variable Name	Relative Location	Absolute Location	Description	Units	Nominal Value
KØPT	IDXV	330	option index	-	0
			For KØPT = 0 S/S rate is set equal to orbit rate, no inputs		
			For KØPT = 1		
ØMPIP(1)	IDXV + 1	331	S/S X-axis rate (constant)	deg/sec	-
ØMPIP(2)	IDXV + 2	332	S/S Y-axis rate (constant)	deg/sec	-
ØMPIP(3)	IDXV + 3	333	S/S Z-axis rate (constant)	deg/sec	-
			For KØPT = 2		
PØMPIP(1)	IDXV + 1	331	S/S X-axis accel. (constant)	deg/sec^2	-
PØMPIP(2)	IDXV + 2	332	S/S Y-axis accel. (constant)	deg/sec^2	-
PØMPIP(3)	IDXV + 3	333	S/S Z-axis accel. (constant)	deg/sec^2	-
R1	IDXV + 4	334	S/S X-axis rate (initial)	deg/sec^2	-
R2	IDXV + 5	335	S/S Y-axis rate (initial)	deg/sec^2	-
R3	IDXV + 6	336	S/S Z-axis rate (initial)	deg/sec^2	-

Input List For Subroutine KINMAT

Variable Name	Relative Location	Absolute Location	Description	Units	Nominal Value
IRØT	INDEXV	300	input rotation sequence	-	321
PHI(1)	INDEXV + 1	301	S/S X-axis rotation angle	deg	- 10
PHI(2)	INDEXV + 2	302	S/S Y-axis rotation angle	deg	0
PHI(3)	INDEXV + 3	303	S/S Z-axis rotation angle	deg	0
NØPRØT	INDEXV + 19	319	# of optional output sequences	-	0
RCHNG	INDEXV + 20	320	optional output rotation sequence	-	-
RCHNG	INDEXV + 21	321	optional output rotation sequence	-	-
RCHNG	INDEXV + 22	322	optional output rotation sequence	-	-

Input List For Subroutine EPHEM 3

Variable Name	Relative Location	Absolute Location	Description	Units	Nominal Value
KØPT	INDEXV	50	input option index	–	3
			For KØPT = 1		
OMEGAØ	INDEXV + 1	51	average orbit rate	rad/sec	–
EB	INDEXV + 2	52	orbit eccentricity	–	–
CLINB	INDEXV + 3	53	orbit inclination	deg	–
WB	INDEXV + 4	54	perigee argument	deg	–
AMU	INDEXV + 5	55	initial true anomaly	deg	–
CAPWB	INDEXV + 6	56	ascending node longitude	deg	–
			For KØPT = 2		
PERIOD	INDEXV + 1	51	nodal period	sec	–
PRAD	INDEXV + 2	52	perigee radius	nm	–
CLINB	INDEXV + 3	53	orbit inclination	deg	–
WB	INDEXV + 4	54	perigee argument	deg	–
U	INDEXV + 5	55	initial satellite argument	deg	–
CAPWB	INDEXV + 6	56	ascending node longitude	deg	–
			For KØPT = 3		
RØMNAK	INDEXV + 1	51	orbit semi-major axis	nm	3843.1
EB	INDEXV + 2	52	orbit eccentricity	–	0.
CLINB	INDEXV + 3	53	orbit inclination	deg	90.
WB	INDEXV + 4	54	perigee argument	deg	90.
AMU	INDEXV + 5	55	initial true anomaly	deg	- 90.
CAPWB	INDEXV + 6	56	ascending node longitude	deg	90.

Input List For Subroutine EPHEM 1

Variable Name	Relative Location	Absolute Location	Description	Units	Nominal Value
KØPT	INDEXV	60	input option index	–	3
			For KØPT = 1		
OMEGAØ	INDEXV + 1	61	average orbit rate	rad/sec	–
EB	INDEXV + 2	62	orbit eccentricity	–	–
CLINB	INDEXV + 3	63	orbit inclination	deg	–
WB	INDEXV + 4	64	perigee argument	deg	–
AMU	INDEXV + 5	65	initial true anomaly	deg	–
CAPWB	INDEXV + 6	66	ascending node longitude	deg	–
			For KØPT = 2		
PERIOD	INDEXV + 1	61	nodal period	sec	–
PRAD	INDEXV + 2	62	perigee radius	nm	–
CLINB	INDEXV + 3	63	orbit inclination	deg	–
WB	INDEXV + 4	64	perigee argument	deg	–
U	INDEXV + 5	65	initial satellite argument	deg	–
CAPWB	INDEXV + 6	66	ascending node longitude	deg	–
			For KØPT = 3		
RØTNAK	INDEXV + 1	61	orbit semi-major axis	nm	22770.8
EB	INDEXV + 2	62	orbit eccentricity	–	.00011
CLINB	INDEXV + 3	63	orbit inclination	deg	.01
WB	INDEXV + 4	64	perigee argument	deg	0
AMU	INDEXV + 5	65	initial true anomaly	deg	0
CAPWB	INDEXV + 6	66	ascending node longitude	deg	15.

Input List For Subroutine EPHEM 2

Variable Name	Relative Location	Absolute Location	Description	Units	Nominal Value
KØPT	INDEXV	70	input option index	–	3
			For KØPT = 1		
OMEGAØ	INDEXV + 1	71	average orbit rate	rad/sec	–
EB	INDEXV + 2	72	orbit eccentricity	–	–
CLINB	INDEXV + 3	73	orbit inclination	deg	–
WB	INDEXV + 4	74	perigee argument	deg	–
AMU	INDEXV + 5	75	initial true anomaly	deg	–
CAPWB	INDEXV + 6	76	ascending node longitude	deg	–
			For KØPT = 2		
PERIOD	INDEXV + 1	71	nodal period	sec	–
PRAD	INDEXV + 2	72	perigee radius	nm	–
CLINB	INDEXV + 3	73	orbit inclination	deg	–
WB	INDEXV + 4	74	perigee argument	deg	–
U	INDEXV + 5	75	initial satellite argument	deg	–
CAPWB	INDEXV + 6	76	ascending node longitude	deg	–
			For KØPT = 3		
RØMNAK	INDEXV + 1	71	orbit semi-major axis	nm	22770.8
EB	INDEXV + 2	72	orbit eccentricity	–	.00011
CLINB	INDEXV + 3	73	orbit inclination	deg	.01
WB	INDEXV + 4	74	perigee argument	deg	0
AMU	INDEXV + 5	75	initial true anomaly	deg	0
CAPWB	INDEXV + 6	76	ascending node longitude	deg	145.

Input List For Subroutine SUN

Variable Name	Relative Location	Absolute Location	Description	Units	Nominal Value
DATE	INDEXV	80	date (month day year)	-	032172
TMØD	INDEXV + 1	81	initial time of day (Greenwich)	sec	21600

Input List For Subroutine INTSS1

Variable Name	Relative Location	Absolute Location		Units	Nominal Value
A	IDXV	90	X-semi axis of ellipsoid	ft	100
B	IDXV + 1	91	Y-semi axis of ellipsoid	ft	100
C	IDXV + 2	92	Z-semi axis of ellipsoid	ft	1
AP(1)	IDXV + 3	93	S/S frame position coordinates of antenna gibmal point	ft	0
AP(2)	IDXV + 4	94		ft	0
AP(3)	IDXV + 5	95		ft	- 50
IRØT	IDXV + 6	96	rotation sequence for following angles	-	321
PHI(1)	IDXV + 7	97	ellipsoid X-axis rotation angle	deg	0
PHI(2)	IDXV + 8	98	ellipsoid Y-axis rotation angle	deg	0
PHI(3)	IDXV + 9	99	ellipsoid Z-axis rotation angle	deg	0

Input List For Subroutine INTSS2

Variable Name	Relative Location	Absolute Location	Description	Units	Nominal Value
A	IDXV	100	X-semi axis of ellipsoid	ft	100
B	IDXV + 1	101	Y-semi axis of ellipsoid	ft	100
C	IDXV + 2	102	Z-semi axis of ellipsoid	ft	1
AP(1)	IDXV + 3	103	S/S frame position coordinates of antenna gimbal point	ft	0
AP(2)	IDXV + 4	104		ft	0
AP(3)	IDXV + 5	105		ft	- 50
IRØT	IDXV + 6	106	rotation sequence for following angles	-	321
PHI(1)	IDXV + 7	107	ellipsoid X-axis rotation angle	deg	0
PHI(2)	IDXV + 8	108	ellipsoid Y-axis rotation angle	deg	0
PHI(3)	IDXV + 9	109	ellipsoid Z-axis rotation angle	deg	0

Input List For Subroutine ANTDYN

Variable Name	Relative Location	Absolute Location	Description	Units	Nominal Value
IAA(1, 1)	IDXV	600	inertia diadic of antenna in antenna reference frame	slug ft^2	1000
IAA(2, 2)	IDXV + 1	601		slug ft^2	1000
IAA(3, 3)	IDXV + 2	602		slug ft^2	2000
IAA(1, 2)	IDXV + 3	603		slug ft^2	0
IAA(1, 3)	IDXV + 4	604		slug ft^2	0
IAA(2, 3)	IDXV + 5	605		slug ft^2	0
MBAR	IDXV + 6	606	reduced mass	slugs	10
R2A(1)	IDXV + 7	607	antenna center of mass to hinge pt. vector in antenna reference frame	ft	0
R2A(2)	IDXV + 8	608		ft	0
R2A(3)	IDXV + 9	609		ft	10
EBETAA(1)	IDXV + 10	610	BETA gimbal axis direction vector in antenna reference frame	-	0
EBETAA(2)	IDXV + 11	611		-	1
EBETAA(3)	IDXV + 12	612		-	0
R1P(1)	IDXV + 13	613	S/S center of mass to hinge pt. vector in S/S reference frame	ft	0
R1P(2)	IDXV + 14	614		ft	0
R1P(3)	IDXV + 15	615		ft	-50
EALFAP	IDXV + 16	616	ALFA gimbal axis direction vector in S/S reference frame	-	1
EALFAP	IDXV + 17	617		-	0
EALFAP	IDXV + 18	618		-	0
ALFA	IDXV + 19	619	initial ALFA gimbal angle	deg	-84.86
ALFAD	IDXV + 20	620	initial ALFA gimbal rate	deg/sec	0
BETA	IDXV + 21	621	initial BETA gimbal angle	deg	0
BETAD	IDXV + 22	622	initial BETA gimbal rate	deg/sec	0
FREQ	IDXV + 23	623	bending mode frequency	rad/sec	.628
			For FREQ $\leq$ 0 no S/S flexibility is accounted for and no further inputs are required		

Input List For Subroutine ANTDYN Continued

Variable Name	Relative Location	Absolute Location	Description	Units	Nominal Value
			For Freq > 0		
MP	IDXV + 24	624	S/S mass	slugs	10000
MPHI	IDXV + 25	625	flexible S/S mass and bending deflection distribution parameters	ft^2	13860
CPHIP(1)	IDXV + 26	626		ft	0
CPHIP(2)	IDXV + 27	627		ft	- 1
CPHIP(3)	IDXV + 28	628		ft	0
CYP(1)	IDXV + 29	629		ft^2	77.88
CYP(2)	IDXV + 30	630		ft^2	0
CYP(3)	IDXV + 31	631		ft^2	0
CEP(1, 1)	IDXV + 32	632		ft^2	.40
CEP(1, 2)	IDXV + 33	633		ft^2	0
CEP(1, 3)	IDXV + 34	634		ft^2	0
CEP(2, 2)	IDXV + 35	635		ft^2	.223
CEP(2, 3)	IDXV + 36	636		ft^2	0
CEP(3, 3)	IDXV + 37	637		ft^2	.241
CNBP(1, 1)	IDXV + 38	638		ft^2	0
CNBP(1, 2)	IDXV + 39	639		ft^2	0
CNBP(1, 3)	IDXV + 40	640		ft^2	0
CNBP(2, 1)	IDXV + 41	641		ft^2	0
CNBP(2, 2)	IDXV + 42	642		ft^2	0
CNBP(2, 3)	IDXV + 43	643		ft^2	62.76
CNBP(3, 1)	IDXV + 44	644		ft^2	0
CNBP(3, 2)	IDXV + 45	645		ft^2	12.76
CNBP(3, 3)	IDXV + 46	646		ft^2	0
PSICP(1)	IDXV + 47	647	bending deformation slope at control position	-	.0175
PSICP(2)	IDXV + 48	648		-	0
PSICP(3)	IDXV + 49	649		-	0

Input List For Subroutine ANTDYN Continued

Variable Name	Relative Location	Absolute Location	Description	Units	Nominal Value
PSIGP(1)	IDXV + 50	650	bending deformation slope at IMU position	-	.0175
PSIGP(2)	IDXV + 51	651		-	0
PSIGP(3)	IDXV + 52	652		-	0
Q	IDXV + 53	653	initial bending coordinate value	-	0
QD	IDXV + 54	654	initial bending coordinate rate	sec^{-1}	0

Input List For Subroutine CNTRL7

Variable Name	Relative Location	Absolute Location	Description	Units	Nominal Value
			ALFA channel parameters:		
K1A	INDEXV	141	attitude gain, pointing mode	deg^{-1}	50
K2A	INDEXV + 1	142	rate gain, pointing mode	$(deg/sec)^{-1}$	500
K3A	INDEXV + 2	143	attitude gain, tracking mode	deg^{-1}	50
K4A	INDEXV + 3	144	rate gain, tracking mode	$(deg/sec)^{-1}$	500
K5A	INDEXV + 4	145	integral gain, tracking mode	sec^{-1}	.02
ALFAB	INDEXV + 5	146	bias	deg	0
			BETA channel parameters:		
K1B	INDEXV + 6	147	attitude gain, pointing mode	deg^{-1}	50
K2B	INDEXV + 7	148	rate gain, pointing mode	$(deg/sec)^{-1}$	500
K3B	INDEXV + 8	149	attitude gain, tracking mode	deg^{-1}	50
K4B	INDEXV + 9	150	rate gain, tracking mode	$(deg/sec)^{-1}$	500
K5B	INDEXV + 10	151	integral gain, tracking mode	sec^{-1}	.02
BETAB	INDEXV + 11	152	bias	deg	0
			resolver characteristics:		
RESØLP	INDEXV + 12	153	position quantization	deg	0
RESØLR	INDEXV + 13	154	rate quantization	deg/sec	0
RESOLI	INDEXV + 14	155	output signal quantization	-	0
			spiral scan parameters:		
TSURCH	INDEXV + 15	156	allowed search duration	sec	5
RØ	INDEXV + 16	157	initial scan radius	deg	.05
VT	INDEXV + 17	158	tangential scan rate	deg/sec	.8
DS	INDEXV + 18	159	radial scan rate	deg/rev	1.0

Input List For Subroutine CNTRL7 Continued

Variable Name	Relative Location	Absolute Location	Description	Units	Nominal Value
			initial conditions:		
REGA	INDEXV + 19	160	ALFA channel integrator	-	0
REGB	INDEXV + 20	161	BETA channel integrator	-	0
QUANTM	INDEXV + 21	162	# of bits in gimbal sensor output	-	0
QUANTP	INDEXV + 22	163	# of bits in computed gimbal output	-	0
QUANTZ	INDEXV + 23	164	# of bits in error signal output	-	0
LSURCH	INDEXV + 24	165	flag: 0 to inhibit spiral scan	-	0

Input List For Subroutine SERVØ, FGEN

Variable Name	Relative Location	Absolute Location	Description	Units	Nominal Value
KGA	INDEXV	181	ALFA channel torque gain	ft-lbs	1
KGB	INDEXV + 1	182	BETA channel torque gain	ft-lbs	1
			Channel 1 of FGEN		
NPTS	INDEXV + 2	183	# of points	-	3
XP(1,1)	INDEXV + 3	184	input value, pt. 1	rad/sec	0
YP(1,1)	INDEXV + 4	185	output value, pt. 1	ft-lbs	.16
XP(1,2)	INDEXV + 5	186	input value, pt. 2	rad/sec	.05
YP(1,2)	INDEXV + 6	187	output value, pt. 2	ft-lbs	.08
XP(1,3)	INDEXV + 7	188	input value, pt. 3	rad/sec	10.
YP(1,3)	INDEXV + 8	189	output value, pt. 3	ft-lbs	.08
			Channel 2 of FGEN		
NPTS	INDEXV + 9	190	# of points	-	3
XP(2,1)	INDEXV + 10	191	input value, pt. 1	rad/sec	0
YP(2,1)	INDEXV + 11	192	output value, pt. 1	ft-lbs	.16
XP(2,2)	INDEXV + 12	193	input value, pt. 2	rad/sec	.05
YP(2,2)	INDEXV + 13	194	output value, pt. 2	ft-lbs	.08
XP(2,3)	INDEXV + 14	195	input value, pt. 3	rad/sec	10.
YP(2,3)	INDEXV + 15	196	output value, pt. 3	ft-lbs	.08

Input List For Surboutine ØBKNMT

Variable Name	Relative Location	Absolute Location	Description	Units	Nominal Value
IRØT	INDEXV	325	input rotation sequence	-	321
PHI(1)	INDEXV + 1	326	S/S X-axis rotation angle	deg	-10.
PHI(2)	INDEXV + 2	327	S/S Y-axis rotation angle	deg	0
PHI(3)	INDEXV + 3	328	S/S Z-axis rotation angle	deg	0

Input List For Subroutine ØBEPH3

Variable Name	Relative Location	Absolute Location	Description	Units	Nominal Value
KØPT	INDXV	500	option index (not used)	-	-
XT(2)	INDEXV + 1	501	time at input point 1	sec	0
RV1(2)	INDEXV + 2	502	earth frame position coordinates of point 1	m.m.	0
RV2(2)	INDEXV + 3	503		m.m.	3844.7
RV3(2)	INDEXV + 4	504		m.m.	0
VV1(2)	INDEXV + 5	505	earth frame velocity components at point 1	ft/sec	0
VV2(2)	INDEXV + 6	506		ft/sec	0
VV3(2)	INDEXV + 7	507		ft/sec	24552.3
XT(3)	INDEXV + 11	511	time at input point 2	sec	1200.
RV1(3)	INDEXV + 12	512	earth frame position coordinates of point 2	m.m.	102.41
RV2(3)	INDEXV + 13	513		m.m.	1167.31
RV3(3)	INDEXV + 14	514		m.m.	3660.26
VV1(3)	INDEXV + 15	515	earth frame velocity components at point 2	ft/sec	-2042.1
VV2(3)	INDEXV + 16	516		ft/sec	-23277.3
VV3(3)	INDEXV + 17	517		ft/sec	7474.1
XT(4)	INDEXV + 21	521	time at input point 3	sec	2400.
RV1(4)	INDEXV + 22	522	earth frame position coordinates of point 3	m.m.	-544.82
RV2(4)	INDEXV + 23	523		m.m.	-3081.21
RV3(4)	INDEXV + 24	524		m.m.	2233.22
VV1(4)	INDEXV + 25	525	earth frame velocity components of point 3	ft/sec	-2484.2
VV2(4)	INDEXV + 26	526		ft/sec	-14049.3
VV3(4)	INDEXV + 27	527		ft/sec	-19972.7

Input List For Subroutine ØBEPH3 Continued

Variable Name	Relative Location	Absolute Location	Description	Units	Nominal Value
XT(5)	INDXV + 31	531	time at input point 4	sec	3600.
RV1(5)	INDXV + 32	532	earth frame position coordinates of point 4	m.m.	-799.44
RV2(5)	INDXV + 33	533		m.m	-2975.0
RV3(5)	INDXV + 34	534		m.m.	-2299.55
VV1(5)	INDXV + 35	535	earth frame velocity components at point 4	ft/sec	3812.4
VV2(5)	INDXV + 36	536		ft/sec	14187.3
VV3(5)	INDXV + 37	537		ft/sec	-19662.8
XT(6)	INDXV + 41	541	time at input point 5	sec	4800.
RV1(6)	INDXV + 42	542	earth frame position coordinates of point 5	m.m.	428.52
RV2(6)	INDXV + 43	543		m.m.	1173.86
RV3(6)	INDXV + 44	544		m.m.	-3634.45
VV1(6)	INDXV + 45	545	earth frame velocity components at point 5	ft/sec	7965.5
VV2(6)	INDXV + 46	546		ft/sec	21795.4
VV3(6)	INDXV + 47	547		ft/sec	7970.7
XT(7)	INDXV + 51	551	time at input point 6	sec	6000.
RV1(7)	INDXV + 52	552	earth frame position coordinates of point 6	m.m.	1628.66
RV2(7)	INDXV + 53	553		m.m.	3481.80
RV3(7)	INDXV + 54	554		m.m.	82.13
VV1(7)	INDXV + 55	555	earth frame velocity components at point 6	ft/sec	-222.4
VV2(7)	INDXV + 56	556		ft/sec	-475.5
VV3(7)	INDXV + 57	557		ft/sec	24546.7

Input List For Surboutine ØBEPH1/SYNCH

Variable Name	Relative Location	Absolute Location	Description	Units	Nominal Value
KØPT	INDXV	560	option index (not used)	-	-
RLØN	INDXV + 1	561	relay satellite longitude	deg	15.

Input List For Subroutine ØBEPH2/SYNCH

Variable Name	Relative Location	Absolute Location	Description	Units	Nominal Value
KØPT	INDXV	580	option index (not used)	-	-
RLØN	INDXV + 1	581	relay satellite longitude	deg	145.

Input List For Subroutine CLBRTN

Variable Name	Relative Location	Absolute Location	Description	Units	Nominal Value
KØPT	IDXV	340	option index (not used)	-	-
ØMEGA	IDXV + 1	341	frequency of sinusoidal corrections	deg/sec	0
TREF	IDXV + 2	342	reference time	sec	0
AA	IDXV + 3	343	ALFA gimbal angle bias corrections	deg	0
BA	IDXV + 4	344	Coeff. of sine correction term (ALFA)	deg	0
CA	IDXV + 5	345	Coeff. of cosine correction term (ALFA)	deg	0
AB	IDXV + 6	346	BETA gimbal angle bias correction	deg	0
BB	IDXV + 7	347	Coeff. of sine correction term (BETA)	deg	0
CB	IDXV + 8	348	Coeff. of cosine correction term (BETA)	deg	0

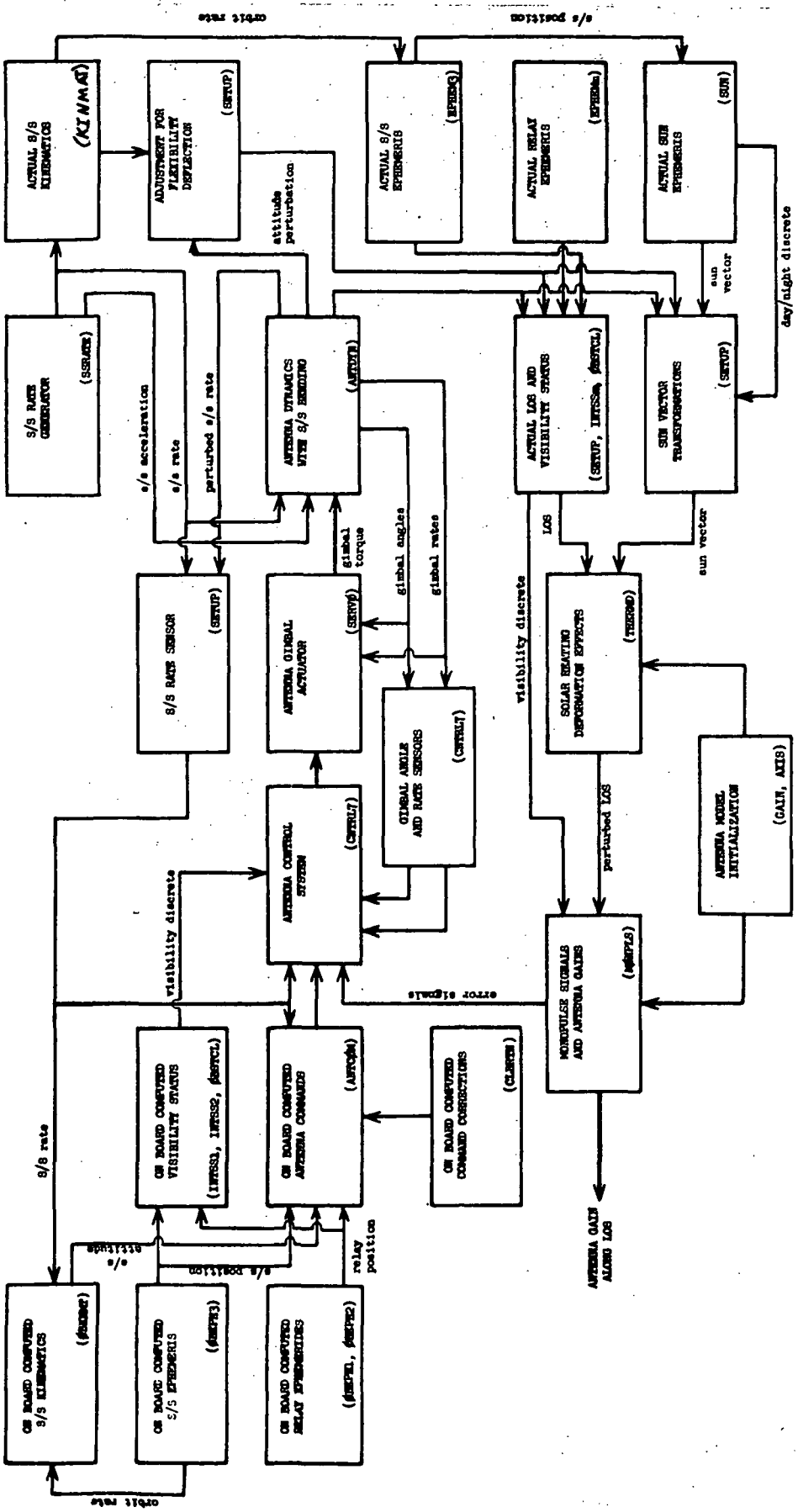

Figure A-1 Functional Block Diagram of Setup/Loop

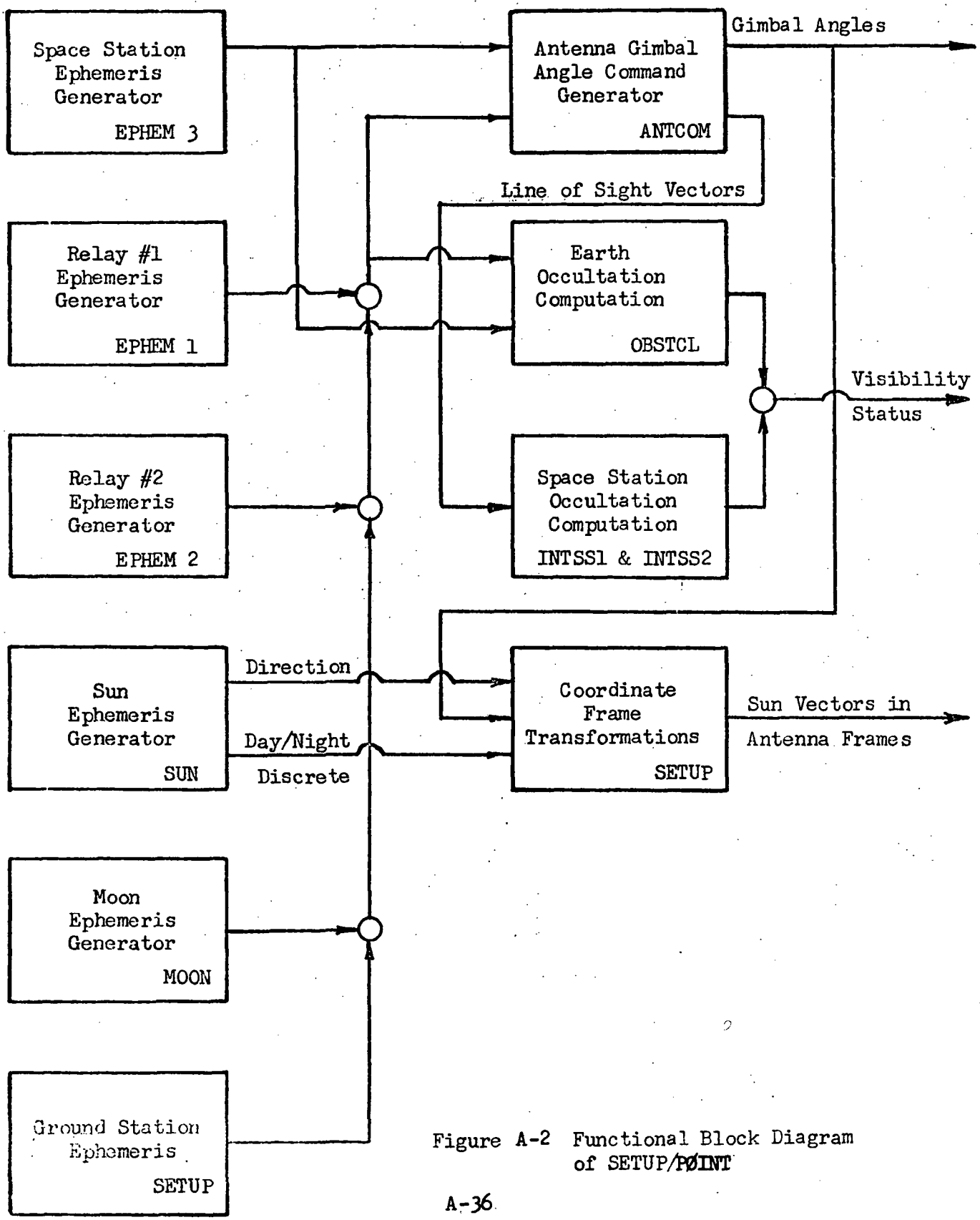

Figure A-2 Functional Block Diagram of SETUP/PØINT

APPENDIX B

BRIEF DESCRIPTION OF THE DEADAM PACKAGE

A real-time simulation analysis can be accomplished with LMSC DEADAM simulation. Figure B-1 illustrates the basic structure of the program. The main program DEADAM acts as the overall executive program which controls the main integration package (ADAMS) and the primary I/O routines. The ADAMS subroutine contains the heart of the integration package. It performs numerical integration of the system of first order ordinary differential equations with piecewise continuous derivatives. The differential equations are usually nonlinear and time varying and can be represented in the following form.

$$\dot{\underline{x}} = \underline{f}(\underline{x}, \underline{u}(t))$$

The above differential equations are defined by the user through the construction of the user executive (SETUP). The integration is performed using a third-order Adams-Bashforth predictor-corrector formula. The step size is adjusted automatically to stay within prescribed error bounds on the difference between predictor and corrector. Hence the step size will vary to allow efficient use of computer time without sacrificing accuracy. A self-starting procedure is used to form the first few differences.

The above features are standard for most Adams-Bashforth methods. In addition, a discontinuity prediction scheme has been incorporated into the DEADAM package. This allows the discontinuity point to be approached without iteration which results again in efficient use of computer time.

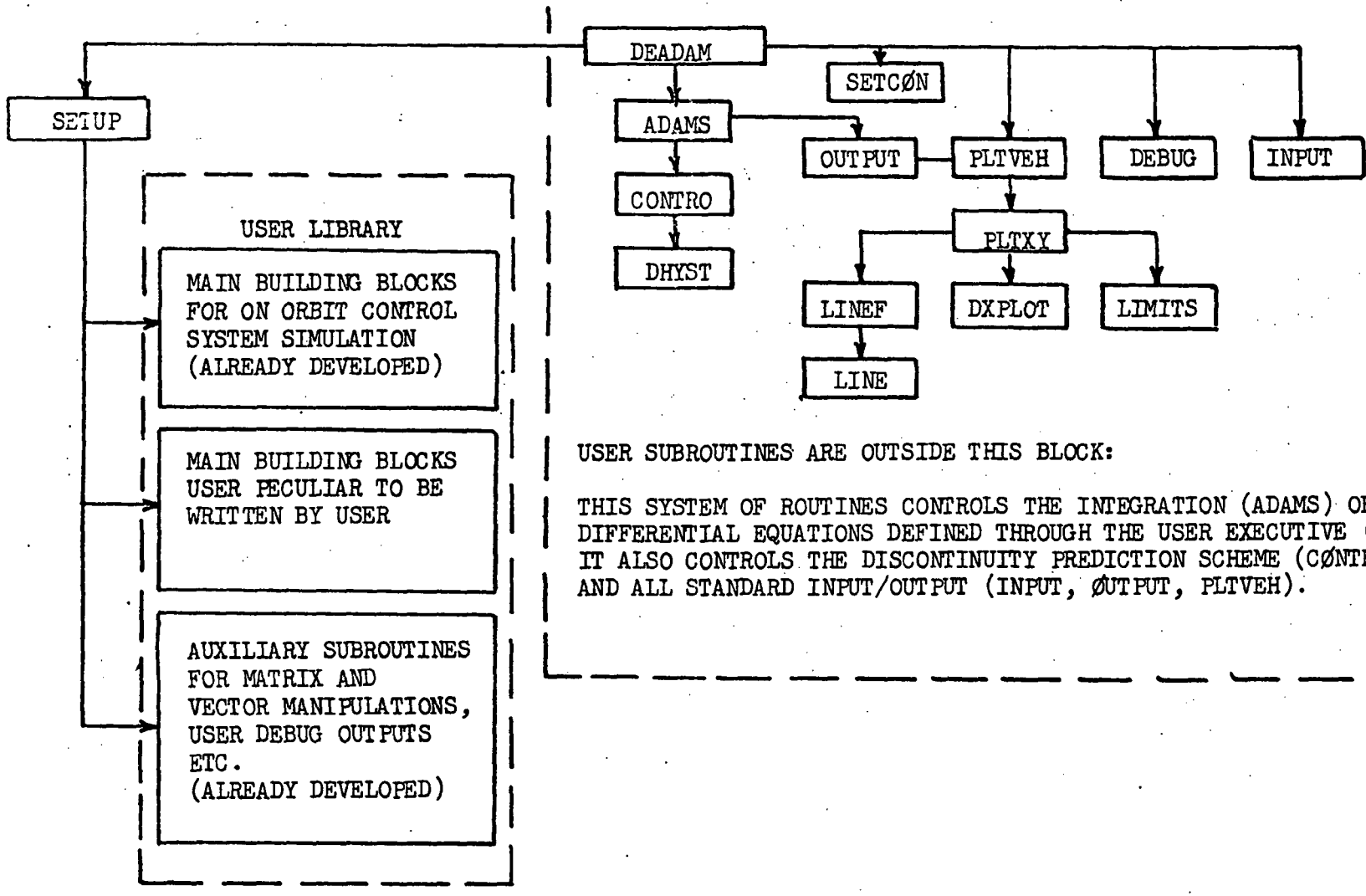

Figure B-1 DEADAM Program

LOCKHEED MISSILES & SPACE COMPANY

APPENDIX B

The user executive (SETUP) must be written for each simulation by the user. It is the organizing subroutine through which the differential equations are defined. The prescription for writing SETUP is contained in the document:

> "DEADAM" A Program Especially Suited for Nonlinear Simulation of Attitude Control Systems," ASCS/2485/6211, 29 Aug. 1969.

Since many aerospace control system simulations have parts in common, a user library has been developed for rapid and easy construction of complicated simulations. Partial lists with brief descriptions of the existing library subroutines are contained in Tables B-2 and B-3. The standarization of these routines allows the construction of sophisticated simulations of highly complex systems in very short periods of time.

The ease in construction of a typical DEADAM simulation can best be illustrated via a simple example. Suppose a simulation was required for a rigid vehicle stabilized by a pitch and yaw wheel during a boost thrust along its x axis. Also suppose there exists a pitch and yaw torque on the rigid body. The problem is to observe the motion of the body and the change in the orbital states.

The user may write a SETUP routine taking advantage of the user library. Such a SETUP is listed on the next page. Note that other outputs which may be desired have not been defined.

There are many fixed input variables which are not shown explicitly in the context of the user executive (SETUP). These are defined indirectly from an input array through the initialization calls to ØRBDYN and KINDYN. Examples of such variables are inertias, initial rigid body orientation, initial rates, inital orbit states. Also initialized through the same input array are the fixed parameters needed by the integration package and those needed by the I/Ø routines. Examples of these are minimum step size, print interval, initial time, maximum time and number of output channels.

```
      SUBRØUTINE SETUP (KP)
      CØMMØN/IØ/ØUT (50, 48)
      CØMMØN/CØNST/DEG, RAD, PI, TPI, PI2, REQ, RPL, GM, QMGE, FTNM
      CØMMØN/SETØUT/ICHANL(96)/SØD/INPADM/MAIN/AID(13),V(300)
      CØMMØN/KNDN/TBØ(3,3), JUNK3(18), PHI(3), RATES(3), ØMEGA(3)
      CØMMØN/ØRBIT/WREF(3), RMAG, RV(3), TØE(9) VMAG, VV(3), ALT, LAT, LØN
      REAL LAT, LØN, TØRQB(3), HWHEEL(3), FØRCE(3), THRUST(3), TEØ(3,3)
      GØ TØ (100, 200, 300, 400, 500, 600, 700,), KP
100   LØ       = 1    ∇Index of initial state variable.
      INPADM   = 100  ∇Index for ADAMS  input data
      RETURN
200   NVØRB    = 1    ∇Index for ØRBDYN input data
      NVKIN    = 50   ∇Index for KINDYN input data
      IDXØRB   = 1    ∇ØRBDYN state index
      CALL ØRBDYN (1, NVØRB, IDXØRB, FØRCE, SMUG)  ∇ Initialization
      IDXKIN   = 8    ∇KINDYN state index
      CALL KINDYN(1, NVKIN, IDXKIN, TORQB, HWHEEL, WRED, RMAG) ∇ Initialization
      NND      = 14   ∇Index of final state variable
      RETURN
300   CALL ØRBDYN (2,NVØRB, IDXØRB, FØRCE, SMUG)  ∇ WRITE ØUT
      CALL KINDYN (2,NVKIN, IDXKIN, TØRQB, HWHEEL, WREF, RMAG)  ∇  WRITE ØUT
      ICHANL(1)= 6H ROLL    ∇Additional output channels heading
      ICHANL(2)= 6H RATE    ∇can be defined here
      RETURN
400   CALL ØRBDYN(3, NVØRB, IDXØRB, FØRCE, SMUG)  ∇ DEFINE ØUTPUT
      CALL KINDYN(3, NVKIN, IDXKIN, TØRQB, HWHEEL, WREF, RMAG) ∇ DEFINE ØUTPUT
      THRUST(1)= 200.       ∇Thrust in lb.
      SMUG     = 100.       ∇Mass in slugs
      CALL TRNPS(TØB, TBØ)
      CALL DDV(TBØ, THRUST, FØRCE)
      CALL ØRBDYN(4, NVØRB, IDXØRB, FØRCE, SMUG)  ∇ DEFINE DERIVATIVES
      TORQB(2) = .5         ∇Pitch torque in ft-lb
      TORQB(3) = .6         ∇Yaw torque in ft-lb
      HWHEEL(2)= 50.        ∇Pitch wheel angular momentum ft-lb-sec
      HWHEEL(3)= 50.        ∇Yaw wheel angular momentum ft-lb-sec
      CALL KINDYN (4, NVKIN, IDXKIN, TØRQB, HWEEL, WREF, RMAG)
      RETURN
500   CALL ØRBDYN(5, NVØRB, IDXØRB, FØRCE, SMUG)  ∇ SPECIAL ØUTPUTS
      CALL KINDYN(5, NVKIN, IDXKIN, TØRQB, HWHEEL, WREF, RMAG)
      ØUT(LØUT,1) = RATES(1)*DEG ∇Additional outputs defined here
      RETURN
600   RETURN
700   CALL ØRBDYN(6, NVØRB, IDXØRB, FØRCE, SMUG)  ∇ DEBUG
      CALL KINDYN(6, NVKIN, IDXKIN, TØRQB, HWHEEL, WREF, RMAG)  ∇ DEBUG
      RETURN
```

Once the user executive (SETUP is written and compiled, the initiation of the program is carried out by

XQT DEADAM

Following by appropriate

DATA CARDS

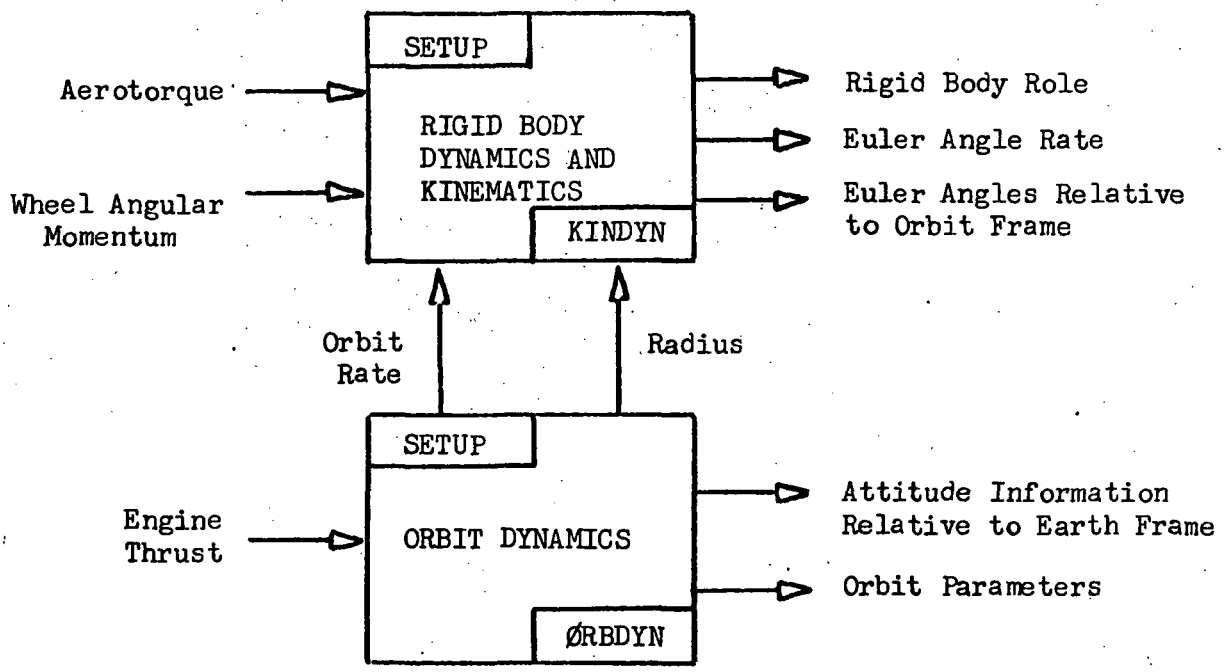

Figure B-2 Functional Block Diagram of Example Simulation

TABLE B-2

USER LIBRARY - AUXILIARY SUBROUTINES (AND FUNCTIONS)

Subroutine Name	Brief Description
ANGLE (X,Y)	Defines angle between X and Y
ANGMOD (X)	X module 2π in radians
ARCTAN (A, B)	Arc tangent function with 4 quadrant return (ATAN2)
ANGLET (A, IAX, D)	D = $[A]_{IAX}$ (transformation for rotation A about axis IAX)
AXEQB5(A,X,B)	Solves AX = B for X (5 x 1)
BOXPRD(X1,X2,X3)	Function = X1, X2, X3
DCTOEA (KS,LS,MS,E,A,B,C,IDEG)	Direction cosing matrix (E) to $[C]_{MS}[B]_{LS}[A]_{KS}$
DCTOEP(D,EP,DMAG)	Direction cosing matrix to Euler parameters
DDD(D1,D2,D3)	D3 = D1*D2 Matrix product (see MAB)
DDV(D,V1,V2)	V2 = D . V1 Linear transformation (3 x 3) of a vector
DIAD(R,S,RST)	RST = R > < S (Diadic)
DINV (D,D1)	DI = (D)
DOTPRD(X,Y)	Dot product of vectors X and Y
EATODC(KS,LS,MS,DC,AN,BN,CN,IDEG)	DC = $[CN]_{MS}[BN]_{LS}[AN]_{KS}$ ((DEG = 0 rad.)
EPTODC(EP,D)	Euler parameters to direction cosines
EULER(IS,JS,KS,WBODY, WREF,A,R,DC,IDEG,IEULER)	IDEG = 0, converts Euler angles (A) and rates (R) to body rates (WBODY) and dir. cos (DC) IDEG = 1, converts (WBODY) and (DC) to (A) and (R), order of A is IS,JS,KS
EAYRP(PSI,PHI,THETA,T)	Direction cosing matrix (T) to Euler angles $[\theta]_2 [\varphi]_1 [\psi]_3$
EPRATE(EPD,EPW)	Rigid body rate (W) to Euler parameter rate (EPD)
EPWINI (Q,W,U,PSI,PHI,THETA,UD,PSID,PHID,THETAD)	Define inertial euler parameters (Q) and body rate (W)
EP2TB1 (TBI,Q)	Euler parameters (Q) to direction cosine matrix (TB1)
LENGTH (X)	Real function determines magnitude of vector X (3x1)
MAC (C,A,B)	C = A*B Matrix multiplication (see DDD)
MABC (D,A,B.C)	D = A * B * C
MABT (C,A,B)	C = A * B^T
MALAT (C,A,I)	C = A_TI A
MATDA (C,D,A)	C = A_TB where B (I,J) = A(I,J) * D (I)

TABLE B-2 (Continued)

MATIA (C,A,I)	$C = A^T\ IA$
MFILL (C,C11, C12, C13, C21, C22, C23, C31, C32, C33)	Fills (3 x 3) matrix
MINV (C,A)	C = (A) (see DINV)
MSUM2 (D,SA,A,SB,D)	D = SA * A + SB * B sums two matrices (SA, SB = scalors)
MSUM2 (D,SA,A,SB,B,SC,C)	$_T$sums three matrices (SA,SB, SC = scalors)
MTR (C,A)	$C = A^T$
PAGE	Skips to new page
TFILL (A, NAXIS, ANGLE)	$A = [\text{Angle}]_{NAXIS}$ (see ANGLET)
TF12 (A, ANGLE1, ANGLE2)	FØRMS Roll/Pitch or 1/2 rotation
TRNPS (D,DT)	$DT = (D)^T$ (see MTR)
VABCTX (V,A,B,C,X)	$V = (A\ B\ C)^T_X$
VABCX (V,A,B,C,X)	V = (A B C).X
VABTX (V,A,B,X)	$V = (AB)^T.X$
VABX (V,A,B,X)	V = (AB).X.
VATX (V,A,X)	$V = A^TX$
VATXSY (V,A,X,S,Y)	$V = A^TX$ + S.Y (S = scaler
VAX (V,A,X)	V = AX (see DDV
VAXSY (V,A,X,S,Y)	V = AX + S . Y (S = scaler
VCOPY (V,I,J,T)	Copies row (I = row) or col. (I = col.) of T into V
VCROSS (Z,S,X,Y)	Z = S . (X cross Y) cross product (S = scalor) (See VXV)
VDX (V,D,X)	V(1) = D(1) . X(I) I = 1,3
VFILL (Z,Z1,Z2,Z3)	Fills (s x 1) vector
VMAG (X)	Forms magnitude of X (function)
VSCALE (X,S)	Rescales X to magnitude S
VSUM2 (Z,S1,X1,S2,X2)	Z = S1 . X1 + Se . X2 (S1, S2 = scalors) sums two vectors
VSUM3 (S,S1,X1,S2,X2,S3,X3)	(see VSUM2)
VSUM4 (S,S1,X1,S2,X2,S3,X3,S4,X4)	(see VSUM2)
VUNIT (X)	Rescales X to unit vector
VXKYSZ(V,X,Y,S,Z)	V = X cross Y + S.Z (S = scalor)
VXDDV(V1,D,V2V3)	V3 = V1 cross D.V2
VXV (Vi,W2,V3)	V3 = V1 cross V2 (cross product) (see VCROSS)

TABLE B-3 - SPECIAL OUTPUT ROUTINES

MLOOK1 (T1,A)	
MLOOK2 (T1,A1,T2,A2)	Prints out (3 x 3) matrices (A_1,A_2,A_3,A_4) with associated titles (T1,T2,T3,T4), titles are 30 spaces long, numbers are in F10.3 format
MLOOK3 (T1,A1,T2,A2,T3,A3)	
MLOOK4 (T1,A1,T2,A2,T3,A3,T4,A4)	
TLOOK1 (T1,A)	
TLOOK2 (T1,A1,T2,A2)	
TLOOK3 (T1,A1,T2,A2,T3,A3)	Same as MLOOK series except F10.6 format
TLOOK4 (T1,A1,T2,A2,T3,A3,T4,A4)	
VLOOK1 (T1,V1,I1)	
VLOOK2 (T1,V1,I1,T2,V2,I2)	Prints out (3 x 1) vectors with associated title (24 spaces long) format is F13.6 times 10 to the I1 power etc. (scaling)
VLOOK3 (T1,V1,I1,T2,V2,I2,T3,V3,I3)	
VLOOK4 (T1,V1,I1,T2,V2,I2,T3,V3,I3,T4,V4,I4)	
VLOOKN (T,V,N)	Prints out (N x 1) vector with associated title (24 spaces long)
BITS (N,DELTA, X)	Function converting X to n bit word with resolution DELTA
SCALE (N, DELTS, X)	Same as BITS but output is (0 - 100) percent of full scale
TRIGGR (D1,D2,D3,D4,D5,D6,D7,D8)	Function which converts 8 real variable discretes (0,1) to 3 octal bit word.

APPENDIX C

TRADE-OFF STUDY SIMULATION RESULTS

During the course of developing and debugging the simulation program described in this report numerous runs were made using typical values for the input parameters of the simulated system. The parameters which determine the response of the antenna pointing control system were adjusted in order to obtain stable, non-oscillatory, and rapidly converging antenna pointing control.

The plots and printed computer output included in this appendix show the behavior of a typical space station computer steered high gain antenna using "optimized" control system gains. The values for all of the input parameters used in the illustrated simulation run are included in the input lists of Appendix A.

The initial conditions were chosen to give a pointing error of about 10° in order to demonstrate the behavior of the controlled antenna during acquisition. When the gimbal angles get within 1.0° of the on board computed values the control system switches to its auto-track mode, using the monopulse error signals (at about 18 seconds in this case). Using an antenna with about a 1.0° half power beam width and monopulse horn separations of 1.0° (total) the antenna control system was able to track the relay satellite within about 0.3°.

The bending input data used in this run was computed from the expressions derived in Section 3.4.2.3 for a space station main body of cylindrical mass distribution (50 ft radius x 100 ft length) weighing 322,000 lbs (10,000 slugs) and with a boom antenna mount which deflects 1.0° angularly for each 1.0 ft translationally. The bending frequency was set at 1/10 Hz (.628 rad/sec) which is considered fairly low (corresponding to a not very stiff space station and boom).

The described bending mode is observed (Fig. C.4) to respond as expected to gimbal torques and space station orbital rate and to have insignificant (10^{-4} deg) effect on pointing.

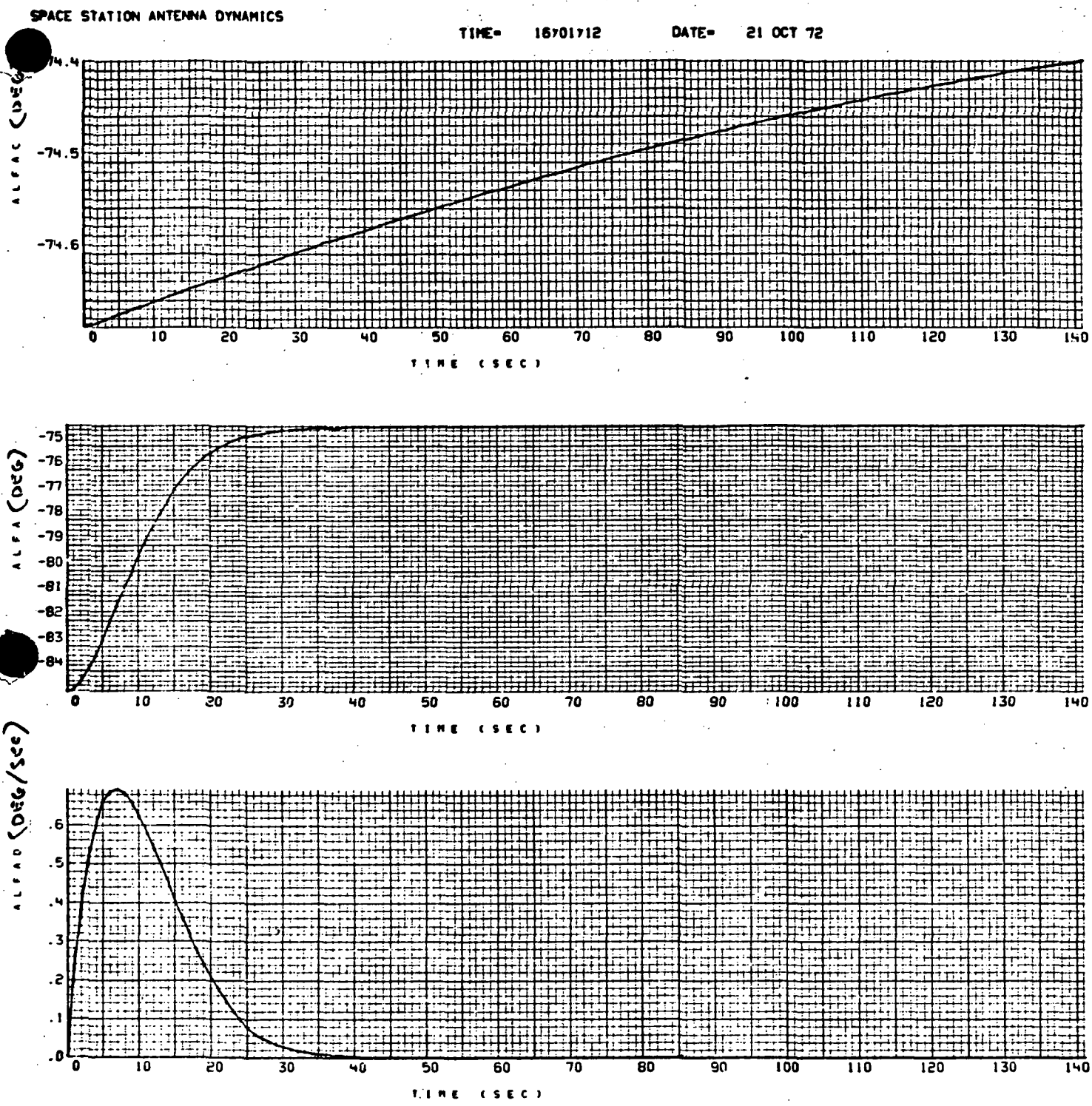

Figure C.1 Computed Gimbal Angle (ALFAC), Actual Gimbal Angle (ALFA), and Gimbal Rate (ALFAD) v.s. Time

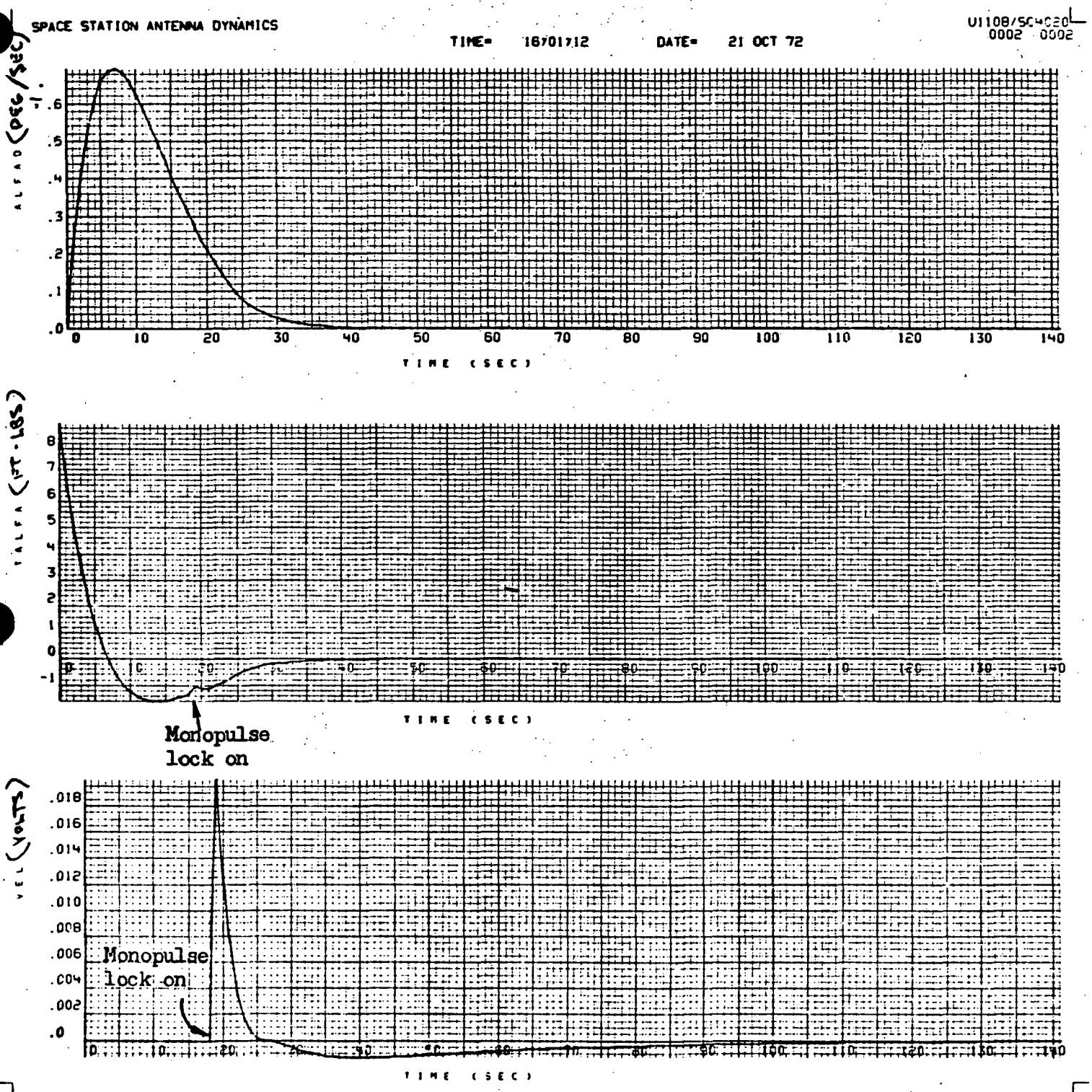

Figure C.2 Gimbal Rate (ALFAD), Gimbal Torque (TALFA), and Monopulse Error Signal (VEL) v.s. Time

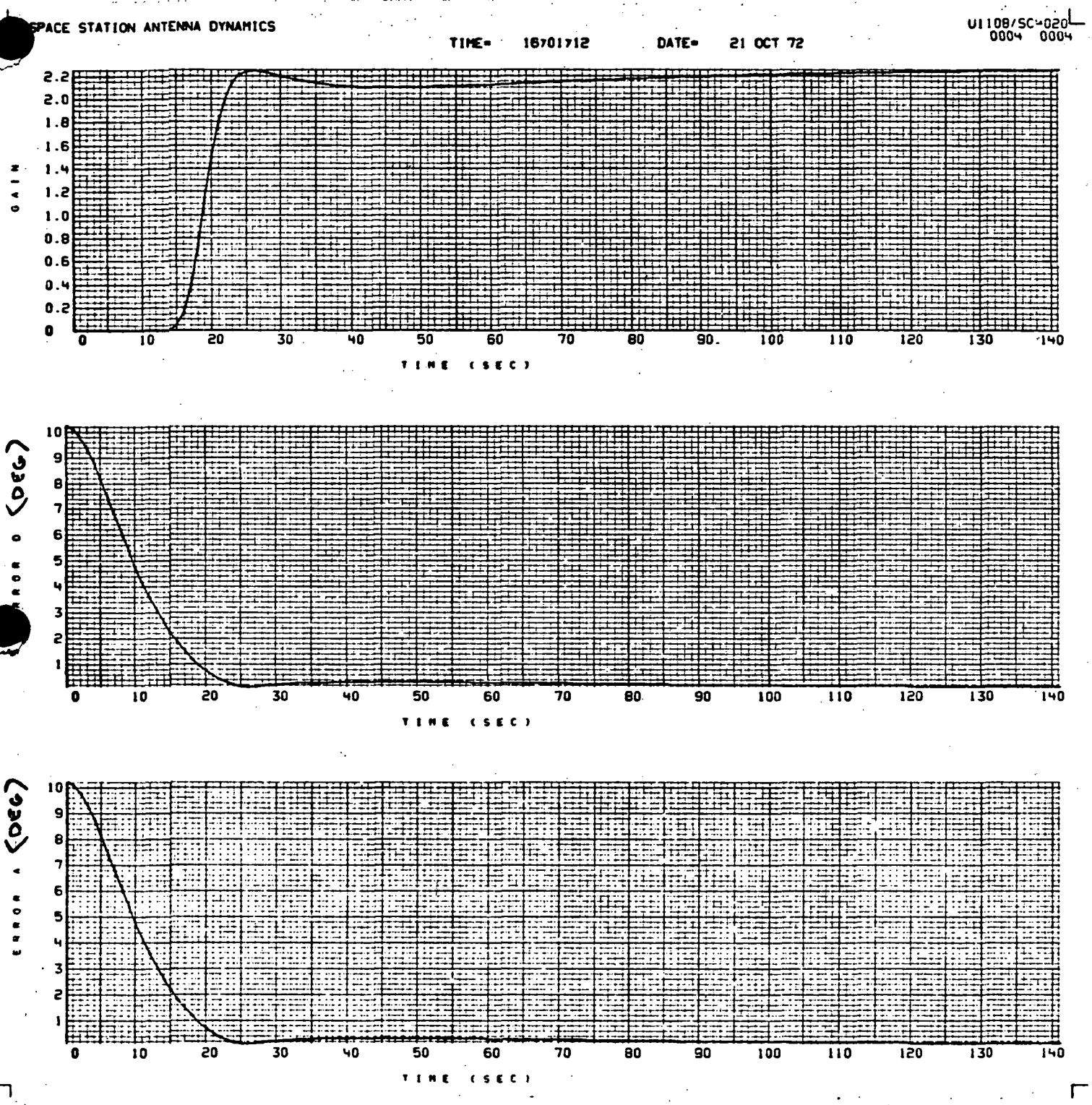

Figure C.3 Antenna Gain (GAIN), Antenna Pointing Error for Thermally Distorted (ERROR D) and Nominal (ERRQR A) Antenna v.s. Time

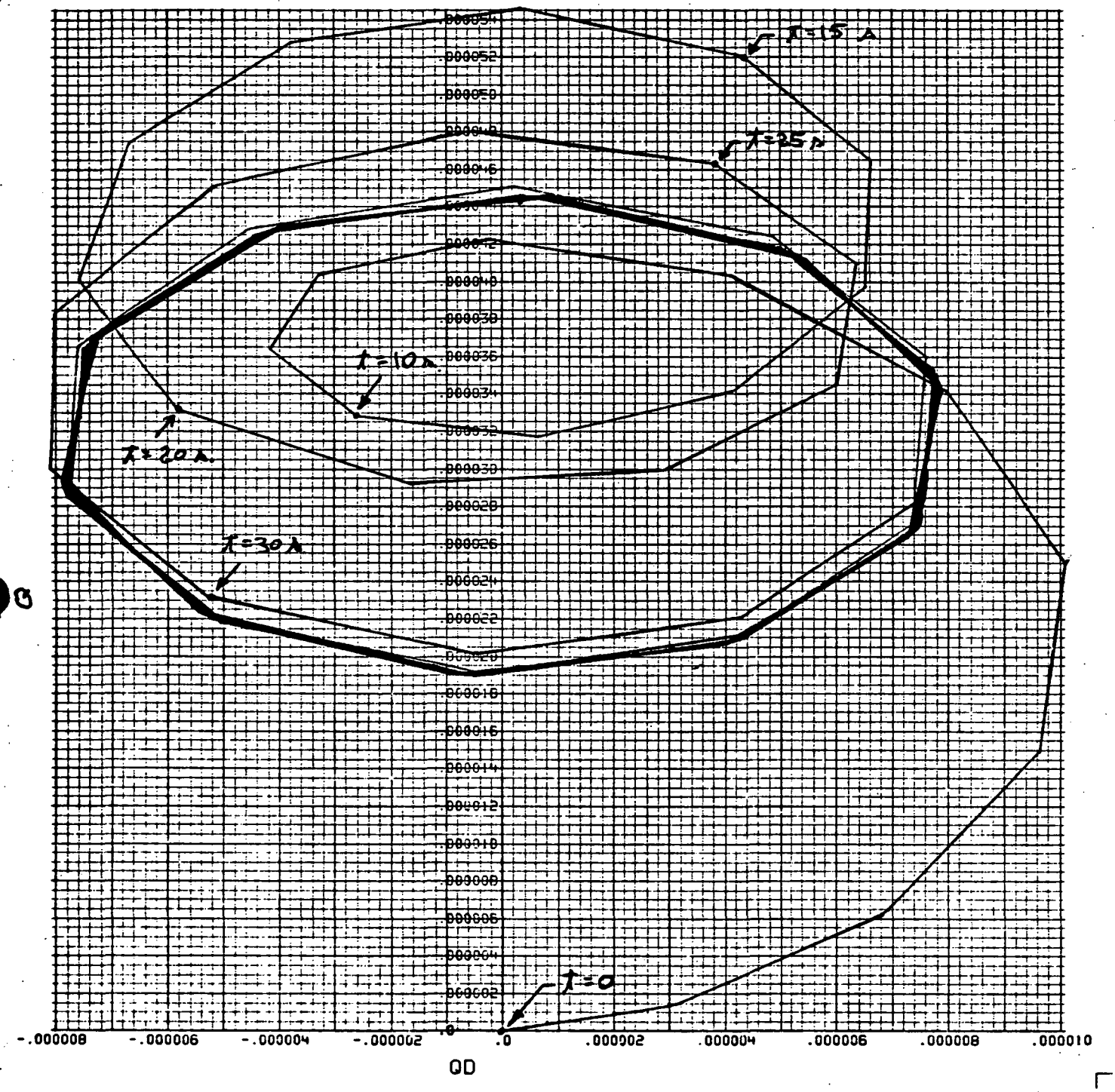

Figure C.4 Bending Mode Coordinate v.s. Derivative

Figure C-5 Computer Printed Output

The following six pages are reproduced from computer printout and show details of the data plotted in Figures C-1 through C-4.

TIME	NI	SSLAT	SSLON	SSALT	SSROLL	SSPITCH	SSYAW	KVIS	NIGHT
.000000	0	.000000	90.0000	400.835	-9.99999	.000000	.000000	.000000	.000000
1.000000	13	-.502081-01	89.9958	400.835	-9.99999	.000000	.000000	.000000	.000000
2.000000	17	.120423	89.9916	400.835	-9.99999	.000000	.000000	.000000	.000000
3.000000	21	.180645	89.9874	400.835	-9.99999	.000000	.000000	.000000	.000000
4.000000	25	.240868	89.9833	400.835	-9.99999	.000000	.000000	.000000	.000000
5.000000	29	.301075	89.9791	400.835	-9.99999	.000000	.000000	.000000	.000000
6.000000	33	.361297	89.9749	400.836	-9.99999	.000000	.000000	.000000	.000000
7.000000	37	.421511	89.9707	400.836	-9.99999	.000000	.000000	.000000	.000000
8.000000	41	.481726	89.9666	400.836	-9.99999	.000000	.000000	.000000	.000000
9.000000	45	.541948	89.9624	400.836	-9.99999	.000000	.000000	.000000	.000000
10.00000	49	.602163	89.9582	400.836	-9.99999	.000000	.000000	.000000	.000000
11.00000	53	.662378	89.9540	400.837	-9.99999	.000000	.000000	.000000	.000000
12.00000	57	.722600	89.9498	400.837	-9.99999	.000000	.000000	.000000	.000000
13.00000	61	.782815	89.9457	400.837	-9.99999	.000000	.000000	.000000	.000000
14.00000	65	.843030	89.9415	400.837	-9.99999	.000000	.000000	.000000	.000000
15.00000	69	.903245	89.9373	400.838	-9.99999	.000000	.000000	.000000	.000000
16.00000	73	.963466	89.9331	400.838	-9.99999	.000000	.000000	.000000	.000000
17.00000	77	1.02368	89.9290	400.838	-9.99999	.000000	.000000	.000000	.000000
18.00000	81	1.08390	89.9248	400.839	-9.99999	.000000	.000000	.000000	.000000
19.00000	104	1.14412	89.9206	400.839	-9.99999	.000000	.000000	.000000	.000000
20.00000	108	1.20433	89.9164	400.840	-9.99999	.000000	.000000	.000000	.000000
21.00000	112	1.26455	89.9122	400.840	-9.99999	.000000	.000000	.000000	.000000
22.00000	116	1.32477	89.9081	400.840	-9.99999	.000000	.000000	.000000	.000000
23.00000	120	1.38498	89.9039	400.841	-9.99999	.000000	.000000	.000000	.000000
24.00000	124	1.44520	89.8997	400.841	-9.99999	.000000	.000000	.000000	.000000
25.00000	128	1.50542	89.8955	400.842	-9.99999	.000000	.000000	.000000	.000000
26.00000	132	1.56564	89.8914	400.843	-9.99999	.000000	.000000	.000000	.000000
27.00000	136	1.62585	89.8872	400.843	-9.99999	.000000	.000000	.000000	.000000
28.00000	140	1.68607	89.8830	400.844	-9.99999	.000000	.000000	.000000	.000000
29.00000	144	1.74629	89.8788	400.844	-9.99999	.000000	.000000	.000000	.000000
30.00000	148	1.80650	89.8746	400.845	-9.99999	.000000	.000000	.000000	.000000
31.00000	152	1.86672	89.8705	400.846	-9.99999	.000000	.000000	.000000	.000000
32.00000	156	1.92694	89.8663	400.846	-9.99999	.000000	.000000	.000000	.000000
33.00000	160	1.98715	89.8621	400.847	-9.99999	.000000	.000000	.000000	.000000
34.00000	164	2.04737	89.8579	400.848	-9.99999	.000000	.000000	.000000	.000000
35.00000	165	2.10759	89.8538	400.848	-9.99999	.000000	.000000	.000000	.000000
36.00000	172	2.16781	89.8496	400.849	-9.99999	.000000	.000000	.000000	.000000
37.00000	176	2.22802	89.8454	400.850	-9.99999	.000000	.000000	.000000	.000000
38.00000	180	2.28824	89.8412	400.851	-9.99999	.000000	.000000	.000000	.000000
39.00000	184	2.34846	89.8370	400.852	-9.99999	.000000	.000000	.000000	.000000
40.00000	188	2.40867	89.8329	400.853	-9.99999	.000000	.000000	.000000	.000000
41.00000	192	2.46889	89.8287	400.853	-9.99999	.000000	.000000	.000000	.000000
42.00000	196	2.52911	89.8245	400.854	-9.99999	.000000	.000000	.000000	.000000
43.00000	200	2.58932	89.8203	400.855	-9.99999	.000000	.000000	.000000	.000000
44.00000	204	2.64954	89.8161	400.856	-9.99999	.000000	.000000	.000000	.000000
45.00000	208	2.70975	89.8120	400.857	-9.99999	.000000	.000000	.000000	.000000
46.00000	212	2.76998	89.8078	400.858	-9.99999	.000000	.000000	.000000	.000000
47.00000	216	2.83019	89.8036	400.859	-9.99999	.000000	.000000	.000000	.000000
48.00000	220	2.89041	89.7994	400.860	-9.99999	.000000	.000000	.000000	.000000
49.00000	224	2.95063	89.7953	400.861	-9.99999	.000000	.000000	.000000	.000000

TIME	NI	ALFAC	ALFA	ALFAD	TALFA	BETAC	BETA	BETAD	TBETA
.000000	0	-74.6800	-84.8600	.000000	8.92073	.000000	.000000	.000000	.487224-01
1.000000	13	-74.6772	-84.7424	.225342	6.85395	.169848-01	.737660-03	.153935-02	.495325-01
2.000000	17	-74.6743	-84.0275	.395920	5.00288	.339693-01	.313506-02	.326227-02	.472919-01
3.000000	21	-74.6715	-83.9660	.521095	3.60885	.509508-01	.726781-02	.504239-02	.430175-01
4.000000	25	-74.6686	-83.4003	.605376	2.37332	.679366-01	.132096-01	.679177-02	.374713-01
5.000000	29	-74.6658	-82.7659	.656482	1.35862	.849227-01	.206389-01	.844297-02	.312920-01
6.000000	33	-74.6630	-82.0920	.685343	.538277	.101909	.300460-01	.995565-02	.249425-01
7.000000	37	-74.6602	-81.4022	.691225	-.112604	.118895	.406674-01	.113057-01	.187652-01
8.000000	41	-74.6574	-80.7151	.680589	-.617117	.135883	.525993-01	.124813-01	.130000-01
9.000000	45	-74.6546	-80.0452	.657342	-.996538	.152871	.655971-01	.134819-01	.781408-02
10.000000	49	-74.6518	-79.4035	.624786	-1.27018	.169860	.795038-01	.143135-01	.331150-02
11.000000	53	-74.6491	-78.7978	.585696	-1.45536	.186849	.941746-01	.149889-01	-.495421-03
12.000000	57	-74.6463	-78.2335	.542382	-1.56758	.203838	.109440	.155216-01	-.357577-02
13.000000	61	-74.6436	-77.7138	.496731	-1.62048	.220825	.125177	.159289-01	-.597480-02
14.000000	65	-74.6408	-77.2403	.450267	-1.62599	.237816	.141262	.162277-01	-.772826-02
15.000000	69	-74.6381	-76.8131	.404197	-1.59450	.254807	.157600	.164360-01	-.891218-02
16.000000	73	-74.6354	-76.4315	.359450	-1.53467	.271800	.174115	.165709-01	-.960934-02
17.000000	77	-74.6327	-76.0934	.316721	-1.45467	.288793	.190726	.166443-01	-.985315-02
18.000000	81	-74.6300	-75.7972	.276508	-1.36020	.305783	.207385	.166733-01	-.975377-02
19.000000	104	-74.6274	-75.5389	.242144	-1.07196	.322777	.223859	.157718-01	-.763575-01
20.000000	108	-74.6247	-75.3125	.210179	-1.15030	.339772	.238715	.140010-01	-.623778-01
21.000000	112	-74.6220	-75.1187	.177556	-1.12231	.356764	.251993	.126102-01	-.493418-01
22.000000	116	-74.6194	-74.9568	.144864	-1.02161	.373761	.264035	.115242-01	-.386331-01
23.000000	120	-74.6168	-74.8238	.119671	-.883296	.390758	.275120	.106875-01	-.297935-01
24.000000	124	-74.6141	-74.7160	.966369-01	-.734973	.407756	.285481	.100557-01	-.224540-01
25.000000	128	-74.6115	-74.6292	.777728-01	-.594126	.424751	.295290	.959300-02	-.163117-01
26.000000	132	-74.6089	-74.5592	.627199-01	-.469709	.441751	.304715	.927454-02	-.111711-01
27.000000	136	-74.6064	-74.5026	.509148-01	-.369421	.458748	.313881	.907732-02	-.684523-02
28.000000	140	-74.6038	-74.4566	.415890-01	-.295240	.475749	.322904	.898426-02	-.320607-02
29.000000	144	-74.6012	-74.4188	.341151-01	-.239232	.492752	.331879	.897572-02	-.103753-03
30.000000	148	-74.5987	-74.3879	.280550-01	-.196058	.509751	.340881	.904317-02	.251276-02
31.000000	152	-74.5961	-74.3624	.230920-01	-.162117	.526755	.349986	.917065-02	.472019-02
32.000000	156	-74.5936	-74.3414	.190067-01	-.134988	.543756	.359247	.935907-02	.659075-02
33.000000	160	-74.5911	-74.3241	.156078-01	-.112958	.560762	.368721	.958873-02	.816024-02
34.000000	164	-74.5886	-74.3100	.127844-01	-.948469-01	.577769	.378440	.985596-02	.947120-02
35.000000	168	-74.5861	-74.2984	.104314-01	-.798045-01	.594773	.388447	.101556-01	.105391-01
36.000000	172	-74.5836	-74.2890	.847029-02	-.672263-01	.611782	.398760	.104801-01	.114061-01
37.000000	176	-74.5811	-74.2814	.683958-02	-.566657-01	.628788	.409415	.108241-01	.120865-01
38.000000	180	-74.5786	-74.2752	.548891-02	-.477846-01	.645798	.420412	.111844-01	.125951-01
39.000000	184	-74.5762	-74.2703	.437303-02	-.402986-01	.662806	.431784	.115558-01	.129446-01
40.000000	188	-74.5737	-74.2664	.345606-02	-.339886-01	.679819	.443532	.119340-01	.131545-01
41.000000	192	-74.5713	-74.2633	.270732-02	-.286778-01	.696829	.455656	.123148-01	.132479-01
42.000000	196	-74.5689	-74.2610	.209772-02	-.241964-01	.713841	.468162	.126965-01	.132225-01
43.000000	200	-74.5665	-74.2591	.160509-02	-.204168-01	.730857	.481043	.130755-01	.130960-01
44.000000	204	-74.5641	-74.2577	.120894-02	-.172329-01	.747870	.494308	.134486-01	.128825-01
45.000000	208	-74.5617	-74.2567	.893047-03	-.145394-01	.764887	.507941	.138149-01	.125852-01
46.000000	212	-74.5593	-74.2559	.646307-03	-.122959-01	.781903	.521936	.141709-01	.122275-01
47.000000	216	-74.5570	-74.2554	.456769-03	-.104311-01	.798920	.536286	.145159-01	.118089-01
48.000000	220	-74.5546	-74.2550	.317604-03	-.892380-02	.815942	.550964	.148480-01	.113522-01
49.000000	224	-74.5523	-74.2547	.219420-03	-.770633-02	.832960	.565970	.151656-01	.108655-01

SPACE STATION ANTENNA DYNAMICS

TIME	NI	GAIN	VEL	VAZ	ERROR D	ERROR A	Q	QD	
.00000	0	.000000	.000000	.000000	10.2076	10.1803	.000000	.000000	.000000
1.00000	13	.000000	.000000	.000000	10.0942	10.0669	.141596-05	.311364-05	.000000
2.00000	17	.000000	.000000	.000000	9.78346	9.75635	.645750-05	.692607-05	.000000
3.00000	21	.221513-33	.000000	.000000	9.32598	9.29905	.148960-04	.964536-05	.000000
4.00000	25	.275158-29	.000000	.000000	8.76435	8.73762	.249716-04	.100749-04	.000000
5.00000	29	.540512-25	.000000	.000000	8.13402	8.10752	.341870-04	.797113-05	.000000
6.00000	33	.845063-21	.000000	.000000	7.46415	7.43757	.403073-04	.407509-05	.000000
7.00000	37	.676939-17	.000000	.000000	6.77828	6.75224	.422164-04	-.188127-06	.000000
8.00000	41	.210754-13	.000000	.000000	6.09517	6.06934	.403246-04	-.329211-05	.000000
9.00000	45	.222869-10	.000000	.000000	5.42929	5.40368	.363877-04	-.416604-05	.000000
10.00000	49	.778700-08	.000000	.000000	4.79157	4.76615	.328153-04	-.241219-05	.000000
11.00000	53	.941840-06	.000000	.000000	4.18991	4.16467	.317355-04	.629050-06	.000000
12.00000	57	.334139-04	.000000	.000000	3.62965	3.60456	.341753-04	.416959-05	.000000
13.00000	61	.862302-03	.000000	.000000	3.11404	3.08909	.396686-04	.650994-05	.000000
14.00000	65	.842967-02	.000000	.000000	2.64465	2.61982	.464387-04	.661658-05	.000000
15.00000	69	.462288-01	.000000	.000000	2.22165	2.19692	.520872-04	.432006-05	.000000
16.00000	73	.180354	.000000	.000000	1.84419	1.81955	.545222-04	.382832-06	.000000
17.00000	77	.390559	.000000	.000000	1.51060	1.48604	.527722-04	-.379002-05	.000000
18.00000	81	.728569	.000000	.000000	1.21865	1.19415	.473742-04	-.668532-05	.000000
19.00000	104	1.11739	.199519-01	-.185073-03	.964974	.940525	.401098-04	-.759168-05	.000000
20.00000	108	1.49146	.124887-01	-.190608-03	.743802	.719405	.331554-04	-.581861-05	.000000
21.00000	112	1.79461	.716446-02	-.203394-03	.556077	.531761	.292674-04	-.171096-05	.000000
22.00000	116	2.00623	.371882-02	-.222514-03	.401428	.377721	.298929-04	.286981-05	.000000
23.00000	120	2.13573	.169007-02	-.247328-03	.279793	.256354	.345113-04	.598951-05	.000000
24.00000	124	2.20472	.617659-03	-.277356-03	.189535	.168370	.409440-04	.637246-05	.000000
25.00000	128	2.23402	.138484-03	-.312293-03	.134396	.120234	.462750-04	.386144-05	.000000
26.00000	132	2.24092	.172757-05	-.351639-03	.119028	.117081	.480213-04	-.552915-06	.000000
27.00000	136	2.23476	-.494704-04	-.395023-03	.133500	.140927	.451131-04	-.512615-05	.000000
28.00000	140	2.22229	-.188109-03	-.441951-03	.158947	.171148	.383295-04	-.803563-05	.000000
29.00000	144	2.20721	-.363782-03	-.491925-03	.185280	.199856	.300063-04	-.809628-05	.000000
30.00000	148	2.19162	-.545776-03	-.544423-03	.209206	.225040	.231266-04	-.523689-05	.000000
31.00000	152	2.17666	-.717364-03	-.598847-03	.229963	.246489	.201658-04	-.510714-06	.000000
32.00000	156	2.16295	-.869631-03	-.654673-03	.247585	.264488	.221375-04	.430824-05	.000000
33.00000	160	2.15073	-.990542-03	-.711248-03	.262367	.279455	.281993-04	.740413-05	.000000
34.00000	164	2.14008	-.110588-02	-.765078-03	.274674	.291824	.359681-04	.741298-05	.000000
35.00000	168	2.13098	-.118958-02	-.814579-03	.284834	.301959	.422240-04	.486486-05	.000000
36.00000	172	2.12325	-.125271-02	-.858260-03	.293173	.310213	.450577-04	.221364-06	.000000
37.00000	176	2.11685	-.129745-02	-.934542-03	.299948	.316860	.428246-04	-.454643-05	.000000
38.00000	180	2.11161	-.132618-02	-.987145-03	.305401	.322151	.365403-04	-.761414-05	.000000
39.00000	184	2.10739	-.134140-02	-.103746-02	.309726	.326291	.285694-04	-.780838-05	.000000
40.00000	188	2.10408	-.134522-02	-.108524-02	.313087	.329449	.219238-04	-.505074-05	.000000
41.00000	192	2.10155	-.133969-02	-.113018-02	.315631	.331777	.191140-04	-.388245-06	.000000
42.00000	196	2.09970	-.132665-02	-.117203-02	.317478	.333400	.211928-04	.440615-05	.000000
43.00000	200	2.09846	-.130754-02	-.121062-02	.318720	.334413	.273538-04	.750879-05	.000000
44.00000	204	2.09772	-.128395-02	-.124568-02	.319450	.334912	.352381-04	.774034-05	.000000
45.00000	208	2.09745	-.125667-02	-.127721-02	.319720	.334950	.418324-04	.501447-05	.000000
46.00000	212	2.09757	-.122689-02	-.130516-02	.319604	.334606	.446168-04	.371190-06	.000000
47.00000	216	2.09803	-.119531-02	-.132983-02	.319142	.333917	.425242-04	-.441918-05	.000000
48.00000	220	2.09878	-.116273-02	-.135025-02	.318395	.332949	.363464-04	-.753691-05	.000000
49.00000	224	2.09980	-.112986-02	-.136756-02	.317378	.331718	.284326-04	-.777777-05	.000000

SPACE STATION ANTENNA DYNAMICS

MONOPULSE ON TIMES AND OFF TIMES

18.8163 .0000

TIME	NI	SSLAT	SSLON	SSALT	SSROLL	SSPITCH	SSYAW	KVIS	NIGHT
50.00000	228	3.01084	89.7911	400.862	-9.99999	.000000	.000000	.000000	.000000
51.00000	232	3.07106	89.7669	400.864	-9.99999	.000000	.000000	.000000	.000000
52.00000	236	3.13128	89.7827	400.865	-9.99999	.000000	.000000	.000000	.000000
53.00000	240	3.19149	89.7785	400.866	-9.99999	.000000	.000000	.000000	.000000
54.00000	244	3.25171	89.7744	400.867	-9.99999	.000000	.000000	.000000	.000000
55.00000	248	3.31192	89.7702	400.868	-9.99999	.000000	.000000	.000000	.000000
56.00000	252	3.37215	89.7660	400.869	-9.99999	.000000	.000000	.000000	.000000
57.00000	256	3.43236	89.7618	400.871	-9.99999	.000000	.000000	.000000	.000000
58.00000	260	3.49258	89.7577	400.872	-9.99999	.000000	.000000	.000000	.000000
59.00000	264	3.55280	89.7535	400.873	-9.99999	.000000	.000000	.000000	.000000
60.00000	268	3.61301	89.7493	400.874	-9.99999	.000000	.000000	.000000	.000000
61.00000	272	3.67323	89.7451	400.876	-9.99999	.000000	.000000	.000000	.000000
62.00000	276	3.73344	89.7409	400.877	-9.99999	.000000	.000000	.000000	.000000
63.00000	280	3.79366	89.7368	400.878	-9.99999	.000000	.000000	.000000	.000000
64.00000	284	3.85388	89.7326	400.880	-9.99999	.000000	.000000	.000000	.000000
65.00000	288	3.91409	89.7284	400.881	-9.99999	.000000	.000000	.000000	.000000
66.00000	292	3.97432	89.7242	400.883	-9.99999	.000000	.000000	.000000	.000000
67.00000	296	4.03453	89.7201	400.884	-9.99999	.000000	.000000	.000000	.000000
68.00000	300	4.09475	89.7159	400.886	-9.99999	.000000	.000000	.000000	.000000
69.00000	304	4.15496	89.7117	400.887	-9.99999	.000000	.000000	.000000	.000000
70.00000	308	4.21518	89.7075	400.889	-9.99999	.000000	.000000	.000000	.000000
71.00000	312	4.27540	89.7033	400.890	-9.99999	.000000	.000000	.000000	.000000
72.00000	316	4.33561	89.6992	400.892	-9.99999	.000000	.000000	.000000	.000000
73.00000	320	4.39583	89.6950	400.893	-9.99999	.000000	.000000	.000000	.000000
74.00000	324	4.45605	89.6908	400.895	-9.99999	.000000	.000000	.000000	.000000
75.00000	328	4.51626	89.6866	400.896	-9.99999	.000000	.000000	.000000	.000000
76.00000	332	4.57648	89.6825	400.898	-9.99999	.000000	.000000	.000000	.000000
77.00000	336	4.63670	89.6783	400.900	-9.99999	.000000	.000000	.000000	.000000
78.00000	340	4.69692	89.6741	400.901	-9.99999	.000000	.000000	.000000	.000000
79.00000	344	4.75713	89.6699	400.903	-9.99999	.000000	.000000	.000000	.000000
80.00000	348	4.81735	89.6657	400.905	-9.99999	.000000	.000000	.000000	.000000
81.00000	352	4.87757	89.6616	400.907	-9.99999	.000000	.000000	.000000	.000000
82.00000	356	4.93778	89.6574	400.908	-9.99999	.000000	.000000	.000000	.000000
83.00000	360	4.99800	89.6532	400.910	-9.99999	.000000	.000000	.000000	.000000
84.00000	364	5.05822	89.6490	400.912	-9.99999	.000000	.000000	.000000	.000000
85.00000	368	5.11843	89.6448	400.914	-9.99999	.000000	.000000	.000000	.000000
86.00000	372	5.17865	89.6407	400.916	-9.99999	.000000	.000000	.000000	.000000
87.00000	376	5.23886	89.6365	400.918	-9.99999	.000000	.000000	.000000	.000000
88.00000	380	5.29909	89.6323	400.919	-9.99999	.000000	.000000	.000000	.000000
89.00000	384	5.35930	89.6281	400.921	-9.99999	.000000	.000000	.000000	.000000
90.00000	388	5.41952	89.6240	400.923	-9.99999	.000000	.000000	.000000	.000000
91.00000	392	5.47973	89.6198	400.925	-9.99999	.000000	.000000	.000000	.000000
92.00000	396	5.53995	89.6156	400.927	-9.99999	.000000	.000000	.000000	.000000
93.00000	400	5.60017	89.6114	400.929	-9.99999	.000000	.000000	.000000	.000000
94.00000	404	5.66038	89.6072	400.931	-9.99999	.000000	.000000	.000000	.000000
95.00000	408	5.72060	89.6031	400.933	-9.99999	.000000	.000000	.000000	.000000
96.00000	412	5.78082	89.5989	400.935	-9.99999	.000000	.000000	.000000	.000000
97.00000	416	5.84103	89.5947	400.937	-9.99999	.000000	.000000	.000000	.000000
98.00000	420	5.90125	89.5905	400.940	-9.99999	.000000	.000000	.000000	.000000
99.00000	424	5.96147	89.5864	400.942	-9.99999	.000000	.000000	.000000	.000000

TIME	NI	ALFAC	ALFA	ALFAD	TALFA	BETAC	BETA	BETAD	TBETA
50.00000	228	-74.5500	-74.2545	.154533-03	-.673750-02	.849981	.581290	.154695-01	.103404-01
51.00000	232	-74.5476	-74.2544	.116113-03	-.597237-02	.867006	.596904	.157581-01	.979837-02
52.00000	236	-74.5453	-74.2543	.964784-04	-.535294-02	.884028	.612805	.160305-01	.924765-02
53.00000	240	-74.5430	-74.2542	.913538-04	-.485653-02	.901052	.628945	.162874-01	.868959-02
54.00000	244	-74.5408	-74.2541	.960764-04	-.445273-02	.918081	.645378	.165282-01	.813335-02
55.00000	248	-74.5385	-74.2540	.108829-03	-.410955-02	.935107	.662016	.167527-01	.759165-02
56.00000	252	-74.5362	-74.2539	.127212-03	-.381145-02	.952135	.678880	.169628-01	.704900-02
57.00000	256	-74.5340	-74.2537	.152825-03	-.364618-02	.969163	.695935	.171566-01	.653538-02
58.00000	260	-74.5318	-74.2536	.184415-03	-.352594-02	.986197	.713188	.173367-01	.602390-02
59.00000	264	-74.5295	-74.2534	.220274-03	-.345829-02	1.00323	.730612	.175024-01	.553858-02
60.00000	268	-74.5273	-74.2531	.261255-03	-.345397-02	1.02026	.748186	.176543-01	.508028-02
61.00000	272	-74.5251	-74.2529	.302236-03	-.347049-02	1.03730	.765910	.177935-01	.464176-02
62.00000	276	-74.5229	-74.2525	.343217-03	-.350746-02	1.05433	.783764	.179199-01	.423517-02
63.00000	280	-74.5208	-74.2522	.380783-03	-.352853-02	1.07137	.801748	.180360-01	.383619-02
64.00000	284	-74.5186	-74.2518	.415788-03	-.350716-02	1.08841	.819841	.181410-01	.346809-02
65.00000	288	-74.5165	-74.2513	.447377-03	-.355435-02	1.10545	.838030	.182349-01	.313347-02
66.00000	292	-74.5143	-74.2509	.477259-03	-.355829-02	1.12249	.856308	.183203-01	.281733-02
67.00000	296	-74.5122	-74.2504	.506296-03	-.357680-02	1.13953	.874667	.183971-01	.252133-02
68.00000	300	-74.5101	-74.2499	.536170-03	-.361715-02	1.15657	.893095	.184654-01	.225372-02
69.00000	304	-74.5080	-74.2493	.567759-03	-.368799-02	1.17362	.911591	.185269-01	.200088-02
70.00000	308	-74.5059	-74.2487	.598835-03	-.376345-02	1.19067	.930149	.185807-01	.177452-02
71.00000	312	-74.5038	-74.2481	.628377-03	-.384791-02	1.20772	.948754	.186265-01	.156565-02
72.00000	316	-74.5017	-74.2475	.656552-03	-.392719-02	1.22477	.967408	.186712-01	.136836-02
73.00000	320	-74.4997	-74.2468	.681311-03	-.398905-02	1.24182	.986095	.187079-01	.119846-02
74.00000	324	-74.4976	-74.2461	.702656-03	-.402993-02	1.25887	1.00482	.187395-01	.104286-02
75.00000	328	-74.4956	-74.2454	.719731-03	-.404502-02	1.27592	1.02357	.187685-01	.891639-03
76.00000	332	-74.4936	-74.2447	.734245-03	-.404517-02	1.29298	1.04236	.187916-01	.764310-03
77.00000	336	-74.4916	-74.2439	.748759-03	-.405738-02	1.31003	1.06116	.188129-01	.642199-03
78.00000	340	-74.4896	-74.2432	.764981-03	-.409521-02	1.32709	1.07998	.188300-01	.535124-03
79.00000	344	-74.4876	-74.2424	.782057-03	-.414657-02	1.34415	1.09882	.188436-01	.444391-03
80.00000	348	-74.4856	-74.2416	.799966-03	-.421410-02	1.36121	1.11767	.188564-01	.347957-03
81.00000	352	-74.4837	-74.2408	.817061-03	-.428561-02	1.37828	1.13653	.188658-01	.271932-03
82.00000	356	-74.4817	-74.2400	.832429-03	-.434312-02	1.39534	1.15540	.188718-01	.212387-03
83.00000	360	-74.4798	-74.2391	.846090-03	-.439329-02	1.41240	1.17427	.188778-01	.146688-03
84.00000	364	-74.4779	-74.2383	.855481-03	-.441379-02	1.42947	1.19316	.188821-01	.840891-04
85.00000	368	-74.4760	-74.2374	.861458-03	-.441094-02	1.44654	1.21204	.188838-01	.404287-04
86.00000	372	-74.4741	-74.2365	.866580-03	-.440587-02	1.46361	1.23092	.188855-01	-.117710-04
87.00000	376	-74.4722	-74.2357	.870849-03	-.439667-02	1.48068	1.24981	.188846-01	-.472479-04
88.00000	380	-74.4703	-74.2348	.876826-03	-.441090-02	1.49776	1.26869	.188838-01	-.872016-04
89.00000	384	-74.4685	-74.2339	.885363-03	-.445184-02	1.51483	1.28758	.188812-01	-.117946-03
90.00000	388	-74.4666	-74.2330	.894755-03	-.450390-02	1.53191	1.30646	.188786-01	-.150532-03
91.00000	392	-74.4648	-74.2321	.904145-03	-.456058-02	1.54899	1.32533	.188744-01	-.170180-03
92.00000	396	-74.4630	-74.2312	.911830-03	-.460920-02	1.56607	1.34420	.188701-01	-.193619-03
93.00000	400	-74.4611	-74.2303	.916953-03	-.463776-02	1.58315	1.36307	.188650-01	-.214951-03
94.00000	404	-74.4593	-74.2294	.920368-03	-.465734-02	1.60023	1.38193	.188590-01	-.227089-03
95.00000	408	-74.4576	-74.2285	.920368-03	-.464847-02	1.61732	1.40079	.188530-01	-.243020-03
96.00000	412	-74.4558	-74.2276	.918660-03	-.462750-02	1.63440	1.41964	.188471-01	-.260799-03
97.00000	416	-74.4540	-74.2266	.916953-03	-.461014-02	1.65149	1.43849	.188402-01	-.271902-03
98.00000	420	-74.4523	-74.2257	.916953-03	-.461582-02	1.66858	1.45732	.188325-01	-.274311-03
99.00000	424	-74.4506	-74.2248	.918660-03	-.463605-02	1.68567	1.47614	.188257-01	-.284002-03

TIME	NI	GAIN	VEL	VAZ	ERROR D	ERROR A	D	DD	
50.00000	228	2.19105	-.109601-02	-.138141-02	.316125	.330257	.217938-04	-.506488-05	.000000
51.00000	232	2.19259	-.106268-02	-.139200-02	.314665	.328595	.189561-04	-.425265-06	.000000
52.00000	236	2.19414	-.102966-02	-.139940-02	.313012	.326748	.209984-04	.437448-05	.000000
53.00000	240	2.19569	-.997218-03	-.140386-02	.311195	.324745	.271408-04	.750646-05	.000000
54.00000	244	2.19726	-.965472-03	-.140546-02	.309227	.322599	.350426-04	.777817-05	.000000
55.00000	248	2.19882	-.934386-03	-.140453-02	.307122	.320322	.416930-04	.508648-05	.000000
56.00000	252	2.20037	-.904220-03	-.140108-02	.304896	.317933	.445584-04	.457105-06	.000000
57.00000	256	2.20192	-.874906-03	-.139548-02	.302567	.315448	.425475-04	-.434637-05	.000000
58.00000	260	2.20344	-.846521-03	-.138787-02	.300140	.312873	.364261-04	-.749395-05	.000000
59.00000	264	2.20493	-.819202-03	-.137803-02	.297627	.310219	.285264-04	-.778690-05	.000000
60.00000	268	2.20640	-.792698-03	-.136676-02	.295044	.307501	.218576-04	-.511331-05	.000000
61.00000	272	2.20785	-.767131-03	-.135389-02	.292393	.304722	.189601-04	-.491913-06	.000000
62.00000	276	2.20926	-.742464-03	-.133970-02	.289687	.301894	.209379-04	.431703-05	.000000
63.00000	280	2.21061	-.718565-03	-.132421-02	.286919	.299010	.270377-04	.748178-05	.000000
64.00000	284	2.21192	-.695541-03	-.130764-02	.284110	.296090	.349364-04	.779686-05	.000000
65.00000	288	2.21318	-.673330-03	-.129020-02	.281268	.293142	.416253-04	.514253-05	.000000
66.00000	292	2.21439	-.651783-03	-.127199-02	.278390	.290162	.445573-04	.529806-06	.000000
67.00000	296	2.21556	-.631107-03	-.125306-02	.275494	.287169	.426160-04	-.428420-05	.000000
68.00000	300	2.21668	-.611121-03	-.123360-02	.272579	.284162	.365414-04	-.746566-05	.000000
69.00000	304	2.21775	-.591833-03	-.121364-02	.269647	.281141	.286479-04	-.780297-05	.000000
70.00000	308	2.21878	-.573172-03	-.119328-02	.266701	.278110	.219428-04	-.516762-05	.000000
71.00000	312	2.21976	-.555197-03	-.117263-02	.263754	.275081	.189802-04	-.563683-06	.000000
72.00000	316	2.22069	-.537773-03	-.115173-02	.260797	.272045	.208889-04	.425510-05	.000000
73.00000	320	2.22158	-.520946-03	-.113077-02	.257848	.269020	.269421-04	.745314-05	.000000
74.00000	324	2.22241	-.504815-03	-.110962-02	.254890	.265989	.348339-04	.781246-05	.000000
75.00000	328	2.22319	-.489339-03	-.108853-02	.251948	.262975	.415586-04	.519608-05	.000000
76.00000	332	2.22392	-.473517-03	-.106730-02	.248997	.259955	.445550-04	.600819-06	.000000
77.00000	336	2.22460	-.458739-03	-.104631-02	.246075	.256966	.426922-04	-.422291-05	.000000
78.00000	340	2.22523	-.444455-03	-.102529-02	.243158	.253984	.366537-04	-.743766-05	.000000
79.00000	344	2.22581	-.430589-03	-.100443-02	.240254	.251017	.287664-04	-.781904-05	.000000
80.00000	348	2.22634	-.417161-03	-.983720-03	.237365	.248067	.220248-04	-.522187-05	.000000
81.00000	352	2.22683	-.404225-03	-.963237-03	.234503	.245146	.189972-04	-.635569-06	.000000
82.00000	356	2.22727	-.391563-03	-.942896-03	.231643	.242226	.208365-04	.419276-05	.000000
83.00000	360	2.22767	-.379301-03	-.922840-03	.228808	.239333	.268423-04	.742396-05	.000000
84.00000	364	2.22802	-.367428-03	-.902953-03	.225988	.236457	.347269-04	.782742-05	.000000
85.00000	368	2.22833	-.355921-03	-.883391-03	.223195	.233609	.414868-04	.524928-05	.000000
86.00000	372	2.22859	-.344741-03	-.864043-03	.220418	.230777	.445475-04	.671949-06	.000000
87.00000	376	2.22881	-.333950-03	-.844987-03	.217658	.227963	.427433-04	-.416109-05	.000000
88.00000	380	2.22898	-.323341-03	-.826210-03	.214927	.225178	.367617-04	-.740885-05	.000000
89.00000	384	2.22911	-.313127-03	-.807694-03	.212213	.222413	.288814-04	-.783429-05	.000000
90.00000	388	2.22919	-.303182-03	-.789513-03	.209523	.219670	.221043-04	-.527542-05	.000000
91.00000	392	2.22923	-.293530-03	-.771656-03	.206858	.216954	.190119-04	-.707165-06	.000000
92.00000	396	2.22923	-.284196-03	-.754076-03	.204218	.214264	.207820-04	.413036-05	.000000
93.00000	400	2.22919	-.275100-03	-.736746-03	.201593	.211589	.267402-04	.739447-05	.000000
94.00000	404	2.22911	-.266293-03	-.719791-03	.199001	.208947	.346170-04	.784191-05	.000000
95.00000	408	2.22900	-.257687-03	-.703102-03	.196423	.206319	.414118-04	.530231-05	.000000
96.00000	412	2.22886	-.249308-03	-.686710-03	.193866	.203712	.445367-04	.743137-06	.000000
97.00000	416	2.22868	-.241166-03	-.670625-03	.191332	.201129	.428016-04	-.409881-05	.000000
98.00000	420	2.22848	-.233344-03	-.654838-03	.188836	.198584	.368674-04	-.737928-05	.000000
99.00000	424	2.22826	-.225870-03	-.639369-03	.186357	.196056	.289949-04	-.784878-05	.000000

SPACE STATION ANTENNA DYNAMICS

MONOPULSE ON TIMES AND OFF TIMES

16.8160 .0000